

Response to reviewers for the paper “A simplified parameterization of isoprene-epoxydiol-derived secondary organic aerosol (IEPOX-SOA) for global chemistry and climate models”

5 We thank the reviewers and Executive Editor for their comments on our paper. To guide the review process we have copied the reviewer comments in black text. Our responses are in regular blue font. We have responded to all the referee comments and made alterations to our paper (**in bold text**). For duplicated responses, we referred to prior comments with underlined links and backlinks, to avoid repeating the text.

10

Executive editor

E1.0) In my role as Executive editor of GMD, I would like to bring to your attention our Editorial version 1.1:

<http://www.geosci-model-dev.net/8/3487/2015/gmd-8-3487-2015.html>

15 This highlights some requirements of papers published in GMD, which is also available on the GMD website in the ‘Manuscript Types’ section:

http://www.geoscientific-model-development.net/submission/manuscript_types.html

In particular, please note that for your paper, the following requirements have not been met in the Discussions paper:

- 20
- "The main paper must give the model name and version number (or other unique identifier) in the title."
 - "If the model development relates to a single model then the model name and the version number must be included in the title of the paper. If the main intention of an article is to make a general (i.e. model independent) statement about the usefulness of a new development, but
25 the usefulness is shown with the help of one specific model, the model name and version number must be stated in the title. The title could have a form such as, "Title outlining amazing generic advance: a case study with Model XXX (version Y)"."
 - "All papers must include a section, at the end of the paper, entitled 'Code availability'. Here, either instructions for obtaining the code, or the reasons why the code is not available should
30 be clearly stated. It is preferred for the code to be uploaded as a supplement or to be made available at a data repository with an associated DOI (digital object identifier) for the exact model version described in the paper. Alternatively, for established models, there may be an existing means of accessing the code through a particular system. In this case, there must exist a means of permanently accessing the precise model version described in the paper. In
35 some cases, authors may prefer to put models on their own website, or to act as a point of contact for obtaining the code. Given the impermanence of websites and email addresses, this is not encouraged, and authors should consider improving the availability with a more permanent arrangement. After the paper is accepted the model archive should be updated to include a link to the GMD paper."

40

Consequently,

- E1.1) add a version number for your new parametrization. Even if this is "only" a parametrization, it might be changed in the future. In this case the version number is important to identify the exact version of the parametrization used.

45 We added a version number to the parameterization (version 1.0), and mentioned this in abstract.

“Here we present three simplified parameterizations (version 1.0) for IEPOX-SOA simulation, based on an approximate analytical/fitting solution of the IEPOX-SOA yield and formation timescale.”

- E1.2) as the main evaluation results are from GEOS-Chem simulations, add this to the title including the version number identifying the modified GEOS-Chem model version unambiguously.

We added a mention of GEOS-Chem and its version number to the title as follows:

55 **“A simplified parameterization of isoprene-epoxydiol-derived secondary organic aerosol (IEPOX-SOA) for global chemistry and climate models: a case study with GEOS-Chem v11-02-rc”**

- E1.3) note that at least the code developments published in the manuscript need to become public themselves. For your article this means that at least the box model needs to be publicly available under a persistent repository or in the supplement BEFORE final acceptance of the paper. It would be best to also make the full modified version of GEOS-Chem available in a public permanent repository, if this is prohibited by license issues, please state this explicitly and add how to get access to the GEOS-Chem code.

60 We recently made the KinSim box model available on the web, as documented in Peng and Jimenez (2019). We have added a citation to this paper.

We have uploaded the different KinSim chemical mechanisms as supplements of the paper, and also to the KinSim chemical mechanisms page.

65 GEOS-Chem is publicly available in GEOS-Chem wiki site, but we are making the full modified version of GEOS-Chem available upon request, because there are technical details that users should be aware of (e.g. the code also requires corresponding run directory, new restart file is needed, etc.). We updated the Code and Data availability section as follows.

70 **“Code and Data Availability. The KinSim box model can be downloaded from <http://tinyurl.com/kinsim-release> (preferred, due to updates) or from the supporting information**

75 **(https://pubs.acs.org/doi/suppl/10.1021/acs.jchemed.9b00033/suppl_file/ed9b00033_si_001.zip) of Peng and Jimenez (2019). The different KinSim chemical mechanisms used for the box model are available in the supplement of this paper, and also at <https://tinyurl.com/kinsim-cases>. They can be directly loaded into KinSim to reproduce the calculations in this work by using “Load_Case” function (see detailed usage on <http://tinyurl.com/kinsim-help>). GEOS-Chem v11-02-rc and meteorological data can be downloaded from GEOS-Chem wiki (http://wiki.seas.harvard.edu/geos-chem/index.php/Downloading_GEOS-Chem_source_code_and_data). GEOS-Chem code modifications for new parameterizations and global model data are available upon email request (duseong.jo@colorado.edu).”**

85

Anonymous Referee #1

R1.0) This manuscript proposed three parameterization methods to reduce the computational cost of simulating Isoprene-derived SOA in GEOS-Chem using the full chemistry model. The parameterization methods were also compared with the volatility-basis-set and fixed yield methods. The results show that the parameterization methods, especially the third one (PAR3), could generally predict the isoprene-derived SOA spatially while reducing the computational cost of using a full chemistry model. The manuscript also suggests that the VBS approach is not accurate in predicting isoprene-derived SOA because the reactive uptake process is the main process for isoprene-derived SOA formation.

The manuscript has clear logic and it provides a useful and efficient parameterization method to calculate isoprene-derived SOA in global models such as GEOS-Chem. The quality of the manuscript is good and the main argument is valid, thus the manuscript is worth being published in Geoscientific Model Development. My main comments are that it occurred in a few places of the manuscript that the assumptions of the model or the detailed processes are not fully clear. I suggest the authors make appropriate changes to the manuscript in the following sections.

R1.1) Line 80: the author states that Pye et al. 2010 used VBS method to predict isoprene derived SOA from first-generation products through partitioning. However, in Pye et al. 2013, the reactive uptake aqueous pathway was already incorporated to the VBS method in predicting the isoprene-derived SOA. The new VBS results have been improved and are consistent with field measurements. The author should at least incorporate the latest model improvement approach by Pye et al. in the manuscript when discussing the VBS method. With the latest method incorporating 2-methyltetrol and 2-methylglyceric acid, it is inaccurate to state that “the default VBS mechanism underestimated the observed isoprene SOA formation by a factor of 3 over the southeast US in summer”.

Pye et al. (2013) updated the CMAQ model to simulate IEPOX reactive uptake in addition to the Odum 2-product SOA model used as default in CMAQ. This work is analogous to the work by Marais et al. (2016), who added the explicit IEPOX reactive uptake pathway in addition to the VBS in GEOS-Chem model. We think these works are unrelated with improving the 2-product or VBS scheme, because they added new gas-phase chemistry to simulate IEPOX and SOA formation and particle-phase reaction processes are not simulated within 2-product or VBS framework.

We understand that the current VBS scheme in GEOS-Chem may not include all the recent findings on SOA formation – wall-corrected yields, volatility-dependent Henry’s law constant, photolysis removal, etc. However, the main purpose of this paper is developing a new SOA parameterization and comparing it with current default parameterization options in GEOS-Chem. We have added the following text to Sect. 2.3 to avoid potential reader confusion as follows.

“We note that there are multiple VBS schemes available in the literature, and their details can vary (e.g., the number of bins, yields, chemical aging, NO_x dependence, photolysis, etc.). In this study we focused on evaluating the current default isoprene VBS scheme in GEOS-Chem.”

R1.2) Line 130-135. The author states that the net effect of the coating effect is to increase the reaction rate of IEPOX with organic coated aerosols. However, both Gaston et al. 2015 and Zhang et al. 2018 show that the uptake coefficient is highly dependent on the diffusion

135 coefficient of IEPOX in the organic layer, the Henry's law of the IEPOX into the organic layer, etc. With different parameters, the resistor model can give drastically different results. The author should explicitly specify what the equations and values were used to calculate the uptake coefficient in Figure S1. Also, why would the uptake coefficient increase at higher organic loading in Figure S1? As shown in Anttila et al., 2006, Gaston et al. 2015, and Zhang et al. 2018, the resistor model will generate monotonically decreasing reactive uptake values as the coating thickness increases.

140 We agree that the resistor model results can be substantially changed with different numerical values of the parameters. We added a supplementary section to provide the detailed information for the resistor model equation and parameters (Section 1 in the supplementary information).

“1 IEPOX reactive uptake coefficient calculation

145 We use the resistor model equation by Gaston et al. (2014b) to calculate the reactive uptake coefficient of IEPOX (γ). The equation is as follows:

$$\frac{1}{\gamma} = \frac{\omega R_p}{4D_{gas}} + \frac{1}{\alpha} + \frac{\omega R_p}{4RTH_{org}D_{org}(q_{org}F - 1)} \quad (S1a)$$

$$F = \frac{\coth(q_{org}) + h(q_{aq}, q_{org}^*)}{1 + \coth(q_{org})h(q_{aq}, q_{org}^*)} \quad (S1b)$$

$$h(q_{aq}, q_{org}^*) = -\tanh(q_{org}^*) \frac{\frac{H_{aq}D_{aq}}{H_{org}D_{org}}(q_{aq} \coth(q_{aq}) - 1) - (q_{org}^* \coth(q_{org}^*) - 1)}{\frac{H_{aq}D_{aq}}{H_{org}D_{org}}(q_{aq} \coth(q_{aq}) - 1) - (q_{org}^* \tanh(q_{org}^*) - 1)} \quad (S1c)$$

150
$$q_{org} = R_p \sqrt{\frac{k_{org}}{D_{org}}}, \quad q_{aq} = R_c \sqrt{\frac{k_{aq}}{D_{aq}}}, \quad q_{org}^* = \frac{R_c}{R_p} q_{org} \quad (S1d)$$

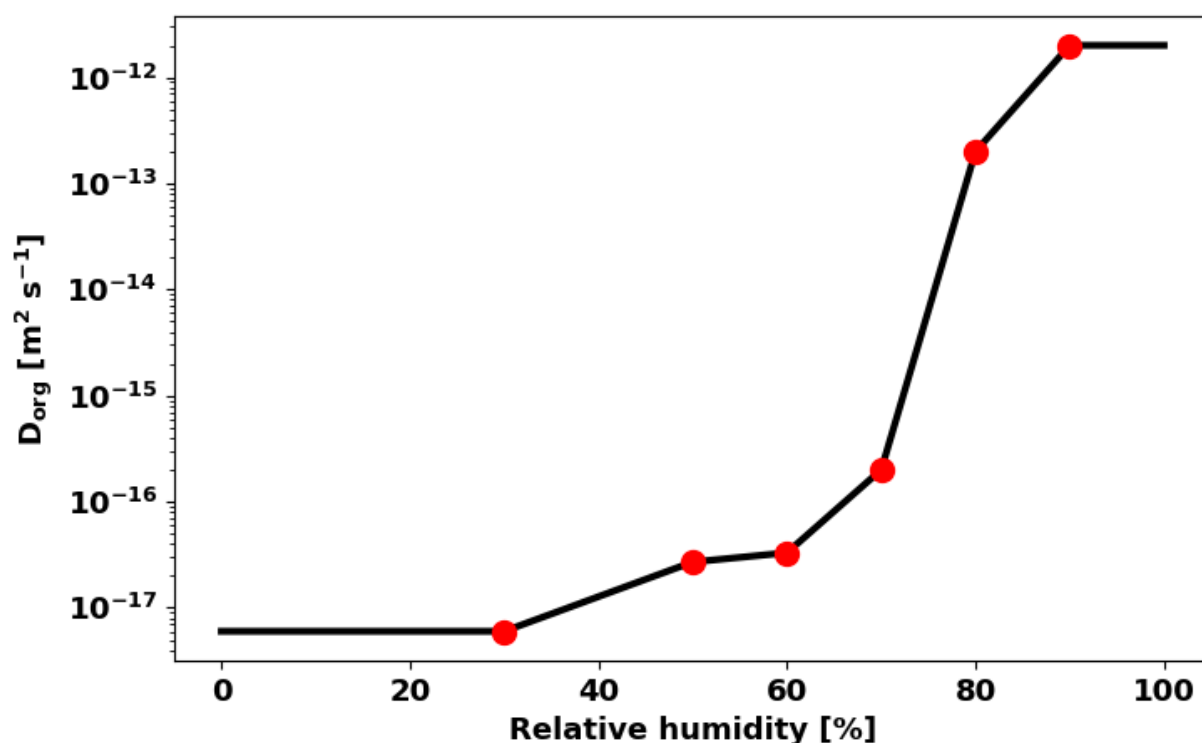
155 where ω is the mean molecular speed of IEPOX ($m s^{-1}$), R_p is the particle radius (m), D_{gas} is the gas-phase diffusion coefficient of IEPOX ($10^{-5} m^2 s^{-1}$), α is the mass accommodation coefficient (0.1), R is the universal gas constant ($8.2057 \times 10^{-2} L atm mol^{-1} K^{-1}$), T is temperature (K), H_{aq} and H_{org} are Henry's law coefficients in the aqueous core ($1.7 \times 10^7 M atm^{-1}$) and in the organic layer ($2 \times 10^6 M atm^{-1}$), D_{aq} and D_{org} are diffusion coefficients of IEPOX in the aqueous core ($10^{-9} m^2 s^{-1}$) and in the organic layer (discussed below), and R_c is the inorganic aqueous core radius (m). k_{aq} is the first-order reaction rate constant in the aqueous phase (s^{-1}), calculated as follows:

$$k_{aq} = (k_{H^+}[H^+]) + (k_{nuc}[nuc]a_{H^+}) + k_{ga}[ga] \quad (S2)$$

160 where k_{H^+} is the reaction rate constant due to acid-catalyzed ring-opening ($0.036 M^{-1} s^{-1}$), $[H^+]$ is the proton concentration (M), a_{H^+} is the proton activity, k_{nuc} is the reaction rate constant due to the presence of specific nucleophiles (sulfate and nitrate) ($2 \times 10^{-4} M^{-1} s^{-1}$), $[nuc]$ is the concentration of nucleophiles (M), k_{ga} is the reaction rate constant due to the presence of general acids (bisulfate) ($7.3 \times 10^{-4} M^{-1} s^{-1}$), and $[ga]$ is the concentration of

165 general acids (M). We assumed the reaction rate coefficient of IEPOX in the organic layer
(k_{org}) is the same as k_{aq} . We note that the equation above is different from the IEPOX
reactive uptake equation used by Zhang et al. (2018), which is based on Gaston et al.
(2014a). The equation from Gaston et al. (2014a) can be derived from the Taylor series
170 approximation by assuming thin coatings (Anttila et al., 2006). Therefore, we used the
equation S1 to avoid some possible errors from the cases that second or higher order
Taylor terms become important.

The diffusion coefficient of IEPOX in the organic layer (D_{org}) substantially changes by
several orders of magnitude over a range of relative humidity (RH) in the atmosphere.
Based on Table S3 of Zhang et al. (2018), we considered the RH dependence for D_{org} values.
175 Table S1 show D_{org} values we used for GEOS-Chem calculation.



180 **Figure S1. The diffusion coefficient of IEPOX in the organic layer (D_{org}) as a function of RH. Red points indicate values calculated by Zhang et al. (2018). Values in between red points are log-linearly interpolated, and values below 30% RH or above 90% are set to be the constant values.”**

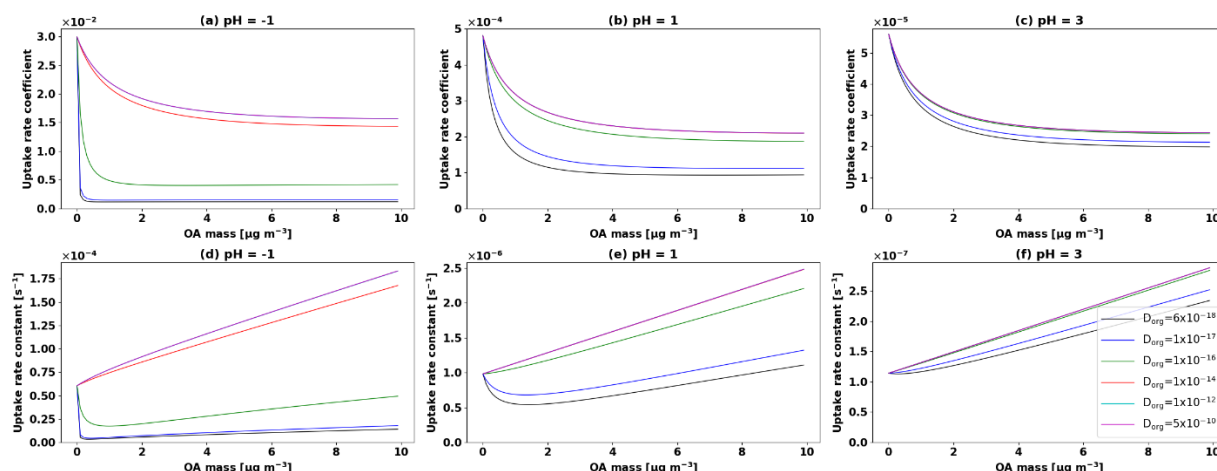
For the uptake coefficient at higher organic loadings, we found an error in our calculation code. It was OK for lower organic loadings, but the bug erroneously increased the uptake coefficient by 30% at higher organic loading conditions. We corrected this error for all the new GEOS-Chem runs shown in the revised paper. New results are shown in Figs. S2 and S3 with the updated main text.
185

“Standard GEOS-Chem assumes no organic coating; only the surface area of inorganic aerosols. We updated the model to include suppression of IEPOX reactive uptake by the

190 organic coating, and to use the available surface area of the total sulfate-ammonium-nitrate-organic aerosols mixture at a given relative humidity with hygroscopic growth factors. We found that the IEPOX reactive uptake coefficient (γ) was always decreased at atmospheric relevant aerosol pH and relative humidity conditions, but the IEPOX reactive uptake rate constant increased in some conditions (high pH and high IEPOX diffusion coefficient in the organic layer, Fig. S2). We note that this is the case for GEOS-Chem v11-02-rc, because GEOS-Chem does not take into account organic aerosol mass for aerosol radius and aerosol surface area calculation when it calculates IEPOX reactive uptake. Therefore, additional OA mass considered in this study increases available aerosol surface area for IEPOX reactive uptake, which compensates or sometimes overcomes the effects by the decrease of γ as shown in Eq. (1) for the first-order uptake rate constant of IEPOX to form IEPOX-SOA:

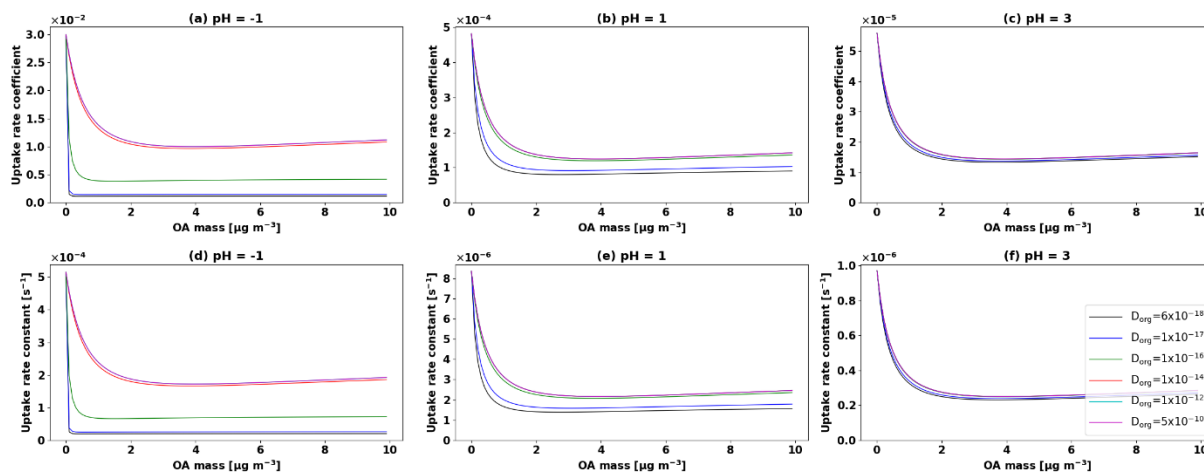
$$200 \quad \text{IEPOX uptake rate constant} = \frac{S_a}{\frac{r_a}{D_g} + \frac{4}{\gamma \times v_{mms}}} \quad (1)$$

S_a is the wet aerosol surface area on which IEPOX can be taken up ($\text{m}^2 \text{m}^{-3}$), r_a is the wet aerosol radius (m), D_g is gas-phase diffusion coefficient of IEPOX ($\text{m}^2 \text{s}^{-1}$), and v_{mms} is the mean molecular speed (m s^{-1}) of gas-phase IEPOX. Again, the effects of organic coating on IEPOX uptake rate constant in this study can be different from previous observational studies (Hu et al., 2016; Zhang et al., 2018), because observational studies used the measured and fixed available aerosol surface area and radius, and they changed organic aerosol layer thickness for their calculations (i.e. inorganic core radius was changed but total particle radius and surface area were not changed). When we assumed the fixed aerosol radius and aerosol surface area, and only organic coating thickness increased as OA mass increased, all the case showed the decreasing IEPOX reactive uptake rate constants (Fig. S3).”



215 **Figure S2. IEPOX reactive uptake coefficient (a,b,c) and uptake rate constant (d,e,f) as a function of OA mass concentrations. Different colors indicate D_{org} values ranging from 6×10^{-18} to $1 \times 10^{-12} \text{ m}^2 \text{ s}^{-1}$. Aerosol pH values were set to be -1 (a,d), 1 (b,e), and 3 (c,f),**

220 respectively. Sulfate aerosol mass concentration was assumed as $10 \mu\text{g m}^{-3}$. Densities of sulfate and organic aerosols were set to be 1.7 and 1.3 g cm^{-3} , respectively, based on densities used by GEOS-Chem v11-02-rc. Initial aerosol radius of 50 nm and aerosol surface area of $3 \times 10^{-6} \text{ cm}^2 \text{ cm}^{-3}$ were assumed for organic aerosol mass = $0 \mu\text{g m}^{-3}$. The changes of aerosol radius and aerosol surface area were calculated as OA mass increases, and aerosol inorganic core radius was fixed as 50 nm .



225 **Figure S3. IEPOX reactive uptake coefficient (a,b,c) and uptake rate constant (d,e,f) as a function of OA mass concentrations. Different colors indicate D_{org} values ranging from 6×10^{-18} to $1 \times 10^{-12} \text{ m}^2 \text{ s}^{-1}$. Aerosol pH values were set to be -1 (a,d), 1 (b,e), and 3 (c,f), respectively. Sulfate aerosol mass concentration was assumed as $1 \mu\text{g m}^{-3}$. Densities of sulfate and organic aerosols were set to be 1.7 and 1.3 g cm^{-3} , respectively, based on densities used by GEOS-Chem v11-02-rc. Initial aerosol radius of 50 nm and aerosol surface area of $3 \times 10^{-6} \text{ cm}^2 \text{ cm}^{-3}$ were assumed for organic aerosol mass = $0 \mu\text{g m}^{-3}$. The changes of aerosol radius and aerosol surface area were fixed regardless of OA mass increase. Aerosol core radius was reduced in proportion to the OA mass increase (i.e. coating thickness increase).**

230 We re-ran GEOS-Chem model to include effects of RH on D_{org} . In addition, soil NO_x emissions were erroneously set as zero for the runs shown in the GMDD paper. We also corrected this error. As a result, Figures 1, 3, 4, 5, and 6 were updated, but conclusions remained the same (PAR2 and PAR3 again showed the best performance). We have updated all the figures and numbers in the main text.

(Backlinks to [R1.10](#), [R2.1](#) and [R2.2](#))

240 R1.3) Line 140. I understand that the author is intended to cross compare parameterizations against the full chemistry model for isoprene formation, however it is inaccurate and a bit misleading to state that “Updating the parameterizations developed here with more accurate values of H or determined in future literature studies would be trivial.” The H or values affect the absolute values of the isoprene-derived SOA significantly, and currently the estimation of the Heryny’s law constant can vary by two orders of magnitudes. Knowing an accurate value of the Heryny’s law constant will help bridge the gap between the model and the field measurement, thus these values are not trivial. I suggest the author revise this sentence.

250 We wanted to deliver the message that our parameterizations do not require any complex refitting processes even if parameters are updated from the future study. I.e. *updating the parameterization with more accurate literature values of H* is trivial, even if *determining accurate values of H* is far from trivial. To avoid possibly misleading the readers with this sentence, we have added the following text:

255 **“Parameters used in this study such as the Henry’s law constant and the IEPOX diffusion coefficient in OA can be easily updated in future studies. Our parameterizations are flexible to the change of these variables, because they use the IEPOX reactive uptake rate (k_{18} in Eqs. (7) and (14) in Sect. 3) rather than using individual input parameters. Therefore, updating the parameterizations developed here with more accurate values of input parameters determined in future literature studies is easy without having to refit the parameterizations.”**

(Backlink to [R2.3](#))

260 R1.4) Please remove the Nault et al. in prep. citation as unpublished work should not appear in the formal citation.

We changed this citation to that of the the AGU conference abstract:

265 **“Effects of sea salt on pH and detailed analysis against the aircraft measurements were discussed in detail by Nault et al. (2018).”**

270 **Nault, B. A., Campuzano-Jost, P., Douglas Day, Hu, W., Palm, B., Schroder, J. C., Bahreini, R., Bian, H., Chin, M., Clegg, S. L., Colarco, P. R., Crouse, J. D., Dibb, J. E., Kim, M. J., Kodros, J., Lopez-Hilfiker, F., Marais, E. A., Middlebrook, A. M., Neuman, J. A., Nowak, J. B., Pierce, J. R., Scheuer, E. M., Thornton, J. A., Veres, P. R., Wennberg, P. O. and Jimenez, J. L.: Global Survey of Submicron Aerosol Acidity (pH), Abstract A53A-06 presented at American Geophysical Union Fall Meeting 2018, 10-14, December, Washington, D.C., 2018.**

275 R1.5) Line 227-230: The author states a numerical fitting method was used to calculate $f(\text{ISOPO}_2\text{-ISOPOOH})$. Which numerical fitting method was selected and why? How good is the fitting result? Please include some details of this fitting in the manuscript.

We attempted various functional forms, independent variables, and initial guesses to get the best results compared to the box model results. We added the following explanation to the main text:

280 **“We tried different functional forms for the equation (polynomial, Gaussian, Lorentzian, exponential, double-exponential, trigonometric, Hill, Sigmoid, etc.), independent variables, and initial guesses for the coefficients. We found that the Hill type equation combined with the production term of ISOPO_2 in exponential form showed the best results compared to the box model calculation.”**

285 The fitting results were very accurate as shown in Figs. 2a and S5a. Because the other parts can be analytically calculated for IEPOX-SOA yield, the fitting for ISOPO_2 self-reaction is the only factor causing the uncertainty of our parameterizations.

(Backlinks to [R1.6](#) and [R1.7](#))

290 R1.6) What is the physical meaning or the rationale of constructing Equation 5c in the current format? Please note that this is a rather complicated fitting equation and I wonder how did the author obtain such format? Why cannot the equation be expressed in other ways? Could the author include the rationale behind constructing this equation in the text, please?

See response to comment [R1.5](#).

295 R1.7) Similar question as the previous one: what are the physical meanings of F? Why is it constructed in such a way? Maybe the author can explain more in the manuscript.

We added the following text to explain the physical meaning of F. The functional form was derived from trial and error as per [R1.5](#).

300 **“We designed the term F to consider contributions of high and low NO_x pathways to the formation timescale in the single equation system. ISOPO₂ + NO pathway is dominant when F = 0 and ISOPO₂ + HO₂ pathway is dominant when F = 1. F cannot be below 0 or above 1 in terms of the physical meaning, but the fitted F can have values outside of 0 to 1 because the numerical fitting works to minimize the total error compared to the box model calculated timescale of IEPOX-SOA”**

305 R1.8) In Figure 2, the e-fold formation timescale from the analytical model was plotted against the full box model. However, unlike the analytical model that has a definition and equation for the formation timescale, there is no definition of the formation timescale in the full box model. How did the author calculate the formation timescale in the full box model? Please specify.

310 We added the text describing the detailed calculation process of the formation timescale from the box model to the caption of Fig. 2:

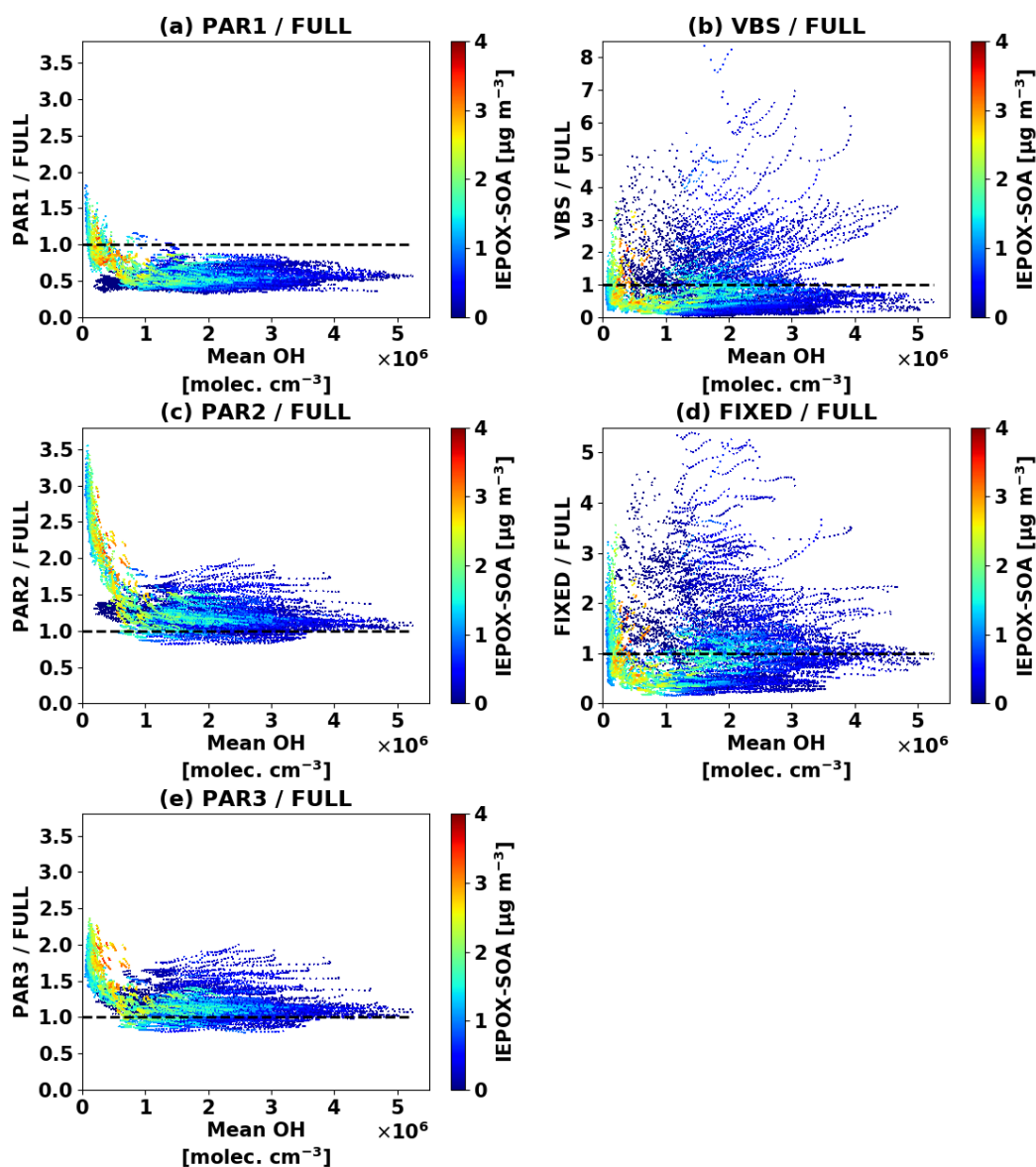
315 **“Formation timescale of the full mechanism box model was calculated as follows. We saved IEPOX concentrations for each timestep. We defined the formation timescale as the time when the IEPOX concentration is closest to the 1 - 1/e (~63%) of the final IEPOX concentration.”**

R1.9) It seems that PAR3 can capture most of the isoprene-derived SOA values when compared with the full chemistry model. However, at isoprene rich areas such as Amazon forest, central Africa and Southeast Asia, the isoprene-derived SOA was overpredicted by PAR3. Are there any reactions causing such overprediction in isoprene-rich areas? It seems to be some sort of systematical error. The author should discuss the drawbacks of PAR3 (such as overprediction in isoprene-rich areas) so as to objectively evaluate the model and educate potential users.

325 We figured out that our parameterizations generally overestimate the IEPOX-SOA when OH concentrations are low (newly added Fig. S9), and OH concentrations are low in Amazon, central Africa, and Southeast Asia regions (Fig. S10). We added the following text with two additional supplemental figures (Figs. S9 and S10) to document these points:

330 **“Contrary to PAR1, which calculated IEPOX-SOA yield at the time of isoprene emission, PAR2 and PAR3 did not show a global underestimation because they only calculated IEPOX yield at the time of isoprene emission, and then simulated the IEPOX reactive uptake explicitly. However, they showed slight overestimations over isoprene source regions such as the Amazon. We found that PAR2 and PAR3 generally overestimate the IEPOX-**

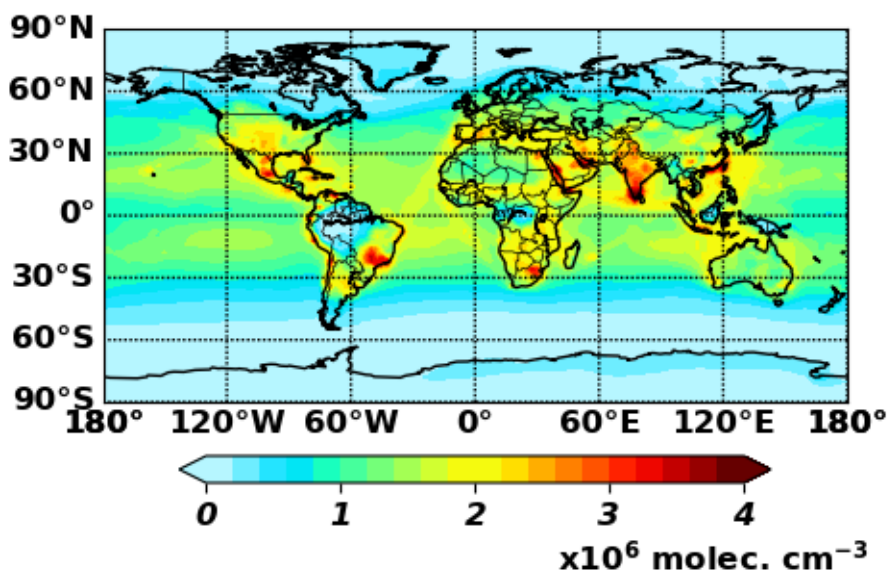
SOA when OH concentrations are low (Fig. S9), and the Amazon is one of low OH regions from GEOS-Chem model (Fig. S10). We attributed this tendency to the effects of lifetime of IEPOX precursor gases, for which OH concentrations are one of the major controlling factors. IEPOX yields in PAR2 and PAR3 are calculated using the instantaneous chemical fields. Therefore, the discrepancies between the explicit chemistry and PAR2-3 are reduced when the lifetimes of precursor gases are short. For the southeastern US where PAR3 did not show an overestimation, the lifetimes of isoprene and ISOPOOH were 0.9 hours and 1.5 hours, respectively. The discrepancies are much larger for the Amazon, the lifetimes of isoprene and ISOPOOH are 12.3 hours and 6.1 hours, respectively, due to low OH concentrations. As a result, the PAR1-3 calculated the similar IEPOX production rate (1.9 Tg yr^{-1}) from the ISOPOOH + OH reaction compared to the full chemistry (1.8 Tg yr^{-1}) for the southeastern US, but the disagreement was larger for the Amazon (4.8 Tg yr^{-1} in the PAR1-3 vs 3.9 Tg yr^{-1} in the full chemistry). We anticipate that the discrepancy in source regions will be reduced in the future version of GEOS-Chem, because GEOS-Chem with the most up to date isoprene mechanism predicts higher OH concentrations (up to 250% increase) in Amazon, central Africa, and Borneo regions compared to the isoprene mechanism used in this study (Fig. S17 in Bates and Jacob, 2019).”



350

Figure S9. Scatterplots of the IEPOX-SOA concentration ratio (five parameterizations against the explicit full chemistry) vs. OH concentration within the PBL. Each point represents the monthly averaged model grid value for four major isoprene source regions [the Southeastern United States: 30°N – 40°N, 100°W – 80°W, Amazon: 10°S – 0°S, 70°W – 60°W, Central Africa: 5°N – 15°N, 10°E – 30°E, Borneo: 5°S – 5°N, 105°E – 120°E]. Colors indicate the IEPOX-SOA concentration simulated by the full chemistry.

355



360

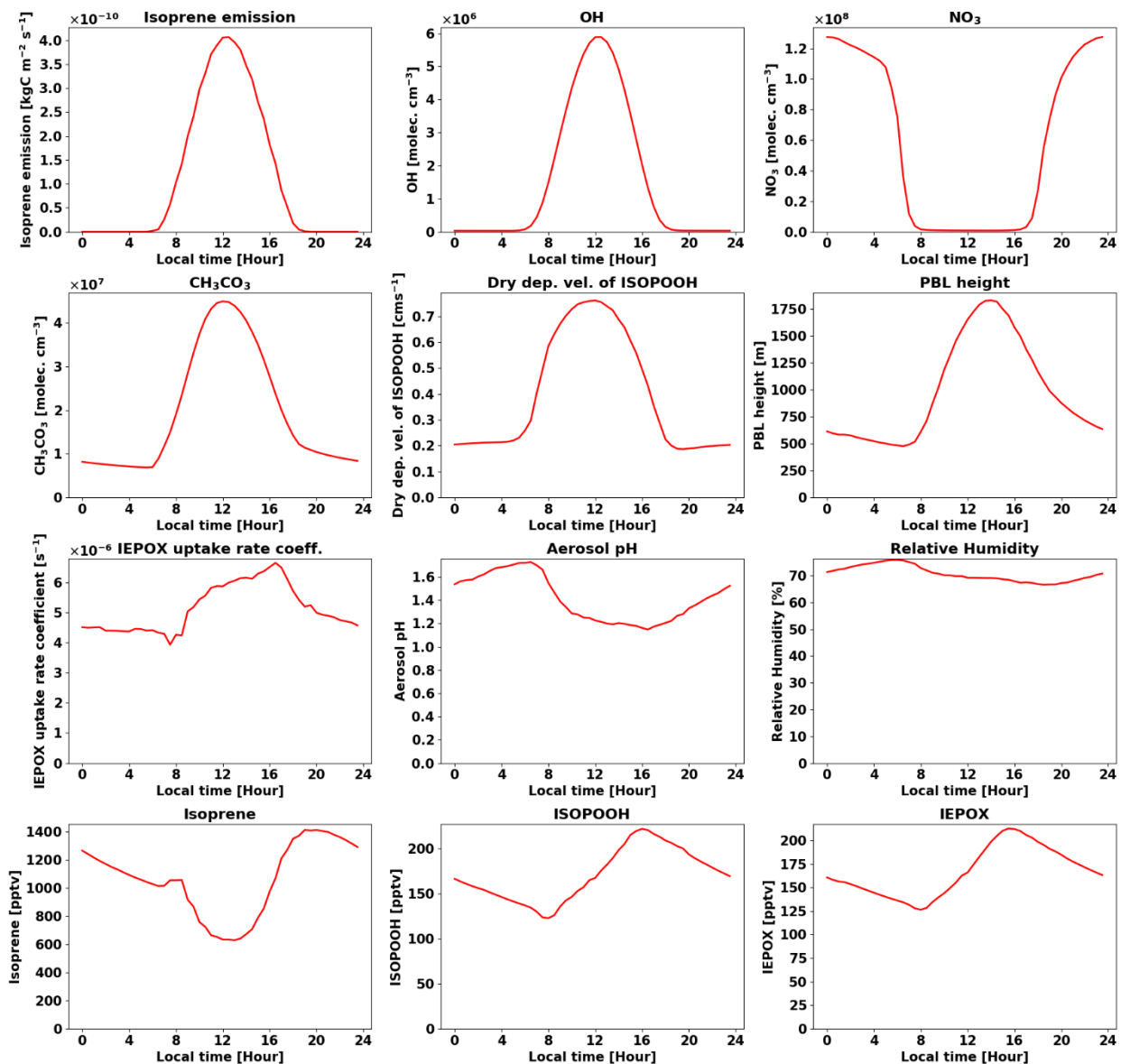
Figure S10. Global annual mean OH concentrations for July 2013 – June 2014 as predicted by the GEOS-Chem v11-02-rc used in this study.

(Backlink to [R2.4](#))

365 R1.10) Why would the IEPOX uptake rate peak at around 6 pm? It seems that the only variable in the IEPOX uptake rate (Equation 7) is $[\text{OH}] \cdot k_{17}$, which is affected by temperature and the OH contraction. However, the product of these two values should not cause the IEPOX uptake rate to peak at 6 pm. Could the author explain why the IEPOX uptake rate peak at around 6 pm?

370 First of all, the IEPOX uptake rate peak changed after we re-ran the model with the updated diffusion coefficient of IEPOX in OA, which changed the organic coating effect (see response to comment [R1.2](#)). IEPOX uptake rate peaks at around 4 p.m., which is used by both the full chemistry and parameterizations. There are many variables affecting the IEPOX uptake rate constant (k_{18}) – aerosol pH, aerosol surface area, temperature, organic coating thickness, etc. $[\text{OH}] \cdot k_{17}$ does not directly affect the IEPOX uptake rate, although it is an important reaction impacting the IEPOX concentration. We found that the diurnal variation of the IEPOX uptake rate constant generally followed aerosol pH variations, which in turn was affected by aerosol water due to relative humidity changes. Aerosol pH was low around at 4 p.m. because H^+ aerosol concentration increased due to low aerosol water content. R^2 between aerosol pH and aerosol water was 0.85. We added the diurnal variation of aerosol pH to Fig. S8.

380



385 **Figure S8. Diurnal variations of chemical/meteorological fields used in box model**
calculation (Fig. 5d). Values were extracted from GEOS-Chem global mean results for four
major isoprene source regions [the Southeastern United States: 30°N – 40°N, 100°W –
80°W, Amazon: 10°S – 0°S, 70°W – 60°W, Central Africa: 5°N – 15°N, 10°E – 30°E, Borneo:
5°S – 5°N, 105°E – 120°E]. Figures represent approximate annual mean diurnal variation
profiles, which were calculated by using the first two days of each month model outputs
at 30 minutes interval averaged within the PBL, averaging points of the same local time.
 390

395 Minor Comments:

R1.11) Please refrain using the word "it" in Line 269 as it makes the sentence confusing. I suggest the author change this part of the sentence to "because of Equation 9 assumes rapid formation of the SOA."

We removed "it" and rephrase the sentence as follows:

400 **"As a result, if the yield from Eq. (9) is used for making IEPOX-SOA, chemical transport models would likely overestimate IEPOX-SOA concentrations locally in isoprene-emitting areas due to the instantaneous formation of IEPOX-SOA from Eq. (9)."**

405 R1.12) The author listed the scatter and correlation plots of PAR1 and PAR3 versus the full mechanism box model in Figure S3 and Figure 2. For consistency I suggest include a similar plot for PAR2 in the SI as well.

PAR2 and PAR3 have the same yield of IEPOX from isoprene (Y_{IEPOX}). PAR3 was developed on top of PAR2 by introducing an intermediate species (SOAP_i). Therefore, Figure 2a covers both PAR2 and PAR3 (Figure 2b is only for PAR3 since PAR2 is not using the formation timescale).

410 We clarified this in the caption of Fig. 2 as follows:

"Scatterplots of the results of parameterizations (y-axis) versus the full mechanism (x-axis) box model results for (a) IEPOX molar yield (PAR2 and PAR3) and (b) formation timescale (PAR3)."

415 R1.13) The phrase "IEPOX condensation rates" in line 391-line 395 should be changed to "IEPOX reactive uptake rates".

We have updated this text as follows:

420 **"For example, the instantaneous IEPOX-SOA yield using both isoprene emission and IEPOX reactive uptake rate constant at noon is lower than the yield calculated using the isoprene emission rate at 12 p.m. and the IEPOX reactive uptake rate constant at 6 p.m, when each process peaks, explaining most of the underestimation in PAR1. Contrary to PAR1, which calculated IEPOX-SOA yield at the time of isoprene emission, PAR2 and PAR3 did not show a global underestimation because they only calculated IEPOX yield at the time of isoprene emission, and then simulated the IEPOX reactive uptake explicitly."**

425

430

Anonymous Referee #2

R2.0) General Comments

435 The manuscript presents a simplified parameterization of isoprene-epoxydiols (IEPOX) derived
secondary organic aerosol (SOA) that exhibits both computational economy and reproducibility
of the explicit or full chemistry (Marais et al., 2016) in simulating IEPOX SOA in global chemistry
and climate models. The new parameterization was developed based on an approximate
analytical fitting in a box model to reproduce the formation yield and time scale of gas-phase
440 intermediates and SOA from isoprene represented by the full chemistry. Three variations of the
simplified parameterization were discussed and evaluated along with fixed yield and VBS
against full chemistry in GEOS-Chem v11-02-rc for IEPOX SOA simulations. Simulations by two
out of the three new parameterizations generally captured the tropospheric burden of IEPOX-
SOA and spatio-temporal profiles of those simulated by the full chemistry while fixed yields and
445 VBS failed to do so. At the same time, the simplified parameterizations were at least 5 times
faster than the full chemistry. The study also highlighted the importance of diurnal variation of
chemical/meteorological fields to different parameterizations under comparison in the study. As
a result, PAR3, the closest to the full chemistry in structure, resembled the full chemistry the
best in terms of the response to the diurnal variation of chemical/meteorological fields.

450 The manuscript is written well and easy to follow. The new parameterization was concluded to
be a good alternative to the full chemical mechanism for accurate and fast simulations of
IEPOX-SOA in climate model applications. The method used to develop the parameterizations
is very repeatable in simplifying other SOA mechanisms and updatable with continuing advance
in isoprene SOA mechanisms. Below are several major and minor comments, which need to be
455 addressed and clarified:

Specific Comments Major

R2.1) Organic coating effects were considered as mentioned in Section 2.2 and results were
plotted as Figure S1. First of all, the equations and parameters used in the implementation of
organic coating effects were not described. Was the resistor representation of uptake coefficient
460 by Gaston et al., (2014) used here? What were the values of the parameters used then? Was
the dependency on the types of organic matters generated in simulations considered? These
need to be clarified. Second, the goal of the paper is to improve computational efficiency while
retaining the ability to predict ground level IEPOX-SOA relative to the full chemistry. However,
the inclusion of organic coating is intended to be realistic, which seems to be beyond the scope.
465 From my understanding, the coating effect was only implemented in the full chemistry where
was modeled explicitly. In other words, the coating effect is now getting “fitted” into the new
parametrization intrinsically as well as the uncertainties going along with it. Please clarify
whether this is the case or not. If it is, the uncertainties must be discussed. In addition, my worry
is that this would make the future efforts to differentiate the inhibiting effects induced by different
470 SOA types under varying environmental conditions hard to implement without fitting a new set of
parameters for each type of organic coating. One should expect that variables like organic
types, thickness of the coating, and relative humidity would change the effect of organic coating
on reactive uptake.

475 We used the resistor model equation by Gaston et al. (2014) in ACP to calculate IEPOX
reactive uptake coefficient. We added a supplementary section to describe the detailed
procedure and parameters for the resistor model (See the response to the comment [R1.2](#) for
details). We did not take into account the changes of IEPOX diffusivity in the organic layer by

480 different SOA types, although this could be easily done in future work by updating the numerical value of that parameter in different regions / times in the model as needed. The diffusivity as a function of relative humidity was newly considered in the revised text (See the response to the comment [R1.2](#)). As a result, Figures 1, 3, 4, and 5 were changed, but conclusions remained the same (PAR2 and PAR3 again showed the best performance). We updated figures and numbers in the main text.

485 The coating effect was implemented not only in the full chemistry but in the parameterizations. Our parameterizations explicitly calculate IEPOX reactive uptake coefficient and rate as does the full chemistry, which avoids having to refit the parameterizations when updated individual parameters become available (e.g. Henry's law constant, diffusivity). As a result, future works making IEPOX reactive uptake rate change can be explicitly reflected in our parameterizations. We clarified this in the main text as follows:

490 **“Parameters used in this study such as the Henry’s law constant and IEPOX diffusion coefficient in OA can be updated in future studies, as new information becomes available in the literature. Our parameterizations are flexible to the change of these variables, because they use the IEPOX reactive uptake rate constant (k_{18} in Eqs. (7) and (14) in Sect. 3) rather than using individual input parameters. Therefore, updating the parameterizations developed here with more accurate values of input parameters determined in future literature studies can be done without refitting.”**
495

R2.2) Line134-136: overestimation compared to the measurements? The organic coating effect is strongly influenced by the composition of the coating and ambient relative humidity, changing the diffusion coefficient of IEPOX in the coating layer. Therefore, not just the Henry’s law constant and the mass accommodation coefficient but the parameterization for organic coating (e.g., diffusion coefficient of IEPOX in the coating layer) could also affect the apparent uptake rate (or heterogenous reaction rate in some literature). It seems that the coating parameterization implemented in this work was not strong enough to counteract the increase in surface as shown by Figure S1, which contradicts with Zhang et al., 2018. Authors should address this or explain why the result is contradictory to the literature. Again, authors should provide the detailed description of the parameterization of the coating effect, and discuss its limitations and uncertainties.
500
505

We examined factors making our calculation deviate from the Figure 1 in Zhang et al. (2018). We found two major differences between our work and Zhang et al.’s work. First one is the diffusivity of IEPOX in the organic layer (D_{org}). We used a D_{org} value of $5 \times 10^{-10} \text{ m}^2 \text{ s}^{-1}$ (Gaston et al., 2014a) in the GMDD version of this paper, while Zhang et al. (2018) used lower D_{org} values (6×10^{-18} and $2.7 \times 10^{-17} \text{ m}^2 \text{ s}^{-1}$ at 30% and 50% RH, respectively). As shown in Fig. S2, D_{org} value of $5 \times 10^{-10} \text{ m}^2 \text{ s}^{-1}$ makes the IEPOX reactive uptake rate increase in all conditions (d,e,f in Fig. S2), but the IEPOX reactive uptake rate decreases in acidic conditions with lower D_{org} values.
510
515

Second, we calculated the case that additional OA mass coated on the surface of inorganic aerosol, which increased the aerosol radius and aerosol surface area (i.e. R_c was fixed, but R_p and S_a were increased.). We calculated the organic coating effects in this way for GEOS-Chem, because the GEOS-Chem standard version only uses inorganic aerosol radius and surface area to calculate IEPOX reactive uptake. However, Zhang et al. (2018) fixed the aerosol radius and surface area, and examined the effects of organic coating thickness on the IEPOX reactive uptake (i.e. R_p and S_a were fixed, but R_c was decreased as organic coating increased). We
520

525 clarified this point in the main text, and we added a Fig. S3 to show IEPOX reactive uptake rate change for the case that R_p and S_a were fixed (similar to the case by Zhang et al., 2018).

See our response to the comment [R1.2](#) for details.

530 R2.3) Line 140: I found the statement here problematic. Literature effective Henry's law constant for IEPOX spans three orders of magnitude (Gaston et al., 2014; Nguyen et al., 2014; Pye et al., 2013; Sareen et al., 2017), the effect of which on uptake coefficient might not be trivial as stated here. Pye et al., 2013 tested the sensitivity of predicted IEPOX SOA to the Henry's law constant. With an increase in the Henry's law constant by a factor of 7, the predicted IEPOX SOA increased by a factor of 5. This scalability indicates that future update on the Henry's law constant may require a full re-evaluation of the parameterization. Besides, author should also
535 note that the Henry's law constant for IEPOX dissolution into the organic layer would be different from that into aqueous aerosol. Zhang et al., estimated the Henry's law constant for IEPOX into the alpha-pinene SOA coating to be $1-5 \times 10^6$ M/atm by fitting a resistor model using experimental data (Zhang et al., 2018). Authors should justify why Henry's law constant was not altered to accommodate the implementation of organic coating.

540 See our response to comment [R1.3](#).

We used Henry's law constant in the organic layer as 2×10^6 M atm⁻¹ based on Zhang et al. (2018). We clarified it in the supplement text.

545 R2.4) Figure 3: PAR2 and PAR3 overpredicted IEPOX SOA in source regions. Is this also a result of differing influence of the diurnal variation profiles of chemical fields compared to the full chemistry? Are there any other reasons? Although this paper focuses on evaluating the new parameterization against the full chemistry, the natural question to ask is does it improve the model performance against measurements? No indication was given in that sense. If the full chemistry model with the coating effect tends to overestimate IEPOX SOA vs. measurements in
550 the source regions, the new parametrizations would worsen the model performance. If the full chemistry underestimates IEPOX SOA, the overestimation of PAR2 and PAR3 offsets the underestimation to some extent and may improve the model performance. The phrase "more accurate" appears a few times in the manuscript including in the conclusion. It should be more carefully used otherwise misleading.

555 The parameterizations developed in this study were designed to reproduce results by the full explicit chemistry. The full chemistry has been evaluated against measurements in prior publications (e.g. Marais et al., 2016). Currently, there are many uncertain parameters substantially affecting the concentrations of IEPOX-SOA (e.g. Henry's law constant and IEPOX diffusivity in OA). We believe that the explicit full chemistry will be improved with future
560 laboratory, field, and modeling studies, and the parameterizations can be updated easily to capture those advances, as long as the structure of the full chemistry mechanism does not change. Therefore, we think addressing the performance against the measurements is beyond the scope of our study, because it involves consideration from various uncertain parameters.

See also the response to [R1.9](#).

565

Minor

R2.5) Figure 1: Which mechanism/parameterization was used to calculate the yields for each step in this figure? Please clarify.

570 We clarified it in the caption as follows. We changed Figure 1 because we re-ran the model to use RH-dependent D_{org} values from Zhang et al. (2018).

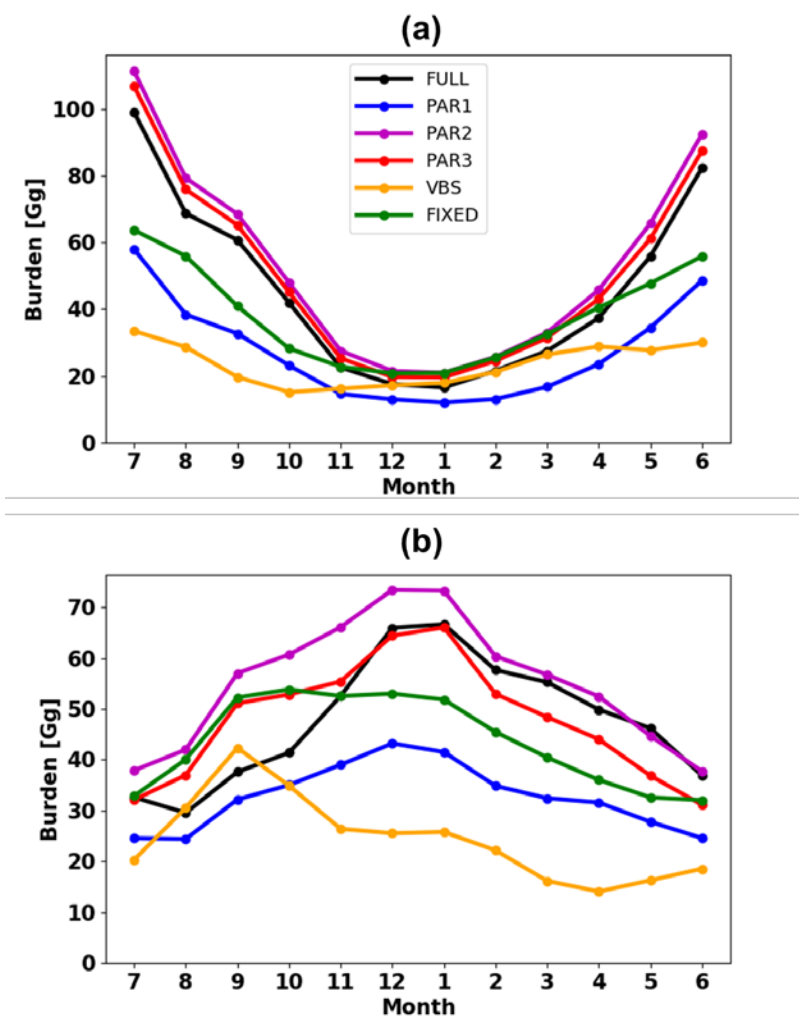
575 **“Figure 1. Schematic diagrams of IEPOX-SOA chemistry for (a) HO₂ and (b) NO dominant regions. Blue arrows indicate IEPOX-SOA formation pathways and red arrows represent other chemical pathways that do not form significant IEPOX-SOA. Values are averaged molar yields relative to the initial oxidation amount of isoprene from GEOS-Chem v11-02-rc results using the explicit full chemistry with updates in this study (see Sect. 2.2) over Borneo (as an example of HO₂ dominant conditions, 5°S – 5°N, 105°E – 120°E) and Beijing (as an example of NO dominant conditions, 35°N – 45°N, 110°E – 120°E) from July 2013 to June 2014. We note that Beijing is located in a region with typically low isoprene emissions, so the appreciable yield of IEPOX-SOA will still result in small ambient concentrations.”**

580

R2.6) Line 400 Figure 4C: Is there a seasonal pattern if the northern and southern hemisphere can be plotted separately?

585 We added a new figure (Fig. S12) to separate the seasonal patterns of the global burdens in both hemispheres. We confirmed that PAR2 and PAR3 again showed better results. We added the following text accordingly:

“It also applied to the seasonal patterns of the hemispheric burden when we separated them for the northern and southern hemispheres, as shown in Fig. S12.”



590 **Figure S12. Same as Fig. 4c but for (a) Northern and (b) Southern Hemisphere.**

R2.7) Technical Corrections: Figure 2(a): Was IEPOX-SOA molar yield or IEPOX yield plotted here? The caption didn't match with axis labels.

595 **We changed the figure caption to correct it.**

References

- Anttila, T., Kiendler-Scharr, A., Tillmann, R. and Mentel, T. F.: On the Reactive Uptake of Gaseous Compounds by Organic-Coated Aqueous Aerosols: Theoretical Analysis and Application to the Heterogeneous Hydrolysis of N₂O₅, *J. Phys. Chem. A*, 110, 10435–10443, doi:10.1021/jp062403c, 2006.
- Bates, K. H. and Jacob, D. J.: A new model mechanism for atmospheric oxidation of isoprene: global effects on oxidants, nitrogen oxides, organic products, and secondary organic aerosol, *Atmos. Chem. Phys. Discuss.*, 2019, 1–46, doi:10.5194/acp-2019-328, 2019.
- Gaston, C. J., Riedel, T. P., Zhang, Z., Gold, A., Surratt, J. D. and Thornton, J. A.: Reactive uptake of an isoprene-derived epoxydiol to submicron aerosol particles, *Environ. Sci. Technol.*, 48, 11178–11186, 2014a.
- Gaston, C. J., Thornton, J. A. and Ng, N. L.: Reactive uptake of N₂O₅ to internally mixed inorganic and organic particles: the role of organic carbon oxidation state and inferred organic phase separations, *Atmos. Chem. Phys.*, 14, 5693–5707, 2014b.
- Hu, W., Palm, B. B., Day, D. A., Campuzano-Jost, P., Krechmer, J. E., Peng, Z., De Sa Suzane, S., Martin, S. T., Alexander, M. L., Baumann, K., Hacker, L., Kiendler-Scharr, A., Koss, A. R., De Gouw, J. A., Goldstein, A. H., Seco, R., Sjostedt, S. J., Park, J. H., Guenther, A. B., Kim, S., Canonaco, F., Prévôt, A. S. H., Brune, W. H. and Jimenez, J. L.: Volatility and lifetime against OH heterogeneous reaction of ambient isoprene-epoxydiols-derived secondary organic aerosol (IEPOX-SOA), *Atmos. Chem. Phys.*, 16, 11563–11580, doi:10.5194/acp-16-11563-2016, 2016.
- Marais, E. A., Jacob, D. J., Jimenez, J. L., Campuzano-Jost, P., Day, D. A., Hu, W., Krechmer, J., Zhu, L., Kim, P. S., Miller, C. C., Fisher, J. A., Travis, K., Yu, K., Hanisco, T. F., Wolfe, G. M., Arkinson, H. L., Pye, H. O. T., Froyd, K. D., Liao, J. and McNeill, V. F.: Aqueous-phase mechanism for secondary organic aerosol formation from isoprene: Application to the southeast United States and co-benefit of SO₂ emission controls, *Atmos. Chem. Phys.*, 16, 1603–1618, doi:10.5194/acp-16-1603-2016, 2016.
- Pye, H. O. T., Pinder, R. W., Piletic, I. R., Xie, Y., Capps, S. L., Lin, Y.-H., Surratt, J. D., Zhang, Z., Gold, A. and Luecken, D. J.: Epoxide pathways improve model predictions of isoprene markers and reveal key role of acidity in aerosol formation, *Environ. Sci. Technol.*, 47, 11056–11064, 2013.
- Zhang, Y., Chen, Y., Lambe, A. T., Olson, N. E., Lei, Z., Craig, R. L., Zhang, Z., Gold, A., Onasch, T. B., Jayne, J. T., Worsnop, D. R., Gaston, C. J., Thornton, J. A., Vizueté, W., Ault, A. P. and Surratt, J. D.: Effect of the Aerosol-Phase State on Secondary Organic Aerosol Formation from the Reactive Uptake of Isoprene-Derived Epoxydiols (IEPOX), *Environ. Sci. Technol. Lett.*, acs.estlett.8b00044, doi:10.1021/acs.estlett.8b00044, 2018.

635

A simplified parameterization of isoprene-epoxydiol-derived secondary organic aerosol (IEPOX-SOA) for global chemistry and climate models: a case study with GEOS-Chem v11-02-rc

5 Duseong S. Jo^{1,2}, Alma Hodzic^{3,4}, Louisa K. Emmons³, Eloise A. Marais⁵, Zhe Peng^{1,2}, Benjamin A. Nault^{1,2}, Weiwei Hu^{1,2}, Pedro Campuzano-Jost^{1,2}, and Jose L. Jimenez^{1,2}

¹Cooperative Institute for Research in Environmental Sciences (CIRES), University of Colorado, Boulder, CO, USA

²Department of Chemistry, University of Colorado, Boulder, CO, USA

³Atmospheric Chemistry Observations and Modeling Lab., National Center for Atmospheric Research, Boulder, CO, USA

⁴Laboratoire d'Aérodynamique, Université de Toulouse, CNRS, UPS, Toulouse, France

10 ⁵Department of Physics and Astronomy, University of Leicester, Leicester, UK

Correspondence to: Jose L. Jimenez (jose.jimenez@colorado.edu)

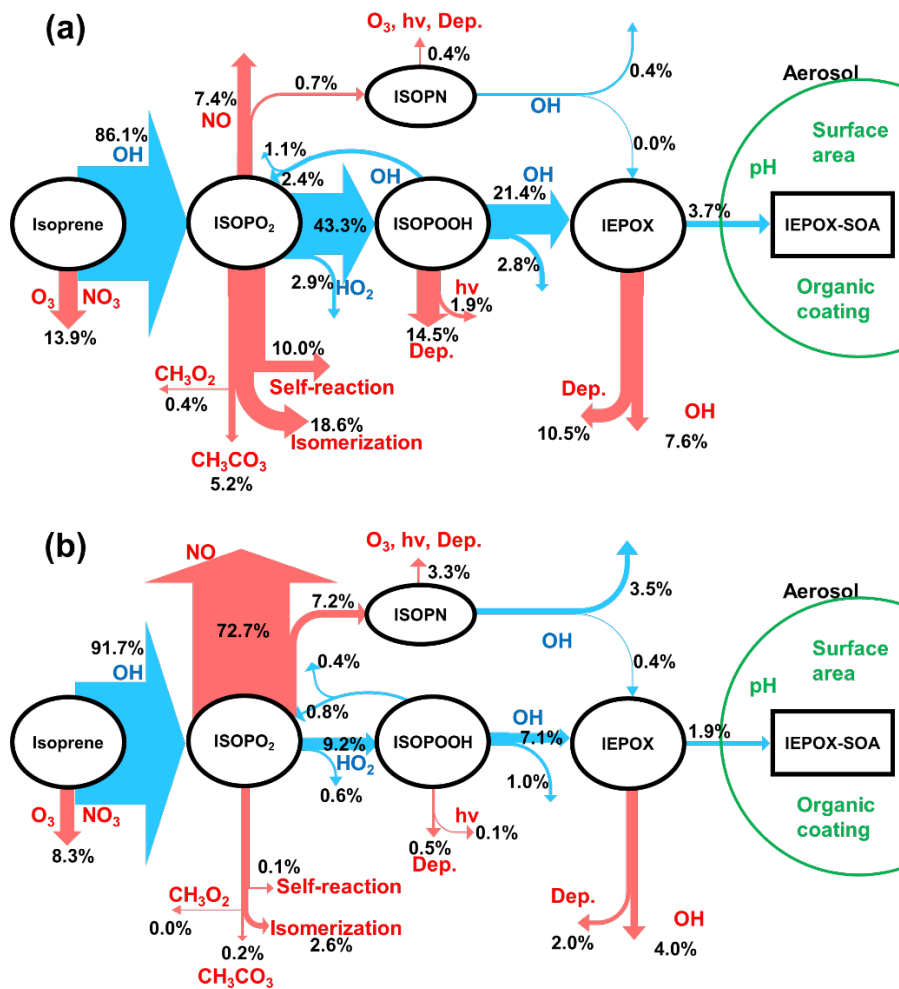
Abstract. Secondary organic aerosol derived from isoprene epoxydiols (IEPOX-SOA) is thought to contribute the dominant fraction of total isoprene SOA, but the current volatility-based lumped SOA parameterizations are not appropriate to represent the reactive uptake of IEPOX onto acidified aerosols. A full explicit modelling of this chemistry is however computationally expensive owing to the many species and reactions tracked, which makes it difficult to include it in chemistry climate models for long-term studies. Here we present three simplified parameterizations (version 1.0) for IEPOX-SOA simulation, based on an approximate analytical/fitting solution of the IEPOX-SOA yield and formation timescale. The yield and timescale can then be directly calculated using the global model fields of oxidants, NO, aerosol pH and other key properties, and dry deposition rates. The advantage of the proposed parameterizations is that they do not require the simulation of the intermediates while retaining the key physico-chemical dependencies. We have implemented the new parameterizations into the GEOS-Chem v11-02-rc chemical transport model, which has two empirical treatments for isoprene SOA (the volatility basis set (VBS) approach and a fixed 3% yield parameterization) and compared all of them to the case with detailed ~~full~~fully explicit chemistry. The best parameterization (PAR3) captures the global tropospheric burden of IEPOX-SOA and its spatio-temporal distribution ($R^2 = 0.9394$) vs. those simulated by the full chemistry, while being more computationally efficient (~5 times faster), and accurately captures the response to changes on NO_x and SO₂ emissions. On the other hand, the constant 3% yield that is now default in GEOS-Chem deviates strongly ($R^2 = 0.65$, ~~63% underestimation~~66), as does the VBS ($R^2 = 0.45$, ~~78~~47, 49% underestimation), with neither parameterization capturing the response to emission changes. With the advent of new mass spectrometry instrumentation, many detailed SOA mechanisms are being developed, which will challenge global and especially climate models with their computational cost. The methods developed in this study can be applied to other SOA pathways, which can allow including accurate SOA simulations in climate and global modeling studies in the future.

35 **1 Introduction**

Secondary organic aerosols (SOA) are a major component of submicron particulate matter globally (Zhang et al., 2007; Jimenez et al., 2009), but are typically poorly predicted by global models (Tsigaridis et al., 2014). Isoprene is the most abundant non-methane volatile organic compound (VOC), whose global emission flux ($\sim 600 \text{ Tg yr}^{-1}$) is much larger than that of monoterpenes ($\sim 100 \text{ Tg yr}^{-1}$) (Sindelarova et al., 2014) and non-methane VOCs from anthropogenic sources ($\sim 130 \text{ Tg yr}^{-1}$) (Lamarque et al., 2010). On account of its global source strength, isoprene oxidation can contribute substantially to SOA in the atmosphere, even if its yield is small (Carlton et al., 2009). There are several isoprene oxidation products that can lead to SOA formation, including isoprene-derived epoxydiols (IEPOX) (Paulot et al., 2009), glyoxal and methyl glyoxal (Fu et al., 2008), gas-phase low volatility organic compounds (LVOC) produced from gas-phase oxidation of hydroxy hydroperoxides (ISOPOOH) (Krechmer et al., 2015; Liu et al., 2016), and methacryloylperoxynitrate (MPAN) (Surratt et al., 2010). Gas-phase IEPOX, mainly formed from the photooxidation of isoprene under low NO conditions (Paulot et al., 2009), can efficiently partition onto aqueous acidic aerosols and produce SOA through aqueous-phase reactions (Paulot et al., 2009; Surratt et al., 2010; Gaston et al., 2014a; Zhang et al., 2018). SOA from IEPOX (“IEPOX-SOA”) is considered at present as the dominant isoprene-derived SOA pathway (Marais et al., 2016; Carlton et al., 2018; Mao et al., 2018), compared to a less efficient formation from glyoxal (Knote et al., 2014).

Ground-based and aircraft field measurements have shown that IEPOX-SOA can contribute to total OA concentrations by as much as 36%, especially for forested regions under low NO across the globe (Hu et al., 2015). Several modeling studies have explicitly simulated IEPOX-SOA by considering detailed isoprene gas-phase chemistry and IEPOX uptake (Marais et al., 2016; Budisulistiorini et al., 2017; Stadtler et al., 2017). Figure 1 shows the main chemical pathways of the IEPOX-SOA chemistry in (a) HO₂ and (b) NO dominant conditions simulated by GEOS-Chem. The fate of isoprene peroxy radicals (ISOPO₂) is substantially affected by the NO and HO₂ concentrations, which modulates the strength of the IEPOX-SOA pathway, consistent with observations in different regions (Hu et al., 2015). In the HO₂ dominant regions (a), most ISOPO₂ reacts with HO₂ to produce ISOPOOH and later IEPOX with a yield of 21.40%. On the other hand, the IEPOX yield is lower (7.52% here) for regions where the NO pathway is dominant (b). An opposite tendency is calculated for an IEPOX-SOA yield from IEPOX, implying the

non-linear chemistry by various factors. The IEPOX-SOA ~~yield~~yields from IEPOX are ~~17.15.2%~~ (~~3%~~
~~3.7.2/21.40~~) and ~~25.3~~20.8% (~~1.9/7.5/7.2~~), respectively for (a) ~~Amazon~~Borneo and (b) Beijing based on
65 GEOS-Chem model calculations, which can be mainly explained by the higher available aerosol surface
area in Beijing compared to ~~Amazon~~Borneo.



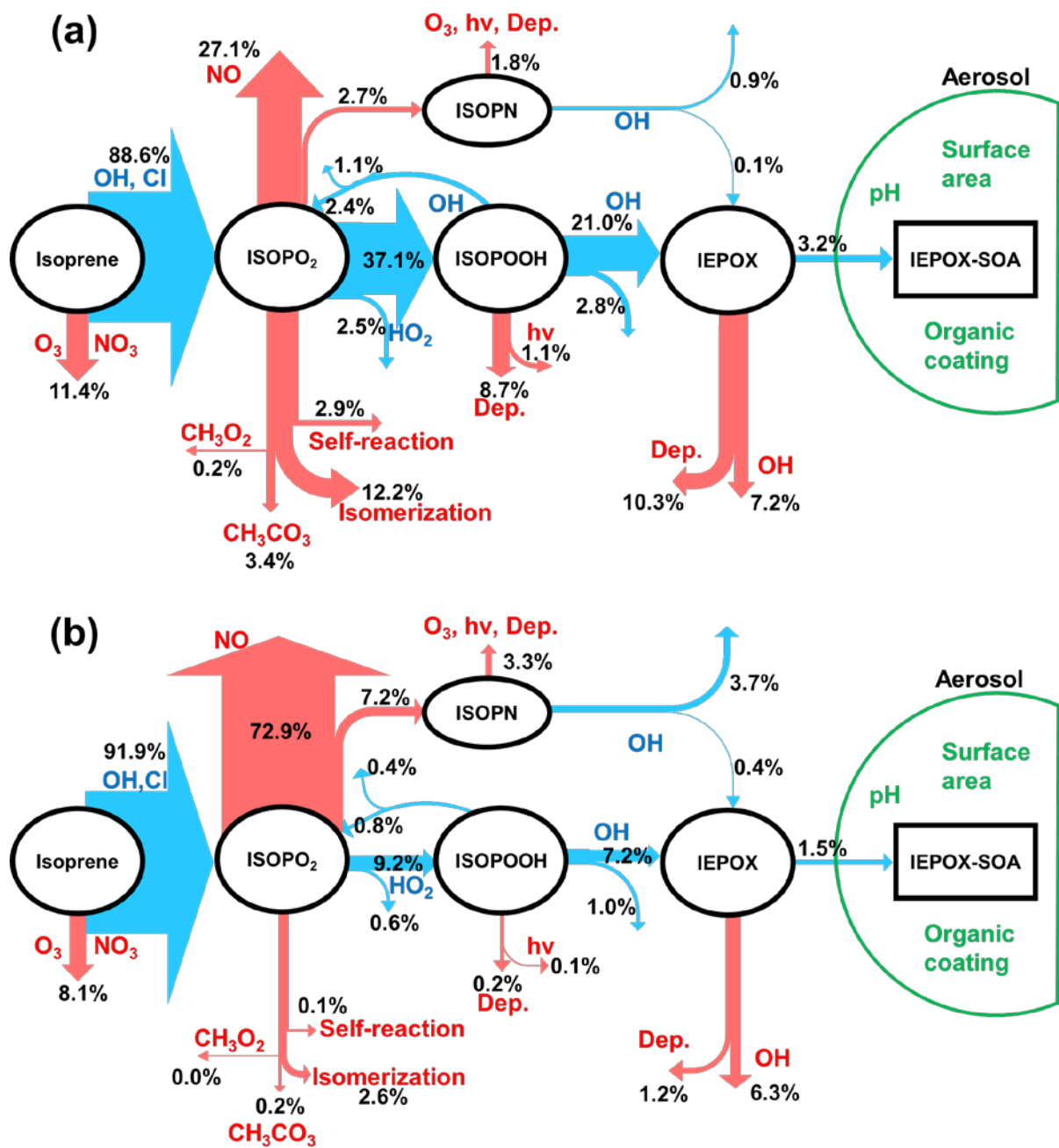


Figure 1. Schematic diagrams of IEPOX-SOA chemistry for (a) HO₂ and (b) NO dominant regions. Blue arrows indicate IEPOX-SOA formation pathways and red arrows represent other chemical pathways that do not form significant IEPOX-SOA. Values are averaged molar yields relative to the initial oxidation amount of isoprene from GEOS-Chem v11-02-rc results using the explicit full chemistry with updates in

75 *this study (see Sect. 2.2) over ~~the Amazon~~Borneo (as an example of HO₂ dominant conditions, ~~105°S – 0°S, 70°W – 60°W~~ 5°N, 105°E – 120°E) and Beijing (as an example of NO dominant conditions, 35°N – 45°N, 110°E – 120°E) from July 2013 to June 2014. We note that Beijing is located in a region with typically low isoprene emissions, so the appreciable yield of IEPOX-SOA will still result in small ambient concentrations.*

80 Marais et al. (2016) reported that the model with the explicit irreversible uptake of isoprene SOA precursors to aqueous aerosols coupled to detailed gas-phase chemistry predicted isoprene SOA better than the default isoprene SOA mechanism based on volatility basis set (VBS) in GEOS-Chem v09-02. The VBS mechanism is based on the reversible partitioning of first-generation semivolatile oxidation products onto pre-existing dry OA (Pye et al., 2010). The default VBS mechanism in GEOS-Chem
85 underestimated the observed isoprene SOA formation by a factor of 3 over the southeast US in summer, whereas the model with the detailed isoprene chemistry showed a close agreement with the measured aircraft and surface isoprene-derived SOA concentrations.

The use of increasingly detailed chemistry in models enables realistic prediction of chemical composition in the atmosphere, but it is limited by the prohibiting computational cost. As a result, most
90 of the models participating in the 5th phase of the Coupled Model Intercomparison Project (CMIP5) (Taylor et al., 2011), which provided results for the recent IPCC report (Stocker et al., 2013), used very simplified approaches, such as assuming a constant fraction of emissions to occur as non-volatile SOA (Tsigaridis and Kanakidou, 2018). ~~These simplified approaches were also used in many models participating in the recent AeroCom intercomparison study of OA (Tsigaridis et al., 2014)~~These
95 simplified approaches were also used in many models participating in the recent AeroCom intercomparison study of OA (Tsigaridis et al., 2014). The modeling community has tried to improve computational efficiency by condensing complex VBS schemes into simpler ones (Shrivastava et al., 2011; Koo et al., 2014) or by developing empirical parameterizations based on field observations (Hodzic and Jimenez, 2011; Kim et al., 2015). In order to avoid the extra computational cost of the full isoprene
100 mechanism, GEOS-Chem v11-02-rc includes a fixed 3% yield of SOA from isoprene emission for most model applications based on the study by Kim et al. (2015) and confirmed by the study with the explicit isoprene SOA mechanism in Marais et al. (2016). However, the 3% yield was derived from the measurements over the southeast US during summer in 2013 (Marais et al., 2016), but the explicit

isoprene SOA mechanism estimated wide range of SOA yields (3 – 13%) in different years (Marais et al., 105 2017), implying that isoprene SOA yields could be different under different physico-chemical environments in other regions and time periods (Hu et al., 2015).

In this study, we develop IEPOX-SOA parameterizations based on approximate analytical solutions of the relevant portion of the isoprene chemical mechanism supplemented with numerical fitting. First, a box model is used to develop and evaluate the parameterizations. We then implement the 110 parameterizations into GEOS-Chem and compare the results against those from the explicit irreversible uptake of isoprene SOA precursors to aqueous aerosols coupled to detailed gas-phase chemistry, the default fixed 3% yield, and the VBS scheme. We investigate the performance and limitations of the new parameterizations in terms of global tropospheric concentrations, vertical profiles, and burdens. Our methods substantially reduce the computational cost of the explicit isoprene SOA mechanism and provide 115 a much-improved simulation compared to the fixed 3% yield and the VBS parameterizations.

2 Global model description

2.1. General

We used the GEOS-Chem (v11-02-rc) global 3-D chemical transport model (Bey et al., 2001) to run the 120 parameterizations described in Sect. 3, as well as the explicit isoprene SOA mechanism, fixed 3% yield, and VBS schemes. The model was driven by Goddard Earth Observing System – Forward Processing (GEOS-FP) assimilated meteorological data from the NASA Global Modeling and Assimilation Office (GMAO) for a year (July 2013 to June 2014) with a spin-up time of two months. Winds, temperature, precipitation, and other meteorological variables are provided at 0.3125° (longitude) \times 0.25° (latitude) 125 and regridded to 2.5° (longitude) \times 2° (latitude) for computational efficiency. GEOS-Chem simulates gas-phase chemistry and aerosol formation including sulfate, ammonium, nitrate (Park et al., 2006), black carbon (Park et al., 2003), OA (Pye et al., 2010; Kim et al., 2015; Marais et al., 2016), sea salt (Jaeglé et al., 2011), and dust (Fairlie et al., 2007). Gas-particle partitioning of inorganic aerosols and aerosol pH

are computed with the ISORROPIA II thermodynamic model (Fountoukis and Nenes, 2007; Pye et al.,
130 2009).

2.2. Update to the full mechanism of IEPOX-SOA uptake

We updated the standard mechanism and code of GEOS-Chem v11-02-rc to include two recent scientific findings influencing IEPOX-SOA uptake rate. ~~First, we considered organic coating effects when we calculated reactive IEPOX uptake by assuming core (inorganic) – shell (organic) mixing state (Gaston et al., 2014a). Standard GEOS Chem assumes no organic coating; only the surface area of sulfate. We updated the model to include suppression of IEPOX reactive uptake by the organic coating, and to use available surface area of the total sulfate-ammonium-nitrate-organic aerosols mixture at a given relative humidity with hygroscopic growth factors. As a result, the inclusion of coating reduces the IEPOX reactive uptake coefficient (γ) (Anttila et al., 2006; Gaston et al., 2014b), but the increased aerosol surface area increases the first order IEPOX loss rate on aerosols as shown in the Eq. (1). The net effect increases the first order IEPOX uptake rate as organic mass increases (Fig. S1). The inclusion of this effect might result in the overestimation of IEPOX-SOA concentration of GEOS-Chem because we did not alter the Henry's law constant of IEPOX ($H = 1.7 \times 10^7 \text{ M atm}^{-1}$) or mass accommodation coefficient ($\alpha = 0.1$) from those used in GEOS-Chem v11-02-rc, which showed the similar IEPOX-SOA concentrations compared to measurements (Marais, 2018). However, it does not affect our conclusions because we compare parameterizations against the explicit isoprene-SOA mechanism, not against measurements. Updating the parameterizations developed here with more accurate values of H or α determined in future literature studies would be trivial. The equation for the uptake rate of IEPOX to form IEPOX-SOA is:~~
135
140
145
150 First, we considered organic coating effects when we calculated reactive IEPOX uptake by assuming core (inorganic) – shell (organic) mixing state (Zhang et al., 2018). The detailed information for the register model and parameters used in this study are given in the supplementary Sect. 1.

IEPOX uptake rate ~~Standard GEOS-Chem assumes no organic coating; only the surface area of inorganic aerosols. We updated the model to include suppression of IEPOX reactive uptake by the organic coating, and to use the available surface area of the total sulfate-ammonium-nitrate-organic aerosols mixture at a given relative humidity with hygroscopic growth factors. We found that the IEPOX reactive~~
155

uptake coefficient (γ) was always decreased at atmospheric relevant aerosol pH and relative humidity conditions, but the IEPOX reactive uptake rate constant increased in some conditions (high pH and high IEPOX diffusion coefficient in the organic layer, Fig. S2). We note that this is the case for GEOS-Chem v11-02-rc, because GEOS-Chem does not take into account organic aerosol mass for aerosol radius and aerosol surface area calculation when it calculates IEPOX reative uptake. Therefore, additional OA mass considered in this study increases available aerosol surface area for IEPOX reactive uptake, which compensates or sometimes overcomes the effects by the decrease of γ as shown in Eq. (1) for the first-order uptake rate constant of IEPOX to form IEPOX-SOA:

IEPOX uptake rate constant =

$$\frac{S_a}{\frac{r_a}{D_g} + \frac{4}{\gamma \times v_{rms}}} \quad (1)$$

S_a is the wet aerosol surface area on which IEPOX can be taken up ($\text{cm}^2 \text{cm}^{-3}$), r_a is the wet aerosol radius (cm), D_g is gas-phase diffusion coefficient of IEPOX ($\text{cm}^2 \text{s}^{-1}$), and v_{rms} is the mean molecular speed (cm s^{-1}) of gas-phase IEPOX.

S_a is the wet aerosol surface area on which IEPOX can be taken up ($\text{m}^2 \text{m}^{-3}$), r_a is the wet aerosol radius (m), D_g is gas-phase diffusion coefficient of IEPOX ($\text{m}^2 \text{s}^{-1}$), and v_{rms} is the mean molecular speed (m s^{-1}) of gas-phase IEPOX. Again, the effects of organic coating on IEPOX uptake rate constant in this study can be different from previous observational studies (Hu et al., 2016; Zhang et al., 2018), because observational studies used the measured and fixed available aerosol surface area and radius, and they changed organic aerosol layer thickness for their calculations (i.e. inorganic core radius was changed but total particle radius and surface area were not changed). When we assumed the fixed aerosol radius and aerosol surface area, and only organic coating thickness increased as OA mass increased as per previous observational studies, all the case showed the decreasing IEPOX reactive uptake rate constants (Fig. S3).

Parameters used in this study such as the Henry's law constant and the IEPOX diffusion coefficient in OA can be easily updated in future studies, as new information becomes available in the literature. Our parameterizations are flexible to the change of these variables, because they use the IEPOX reactive uptake rate constant (k_{18} in Eqs. (7) and (14) in Sect. 3) rather than using individual input parameters.

Therefore, updating the parameterizations developed here with more accurate values of input parameters determined in future literature studies is easy without having to refit the parameterizations.

185 Second, we calculate the submicron aerosol pH without sea salt based on the results from previous studies (Noble and Prather, 1996; Middlebrook et al., 2003; Hatch et al., 2011; Allen et al., 2015; Guo et al., 2016; Bondy et al., 2018; Murphy et al., 2018), which showed that sea salt aerosols were dominantly externally mixed with sulfate-nitrate-ammonium rather than internally mixed. Therefore, sea salt is not expected to impact submicron aerosol pH significantly in the real atmosphere. ~~Effects of sea salt on pH and detailed analysis against the aircraft measurements will be separately discussed in Nault et al. (2019, in preparation).~~ Effects of sea salt on pH and detailed analysis against the aircraft measurements were discussed in detail by Nault et al. (2018).

190

2.3. Isoprene SOA simulations

In this section, we briefly describe three different schemes for isoprene SOA simulations used in GEOS-Chem v11-02-rc: the explicit scheme (Marais et al., 2016), the VBS (Pye et al., 2010), and the fixed 3% parameterization (Kim et al., 2015). In the explicit scheme, isoprene and its products, and related processes including chemistry, dry and wet deposition, and transport are explicitly calculated in GEOS-Chem. The chemical mechanism related to IEPOX-SOA formation ~~mechanism~~ is shown in Table S1. Gas-phase concentrations of isoprene, ISOPO₂, ISOPOOH, IEPOX, and isoprene nitrate (ISOPN) are explicitly calculated in every model grid point. All the species (except for ISOPO₂ because of its short ~~life-time~~ lifetime) are transported in the model. More detailed information can be found in Marais et al. (2016), with some updates for isomer reactions described in Sect. 3.1.

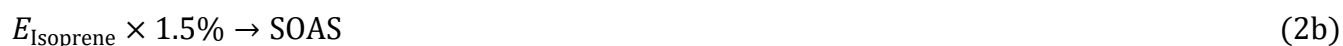
200

The VBS scheme implemented in GEOS-Chem uses six tracers to simulate isoprene SOA, three for gas-phase and three for aerosol-phase concentrations. This scheme calculates semi-volatile products from the isoprene + OH reaction and ~~distribute~~ distributes them into three saturation vapor pressure bins ($C^* = 1, 10, 100 \mu\text{g m}^{-3}$). These products are partitioned into gas (ISOG1–3 in GEOS-Chem) and aerosol phase (ISOA1–3 in GEOS-Chem) at every model timestep based on equilibrium partitioning (Pankow, 1994). Dry and wet deposition are calculated for both gas and aerosol species, with a Henry's law solubility coefficient of 10^5 M atm^{-1} (similar to HNO₃) for gas species. More detailed description is available in Pye

205

et al. (2010). We note that there are multiple VBS schemes available in the literature, and their details can vary (e.g., the number of bins, yields, chemical aging, NO_x dependence, photolysis, etc.). In this study we focused on evaluating the current default isoprene VBS scheme in GEOS-Chem.

The fixed 3% parameterization applies the fixed 3% mass yield to isoprene emissions to produce two tracers including the gas-phase SOAP (SOA precursor, with 1.5% mass yield) and the aerosol product SOAS (“simple” SOA, with the 1.5% yield). The gas-phase tracer SOAP is further aged with a fixed 1-day conversion timescale to SOAS. There are no losses in the gas-phase for SOAP other than ~~formation of~~ the conversion process to SOAS.



Since the fixed 3% and the VBS scheme do not separate IEPOX-SOA from isoprene SOA, we directly compared isoprene SOA from the VBS and the fixed 3% with the parameterizations developed in Sect. 3. Because IEPOX-SOA is thought to comprise the dominant fraction of isoprene SOA, we think this assumption will not significantly affect our conclusions. Furthermore, isoprene SOA from the VBS and the fixed 3% parameterizations ~~substantially~~ underestimate the predicted IEPOX-SOA concentrations (See Fig. 4), implying that the underestimation will be even larger for total isoprene SOA, if other pathways are significant.

3 Parameterization Development

3.1. Chemical reactions

We use the explicit isoprene SOA formation mechanism coupled to detailed gas-phase isoprene chemistry from GEOS-Chem v11-02-rc (Yantosca, 2018) as the complete mechanism from which to develop the parameterization. The IEPOX-SOA formation pathway in v11-02-rc is mostly based on Marais et al. (2016), with updates for the inclusion of isomers of ISOPOOH and IEPOX (Bates et al., 2014; St. Clair et al., 2016). As in Marais et al. (2016), we lumped together isomers of the same species to make the resulting parameterizations simpler. Listed in Table S1 are the mechanism used in GEOS-Chem v11-02-rc and the isomer-lumped mechanism, which were used as a starting point for our work. Most reactions

235 forming IEPOX-SOA were included, but we excluded a minor pathway from the isoprene + NO₃ reaction, which contributed only 0.06% of global annual IEPOX production using GEOS-Chem (July 2013 to June 2014). We compared IEPOX-SOA molar yields from isoprene between the isomer-resolved and the isomer-lumped mechanisms for 14,000 different input parameter combinations (using the box model described in Sect. 3.2), which showed nearly identical results (Fig. S2S4; slope = 1.00 and R² = 1.00).
240 Hereinafter, we use the word “the full chemistry” or “FULL” to refer to “the explicit IEPOX-SOA formation mechanism coupled to the detailed gas-phase isoprene chemistry”, for brevity.

3.2. Box model calculation

We used a box model (KinSim v3.71 in Igor Pro 7.08 ~~(Peng et al., 2015) to simulate IEPOX-SOA concentrations and develop parameterizations.~~) (Peng and Jimenez, 2019) to simulate IEPOX-SOA concentrations and develop parameterizations.
245 concentrations and develop parameterizations. Box model simulations were computed for 10 days with 400 second output timesteps for the complete consumption of isoprene and intermediates. We evaluate the developed parameterization in Sect. 3.3 by the mechanism over a very wide range of all the key parameters. We conducted 14,000 box model simulations by varying key species concentrations, aerosol pH and physical properties, temperature, and planetary boundary layer (PBL) height logarithmically over
250 their relevant global tropospheric ranges (Table S2). Aerosol properties are used for the calculation of the IEPOX uptake reaction (R18) (Gaston et al., 2014a, 2014b; Hu et al., 2016). Dry deposition frequencies (R21-22R22-23) were estimated as 2.5 cm s⁻¹ / [PBL height] based on measured dry deposition velocity over the southeast United States temperate mixed forest in the summer (Nguyen et al., 2015).

3.3. Parameterization 1

255 We developed three IEPOX-SOA parameterizations based on an approximation of the analytical solution to the chemical mechanism in Table S1. The development of the first parameterization (PAR1) is described here. First, we divided the IEPOX-SOA formation pathway into four parts:

$$\begin{aligned} \text{IEPOX-SOA} &= E_{\text{Isoprene}} \times Y_{\text{IEPOX-SOA}} \\ &= E_{\text{Isoprene}} \times f_{\text{Isoprene} \rightarrow \text{ISOPO}_2} \times f_{\text{ISOPO}_2 \rightarrow \text{ISOPOOH}} \times f_{\text{ISOPOOH} \rightarrow \text{IEPOX}} \times f_{\text{IEPOX} \rightarrow \text{IEPOX-SOA}} \quad (3) \end{aligned}$$

260 where $IEPOX-SOA$ and $E_{Isoprene}$ are the formation rate and emissions of those species [$\text{molec. m}^{-2} \text{ s}^{-1}$]. $Y_{IEPOX-SOA}$ is the molar yield from isoprene. $f_{A \rightarrow B}$ means the mole fraction of product species B formed upon consumption of precursor species A . For example, if $f_{A \rightarrow B}$ is 0.3, 30% of A produces B , and the remaining 70% of A is lost by other chemical reaction pathways. Each fraction can be estimated using the instantaneous reaction rates and species concentrations. For example, the first fraction can be written as:

$$265 \quad f_{\text{Isoprene} \rightarrow \text{ISOPO}_2} = \frac{k_1 \times [\text{OH}] + k_4 \times [\text{Cl}]}{k_1 \times [\text{OH}] + k_2 \times [\text{O}_3] + k_3 \times [\text{NO}_3] + k_4 \times [\text{Cl}]} \quad (4)$$

where k_n represents the reaction rate constant of reaction number n in Table S1. Brackets refer to species concentrations in molec. cm^{-3} .

Deriving the second conversion fraction ($\text{ISOPO}_2 \rightarrow \text{ISOPOOH}$) in Eq. (3) is not straightforward, due to the ISOPO_2 self-reaction (R8). ISOPO_2 concentrations change with time and species concentrations. 270 Therefore, we constrained this fraction by performing a numerical fitting method (using the curve fitting analysis tools within Igor Pro) to the output of the box model for the 14,000 independent simulations discussed above. We tried different functional forms for the equation (polynomial, Gaussian, Lorentzian, exponential, double-exponential, trigonometric, Hill, Sigmoid, etc.), independent variables, and initial guesses for the coefficients. We found that the Hill type equation combined with the production term of 275 ISOPO_2 in exponential form showed the best results compared to the box model calculation. The result was as follows:

$$f_{\text{ISOPO}_2 \rightarrow \text{ISOPOOH}} = Y_5 \times \frac{k_5 \times [\text{HO}_2]}{L_{\text{ISOPO}_2\text{-others}} + L_{\text{ISOPO}_2\text{-self}}} \quad (5a)$$

$$L_{\text{ISOPO}_2\text{-others}} = k_5 \times [\text{HO}_2] + k_6 \times [\text{NO}] + k_7 \times [\text{CH}_3\text{O}_2] + k_9 \times [\text{CH}_3\text{CO}_3] + k_{10} \quad (5b)$$

$$L_{\text{ISOPO}_2\text{-self}} = C_1 \times \left(1 - \left(\frac{L_{\text{ISOPO}_2\text{-others}}^{C_2}}{L_{\text{ISOPO}_2\text{-others}}^{C_2} + C_3^{C_2}} \right) \right) \quad (5c)$$

280 Where $C_1 = 1.207 \times 10^{-2} - 1.048 \times 10^{-2} \times \exp(-2260 \times [P_{\text{ISOPO}_2}])$, $C_2 = 1.24$, and $C_3 = 3.667 \times 10^{-2} - 3.149 \times 10^{-2} \times \exp(-2411 \times [P_{\text{ISOPO}_2}])$. Y_n means the product yield parameter of reaction number n in Table S1 (i.e., $Y_5 = 0.937$). If the number of products of interest in a single reaction is larger than 1, we used the notation $Y_{n,m}$ where n denotes the reaction and m the product number (see Eq. (8) below and R6

in Table S1 for example). P_{ISOPO_2} is the production frequency term of ISOPO₂ from isoprene ($= k_1 \times [OH] + k_4 \times [Cl]$). The need for this numerical fitting function reflects the fact that ISOPO₂ concentration is affected by the loss frequency ($L_{ISOPO_2_others}$) and the production frequency (P_{ISOPO_2}) of ISOPO₂.

The third conversion fraction in Eq. (3) includes the regeneration of ISOPO₂ from ISOPOOH (R11). To consider this regeneration, the resulting ~~IEPOX formation rate~~ $f_{isoprene \rightarrow IEPOX, HO_2}$ [$\text{molec. m}^{-2} \text{s}^{-1}$] (IEPOX formation fraction from isoprene via ISOPO₂ + HO₂ pathway) can be calculated using a geometric series:

$$f_{isoprene \rightarrow IEPOX, HO_2} = f_{isoprene \rightarrow ISOPO_2} \times f_{ISOPO_2 \rightarrow ISOPOOH} \times f_{ISOPOOH \rightarrow IEPOX} + f_{isoprene \rightarrow ISOPO_2} \times f_{ISOPO_2 \rightarrow ISOPOOH} \times f_{ISOPOOH \rightarrow ISOPO_2} \times f_{ISOPO_2 \rightarrow ISOPOOH} \times f_{ISOPOOH \rightarrow IEPOX} + \dots \quad (6a)$$

$$f_{ISOPOOH \rightarrow IEPOX} = Y_{12} \times \frac{k_{12} \times [OH]}{k_{11} \times [OH] + k_{12} \times [OH] + k_{21} + k_{22}} \quad (6b)$$

$$f_{ISOPOOH \rightarrow ISOPO_2} = Y_{11} \times \frac{k_{11} \times [OH]}{k_{11} \times [OH] + k_{12} \times [OH] + k_{21} + k_{22}} \quad (6c)$$

Equation (6a) can be solved as $f_{isoprene \rightarrow IEPOX, HO_2} = a / (1 - r)$, where

$$a = f_{isoprene \rightarrow ISOPO_2} \times f_{ISOPO_2 \rightarrow ISOPOOH} \times f_{ISOPOOH \rightarrow IEPOX} \quad (6d)$$

$$r = f_{ISOPOOH \rightarrow ISOPO_2} \times f_{ISOPO_2 \rightarrow ISOPOOH} \quad (6e)$$

300 Finally, the fourth function can be calculated as:

$$f_{IEPOX \rightarrow IEPOX-SOA} = \frac{k_{18}}{k_{17} \times [OH] + k_{18} + k_{23}} \quad (7)$$

Analogously, the IEPOX formation ~~rate~~ fraction from the ISOPO₂ + NO pathway can be calculated as follows:

$$f_{isoprene \rightarrow IEPOX, NO} = \frac{k_1 \times [OH] + k_4 \times [Cl]}{k_1 \times [OH] + k_2 \times [O_3] + k_3 \times [NO_3] + k_4 \times [Cl]} \times \left\{ \frac{k_6 \times [NO]}{L_{ISOPO_2_others} + L_{ISOPO_2_self}} \times (Y_{6,1} \times Y_{13} \times \frac{k_{13} \times [OH]}{k_{13} \times [OH] + k_{15} \times [O_3]} + Y_{6,2} \times Y_{14} \times \frac{k_{14} \times [OH]}{k_{14} \times [OH] + k_{16} \times [O_3]}) \right\} \quad (8)$$

With both HO₂ and NO pathways combined, the IEPOX-SOA yield ($Y_{IEPOX-SOA}$) is

$$Y_{\text{IEPOX-SOA}} = (f_{\text{isoprene} \rightarrow \text{IEPOX,HO}_2} + f_{\text{isoprene} \rightarrow \text{IEPOX,NO}}) \times f_{\text{IEPOX} \rightarrow \text{IEPOX-SOA}} \quad (9)$$

From Eq. (9), we can calculate the IEPOX-SOA molar yield with instantaneous meteorological and chemical fields in each grid box. We evaluated this instantaneous IEPOX-SOA molar yield against the
 310 calculated IEPOX-SOA yield using the full mechanism with the box model (Fig. S3a-S5a). Each point indicates the IEPOX-SOA yield with randomly selected input variables in the parameter space shown in Table S2. We confirmed that the yield from Eq. (9) very accurately regenerated the simulated yield from the full mechanism with the box model (Fig. S3S5).

Equation (9) gives the instantaneous yield if all the reactions were extremely fast, but it takes time to
 315 produce IEPOX-SOA in the full chemistry model as well as in the real atmosphere. As a result, if the yield from Eq. (9) is used for making IEPOX-SOA, chemical transport models would likely overestimate IEPOX-SOA concentrations locally in isoprene-emitting areas ~~because of its too rapid~~ due to the instantaneous formation of IEPOX-SOA from Eq. (9). To simulate the formation of IEPOX-SOA with a realistic timescale, we introduced a single gas-phase intermediate, similarly to the 3% parameterization
 320 in GEOS-Chem v11-02-rc. The gas-phase intermediate is then converted to IEPOX-SOA with a first order timescale that depends on the local conditions. The final form of parameterization PAR1 is:



SOAP stands for the gas-phase precursor of IEPOX-SOA (using the same terminology as in the 3% parameterization in GEOS-Chem), and τ is the formation timescale. *SOAP* represents the lumped species
 325 of isoprene, ISOPOOH, and IEPOX, and it undergoes wet deposition with the effective Henry's law solubility coefficient of 10^5 M atm^{-1} (the value used for the gas-phase semivolatile products of isoprene SOA simulated by the VBS in GEOS-Chem). Dry deposition of *SOAP* was not simulated in GEOS-Chem, because dry deposition of intermediate species was already included in the parameterization (R22 and R23). On the other hand, *SOAP* in the 3% parameterization is not dry or wet deposited, as described in
 330 Sect. 2.3. (Kim et al., 2015; Yantosca, 2016). IEPOX-SOA formation is calculated at each timestep (Δt) in the model as follows:

$$\text{IEPOX-SOA}(t+\Delta t) = \text{IEPOX-SOA}(t) + \left\{1 - \exp\left(-\frac{\Delta t}{\tau}\right)\right\} \times \text{SOAP}(t) \quad (11)$$

We conducted numerical fitting to calculate the value of τ , due to the fact that many processes in the mechanism can affect the formation timescale of IEPOX-SOA. ~~The~~Again, the best fitting results were obtained from Hill equation formulas with the loss rates of different precursors as shown in Eq. (12) below.

$$\tau = C_0 + C_1 \times \frac{L_{\text{ISOP}}^{C_2}}{L_{\text{ISOP}}^{C_2} + C_3^{C_2}} + C_4 \times \frac{L_{\text{ISOPOOH}}^{C_5}}{L_{\text{ISOPOOH}}^{C_5} + C_6^{C_5}} \times F + C_7 \times \frac{L_{\text{ISOPN}}^{C_8}}{L_{\text{ISOPN}}^{C_8} + C_9^{C_8}} \times (1 - F) + C_{10} * \frac{L_{\text{IEPOX}}^{C_{11}}}{L_{\text{IEPOX}}^{C_{11}} + C_{12}^{C_{11}}} \quad (12a)$$

$$F = C_{13} + C_{14} \times \exp\left(-C_{15} \times \frac{P_{\text{ISOPOOH}}}{L_{\text{ISOPO}_2}}\right) + C_{16} \times \exp\left(-C_{17} \times \frac{P_{\text{ISOPN}}}{L_{\text{ISOPO}_2}}\right) \quad (12b)$$

Where L stands for the loss frequency of a species [s^{-1}], and P represents the production frequency of a species [s^{-1}]. Constants are listed in Table S3. Equation (12a) has five parts – constant (C_0), isoprene (ISOP) loss (C_1 – C_3), ISOPOOH loss (C_4 – C_6), ISOPN loss (C_7 – C_9), and IEPOX loss (C_{10} – C_{12}). All precursor loss rates affect the formation timescale except for ISOPO₂ loss. The loss rate of ISOPO₂ is very fast, therefore, it rarely influences the formation timescale of IEPOX-SOA. There are two different ISOPO₂ loss pathways leading to IEPOX. ~~We included these pathways by calculating Eq. (12b) with HO₂/NO branching ratio from ISOPO₂ oxidation. As shown in Fig. S3b~~We designed the term F to consider contributions of high and low NO_x pathways to the formation timescale in the single equation system. ISOPO₂ + NO pathway is dominant when F = 0 and ISOPO₂ + HO₂ pathway is dominant when F = 1. F cannot be below 0 or above 1 in terms of the physical meaning, but the fitted F can have values outside of 0 to 1 range because the numerical fitting works to minimize the total error compared to the box model calculated timescale of IEPOX-SOA. As shown in Fig. S5b, the formation timescale by box model was generally well captured by the parameterization over the entire input parameter space (slope = 0.98 and R² = 0.98).

3.4. Parameterizations 2 and 3

PAR1 showed some limitations in performance (discussed ~~below~~in Sect. 4), which were related to the calculation of $Y_{\text{IEPOX-SOA}}$ based on the local conditions when isoprene is emitted. Since the time to form and uptake IEPOX can be significant, and some parametric dependences are quite nonlinear (especially

for IEPOX reactive uptake), this approximation can result in some deviations between the parameterization and the full chemistry since the local conditions at the time of IEPOX uptake may be different than those at the time of isoprene emission. To address this problem and improve performance, a modified second parameterization (PAR2) was developed, where the gas-phase IEPOX(~~g~~) yield is calculated with the local conditions at the point of isoprene emissions, while the IEPOX uptake to form IEPOX-SOA is calculated explicitly using Eq. (14). Y_{IEPOX} was calculated from Eq. (9), by eliminating $f_{IEPOX \rightarrow IEPOX-SOA}$ from the right side of the equation. The form of PAR2 is:

$$365 \quad E_{\text{Isoprene}} \times Y_{\text{IEPOX}} \rightarrow \text{IEPOX} \xrightarrow{f_{\text{IEPOX} \rightarrow \text{IEPOX-SOA}}} \text{IEPOX-SOA} \quad (13)$$

IEPOX-SOA formation is calculated at each timestep (Δt) in the model as follows:

$$\begin{aligned} \text{IEPOX-SOA}(t+\Delta t) = & \text{IEPOX-SOA}(t) + \{1 - \exp(-\Delta t \times (k_{17} \times [\text{OH}] + k_{18} + k_{23}))\} \\ & \times \text{IEPOX}(t) \times \frac{k_{18}}{k_{17} \times [\text{OH}] + k_{18} + k_{23}} \end{aligned} \quad (14)$$

PAR2 effectively replaces the generic SOAP gas-phase intermediate of PAR1 with a chemically-meaningful gas-phase intermediate (IEPOX).

Because IEPOX is formed immediately after isoprene emission in PAR2, it can result in an overestimated IEPOX concentrations since the gas-phase chemistry has a limited rate. Therefore, we developed a 3rd parameterization (PAR3) by modifying PAR2 by representing the formation timescale for IEPOX by adding a second intermediate:

$$375 \quad E_{\text{Isoprene}} \times Y_{\text{IEPOX}} \rightarrow \text{SOAP}_I \xrightarrow{\tau_I} \text{IEPOX} \xrightarrow{f_{\text{IEPOX} \rightarrow \text{IEPOX-SOA}}} \text{IEPOX-SOA} \quad (15)$$

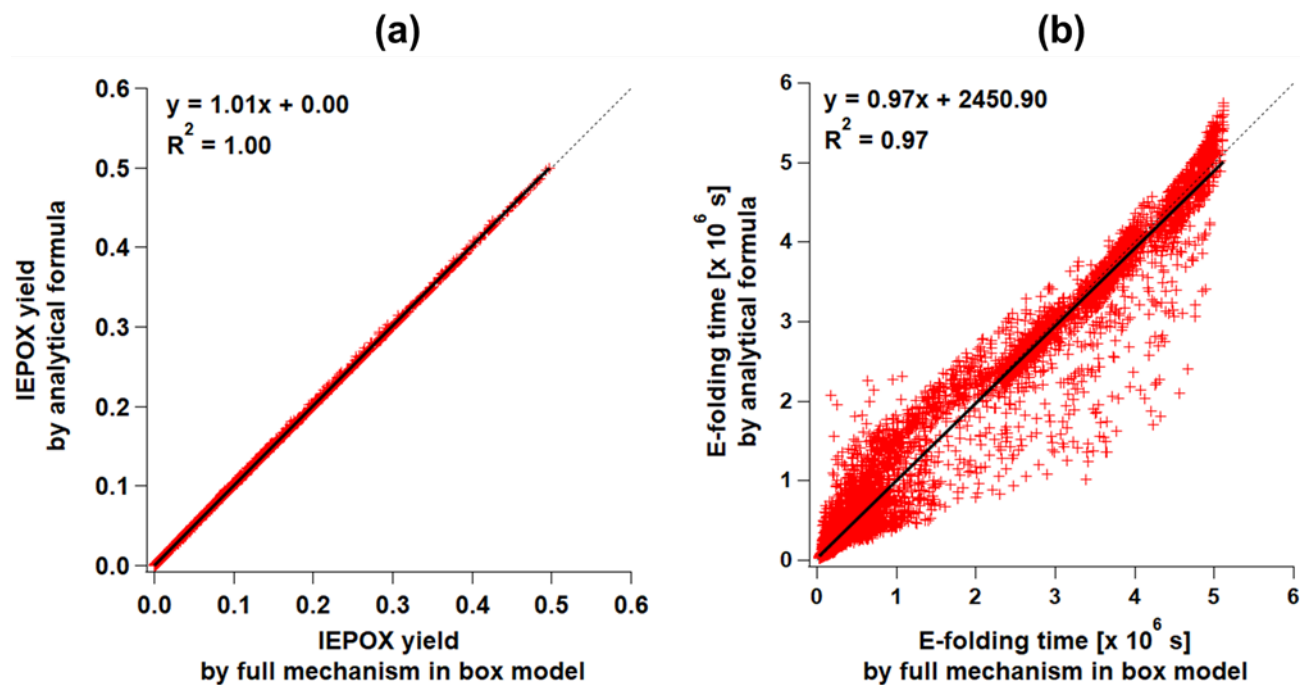
Where τ_I is the formation timescale of IEPOX, which is calculated using the equation below.

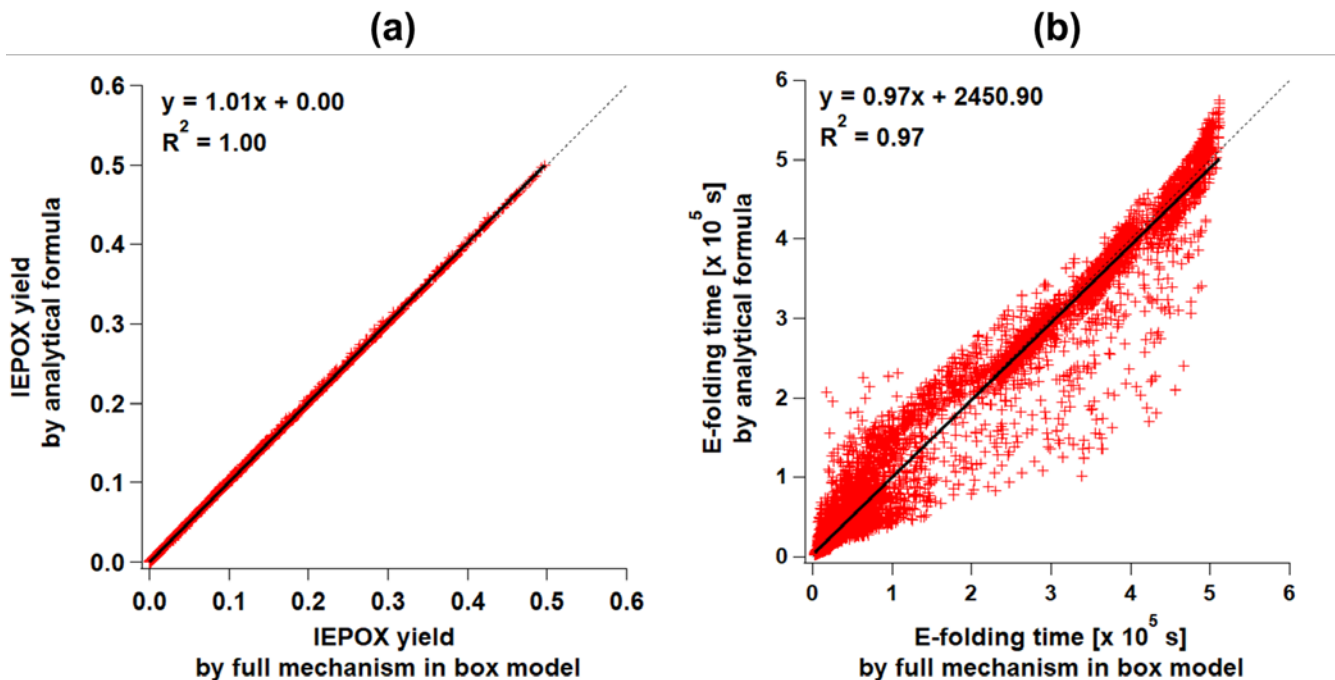
$$\tau_I = C_0 + C_1 \times \frac{L_{\text{ISOP}}^{C_2}}{L_{\text{ISOP}}^{C_2} + C_3^{C_2}} + C_4 \times \frac{L_{\text{ISOPPOOH}}^{C_5}}{L_{\text{ISOPPOOH}}^{C_5} + C_6^{C_5}} \times F + C_7 \times \frac{L_{\text{ISOPN}}^{C_8}}{L_{\text{ISOPN}}^{C_8} + C_9^{C_8}} \times (1 - F) \quad (16)$$

The functional form of Eq. (16) is the same as Eq. (12a) but excludes the last term (IEPOX loss). F is calculated using Eq. (12b) but with different constant values, which are provided in Table S3. Similar to the evaluation of PAR1, Y_{IEPOX} and τ_I were generally well predicted compared to 14,000 box model simulations (Fig. 2).

Three parameterizations from Eqs. (10), (13), and (15) were implemented in GEOS-Chem and evaluated in the rest of the paper. For brevity, hereinafter the parameterization using Eq. (10), Eq. (13), and Eq. (15) are referred to simply as “PAR1”, “PAR2”, and “PAR3”, respectively.

385





390 *Figure 2. Scatterplots of the results of ~~parameterization PAR3~~ parameterizations (y-axis) versus the full mechanism (x-axis) box model results for (a) IEPOX-SOA molar yield (PAR2 and PAR3) and (b) formation timescale- (PAR3). Formation timescale of the full mechanism box model was calculated as follows. We saved IEPOX concentrations for each timestep. We defined the formation timescale as the time when the IEPOX concentration is closest to the $1 - 1/e$ (~63%) of the final IEPOX concentration.*

395

4 Results

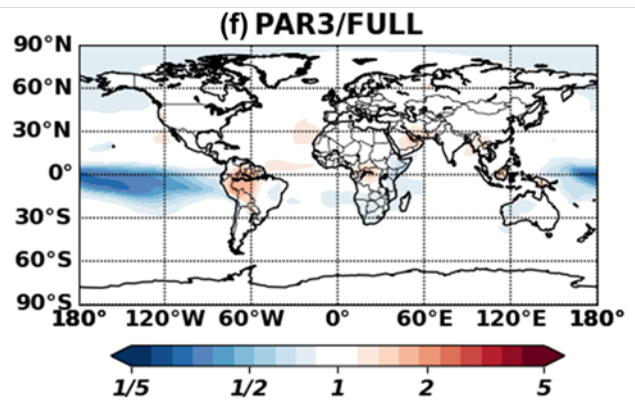
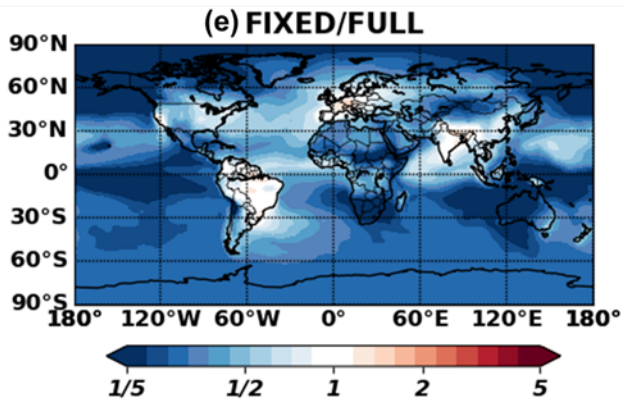
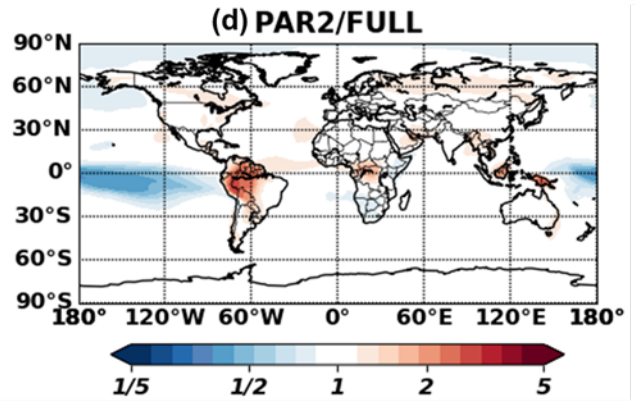
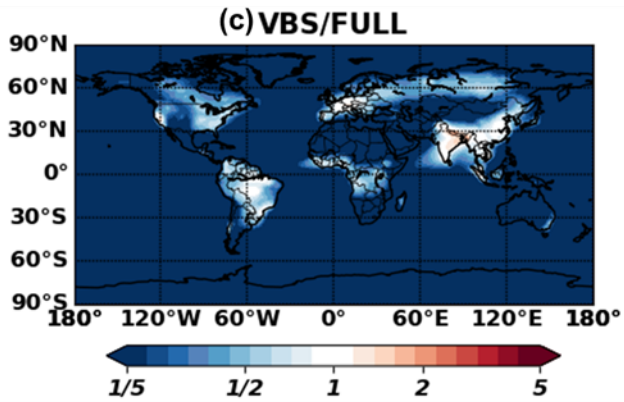
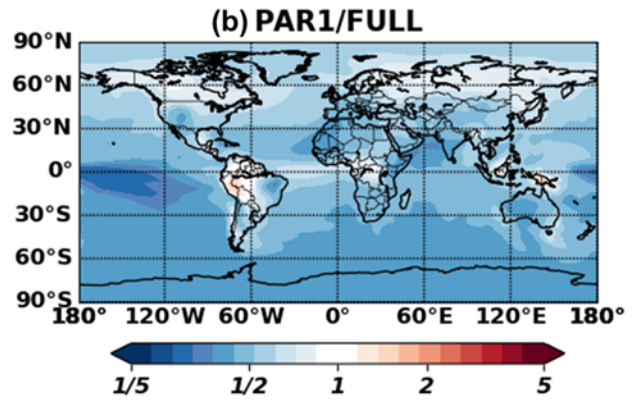
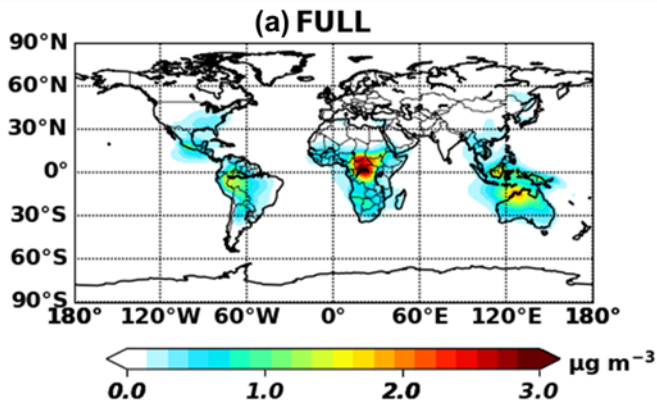
4.1. Full chemistry vs. Parameterizations

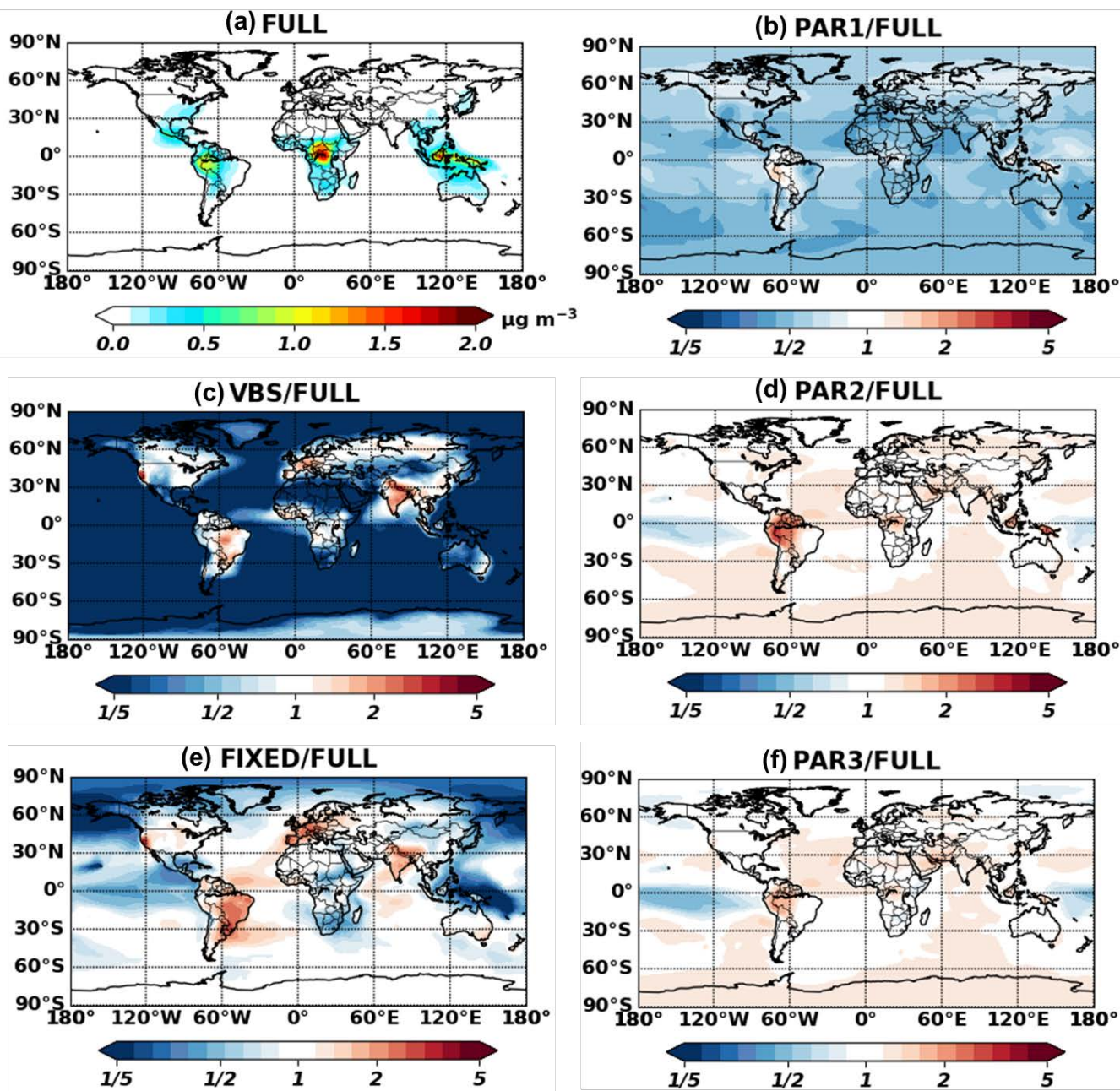
Figure 3 shows global annual surface maps of simulated IEPOX-SOA concentrations by using the full chemistry and the five parameterizations, while Figure 4 compares the concentrations and burdens. The fixed 3% yield parameterization (FIXED) ~~substantially~~ underestimated IEPOX-SOA concentrations with a slope of 0.34. ~~This underestimation became even worse for IEPOX-SOA concentrations below $0.1 \mu\text{g m}^{-3}$ where most of the points are located (Fig. S4).~~

400

66. Similar to the 3% parameterization, isoprene SOA concentrations with the VBS were substantially lower than those with the full chemistry and parameterizations. Isoprene SOA ratios of the VBS to the full chemistry were less than 20% except for the aerosol source regions (Fig. 3c), because more semi-volatile products can exist in aerosol phase due to high pre-existing aerosol concentrations in the source regions. Furthermore, the VBS/Full chemistry ratios were even higher than 1 for anthropogenic source dominant regions (California, western Europe, and Asia), where NO concentrations are high. However, the VBS predicted very low isoprene SOA concentrations in remote regions, leading to a low global burden (Fig. 4c). This dramatic difference came from the fact that the IEPOX-SOA is non-volatile in the full chemistry, but the isoprene SOA is treated as semi-volatile using the partitioning theory in the VBS. The VBS simulated most of the semi-volatile products as gas-phase (tropospheric burden of 237232 Gg) rather than aerosol-phase (tropospheric burden of 4948 Gg), especially for remote regions where pre-existing aerosol concentrations were low.

PAR1 generally underestimated IEPOX-SOA concentrations compared to the full chemistry simulation (slope = 0.6872; $R^2 = 0.989$), although with less bias and better skill than the default VBS (slope = 0.2958; $R^2 = 0.45$) and the fixed 3% yield simulation (slope = 0.34; $R^2 = 0.6547$). An important driver of the low bias vs. the full chemistry was the diurnal variation of the chemical fields. $Y_{IEPOX-SOA}$ is calculated in PAR1 using the instantaneous chemical fields at the time of isoprene emission, while in the full chemistry simulation (and in the real atmosphere), some processes proceed at different rates due to the different diurnal variations of key parameters.





425 **Figure 3.** Annual mean (July 2013 – June 2014) surface concentrations for IEPOX-SOA as predicted by full chemistry (a). Ratio of parameterized IEPOX-SOA concentrations to the full chemistry case are shown in (b,c,d,e,f).

To directly investigate the effect from the diurnal variation of the chemical fields, we used the box model to exclude other factors such as transport and deposition processes. First, we extracted isoprene emissions and chemical/meteorological fields affecting the IEPOX-SOA formation pathway from GEOS-Chem with 30 minutes temporal resolution (equivalent to the chemistry timestep of GEOS-Chem used in this study). Then we averaged global chemical/meteorological fields within the PBL based on local time at each grid point for four major isoprene source regions (the Southeastern United States, Amazon, Central Africa, and Borneo). In this way, we constructed the source regions–averaged diurnal profile of chemical species, temperature, boundary layer height, isoprene emission, and reaction rate constants as inputs of the box model. The underestimation of IEPOX-SOA concentrations by PAR1 also occurred when we calculated IEPOX-SOA with the box model (Fig. 4d). This was caused by the diurnal variation of chemical/meteorological fields, as PAR1 successfully captured the timeseries of IEPOX-SOA when we used constant input values (Fig. S5S7).

The box model simulation with the source regions–averaged diurnal cycle resulted in similar IEPOX-SOA concentrations between the two parameterizations directly calculating IEPOX (PAR2 and PAR3) and the full chemistry (Fig 4d). PAR2 and PAR3 also showed similar global spatial patterns vs. the full chemistry, althoughbut they slightly overestimated IEPOX-SOA over source regions (Amazon, Central Africa, and Southeast Asia) (Fig. 3d and 3f-), which was discussed in detail below.

The different performance between PAR1 and ~~PAR2~~ PAR3 was mainly caused by the differing influence of the diurnal variation profiles of chemical fields (Fig. S6). S8). Furthermore, the diurnal variation effect influenced the IEPOX-SOA yield differently for each IEPOX-SOA precursor. Compared to the chemical pathways simulated by the full chemistry, PAR1 calculated higher chemical losses for isoprene but lower chemical losses for ISOPO₂ as revealed in global budget analysis (Fig. 5).

The underestimation of PAR1 was mainly caused by two reactions – IEPOX + OH and IEPOX reactive uptake. During the daytime when OH concentration was high, IEPOX + OH reaction became dominant, which reduced the IEPOX-SOA yield by PAR1. However, in the full chemistry model, IEPOX was less consumed by OH because IEPOX was not formed immediately from isoprene emissions. IEPOX peaked around 4 p.m. (Fig. S8). Therefore, PAR1 overestimated the loss of IEPOX because it used higher IEPOX loss rate compared to the full chemistry. In a similar way, PAR1 underestimated the IEPOX reactive

uptake. In the full chemistry model, isoprene emission and OH peaked around local noon, but the IEPOX uptake rate constant peaked around 64 p.m. ~~Because it takes several hours to convert the emitted isoprene to IEPOX in the full chemistry case (Fig. 5a), the~~S8). The IEPOX-SOA yield calculated at the time of isoprene emission (in PAR1) ~~could underestimate~~underestimated the real IEPOX-SOA yield. For example, the instantaneous IEPOX-SOA yield using both isoprene emission and IEPOX ~~condensation rates~~reactive uptake rate constant at noon is lower than the yield calculated using the isoprene emission rate at 12 p.m. and the IEPOX ~~condensation~~reactive uptake rate constant at 64 p.m, when each process peaks, ~~explaining most of the underestimation in PAR1.~~

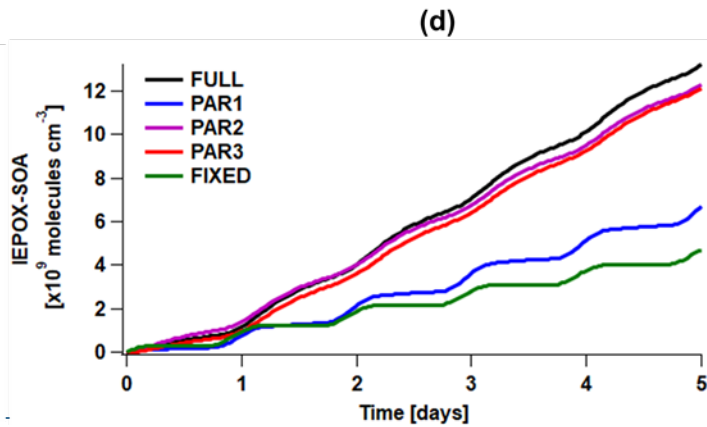
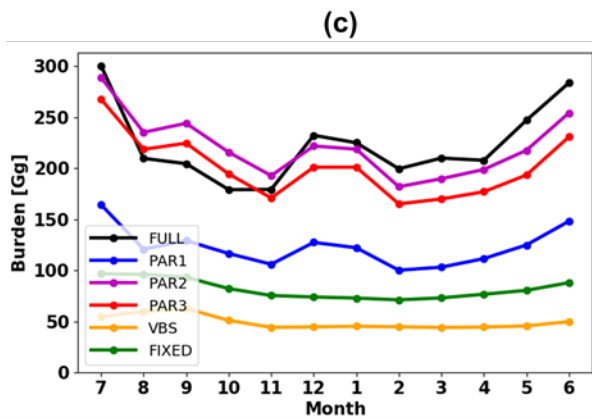
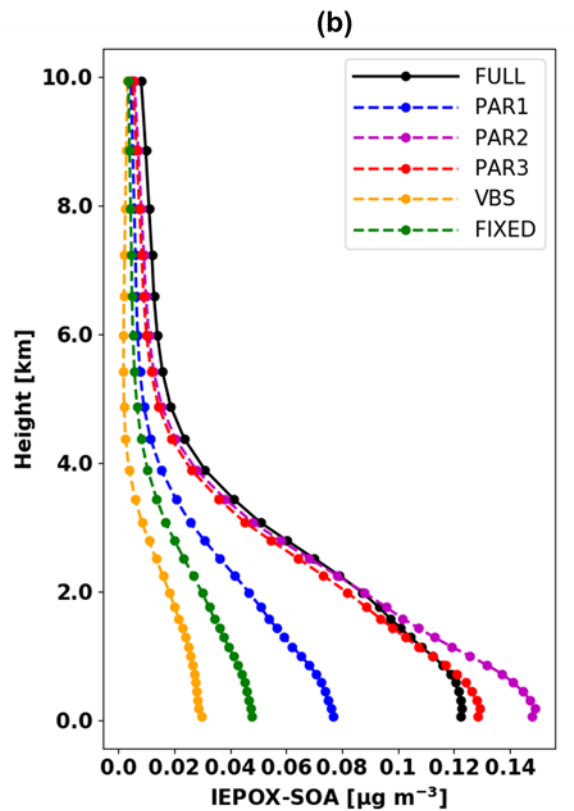
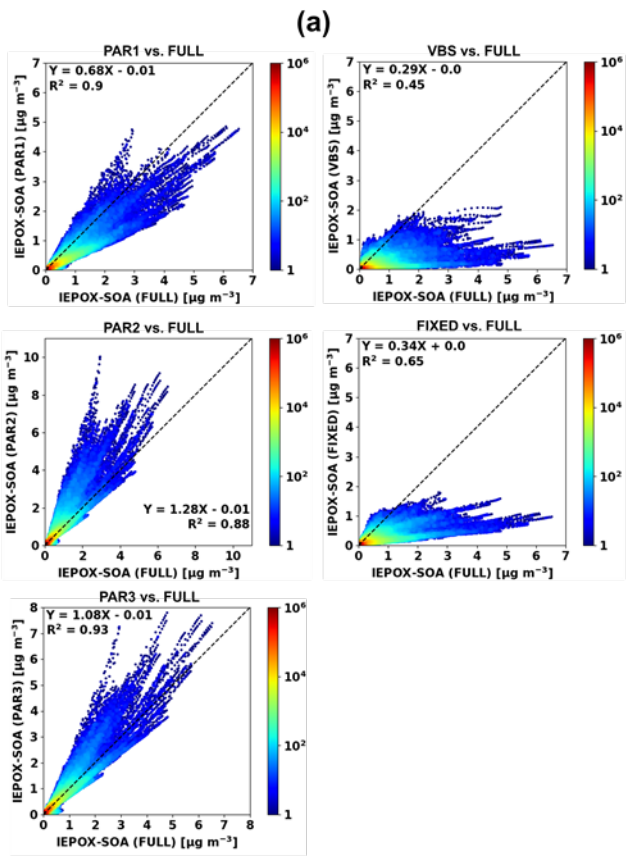
465 Contrary to PAR1, which calculated IEPOX-SOA yield at the time of isoprene emission, PAR2 and PAR3 did not show a global underestimation because they only calculated IEPOX yield at the time of isoprene emission, and then simulated the IEPOX ~~condensation rate explicitly. The 3% parameterization underestimated IEPOX-SOA globally except for Amazon, India, and Western Europe.~~reactive uptake explicitly. However, they showed slight overestimations over isoprene source regions such as the Amazon.

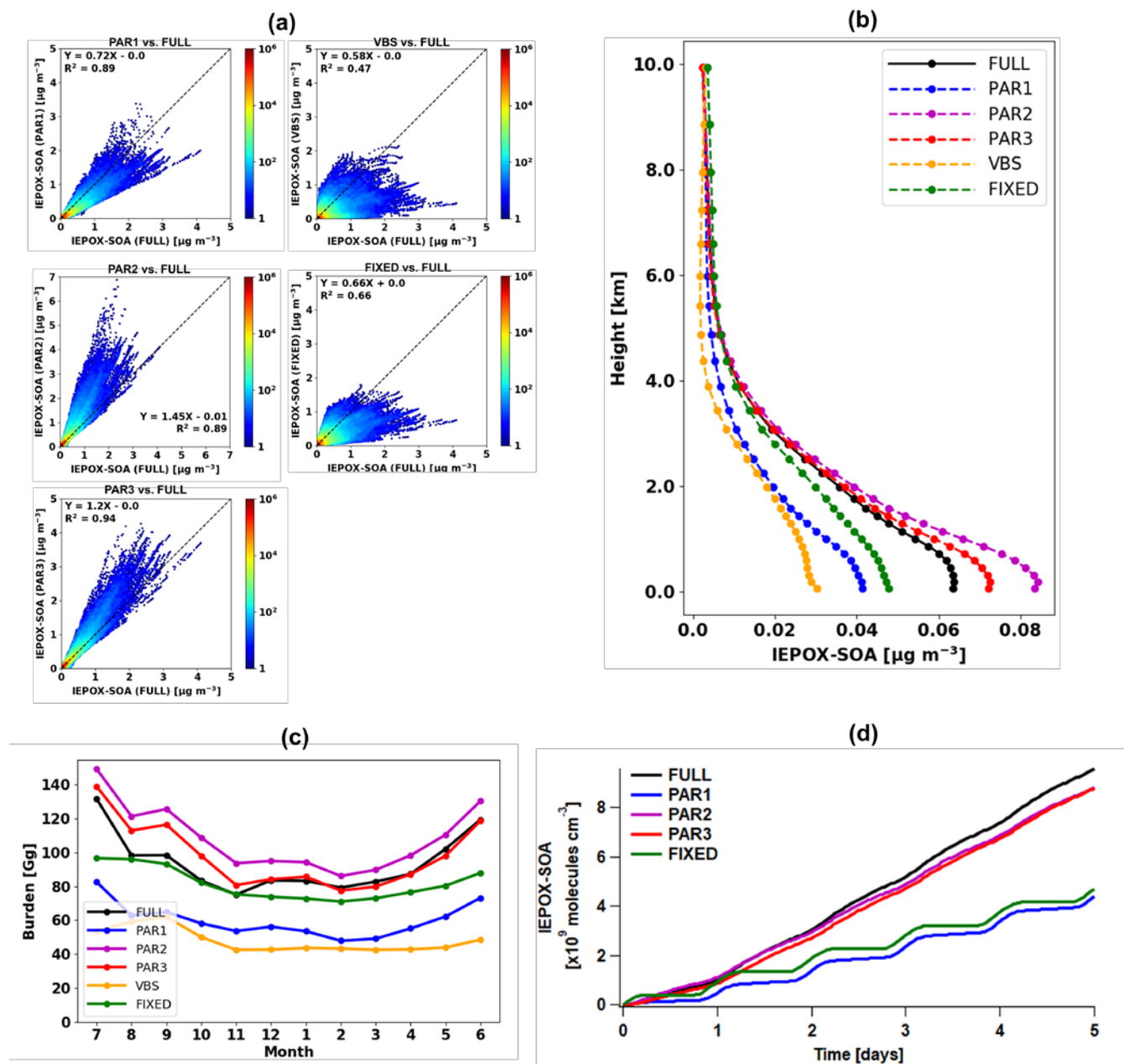
470 We found that PAR2 and PAR3 generally overestimate the IEPOX-SOA when OH concentrations are low (Fig. S9), and the Amazon is one of low OH regions from GEOS-Chem model (Fig. S10). We attributed this tendency to the effects of lifetime of IEPOX precursor gases, for which OH concentrations are one of the major controlling factors. IEPOX yields in PAR2 and PAR3 are calculated using the instantaneous chemical fields. Therefore, the discrepancies between the explicit chemistry and PAR2-3

475 are reduced when the lifetimes of precursor gases are short. For the southeastern US where PAR3 did not show an overestimation, the lifetimes of isoprene and ISOPOOH were 0.9 hours and 1.5 hours, respectively. The discrepancies are much larger for the Amazon, the lifetimes of isoprene and ISOPOOH are 12.3 hours and 6.1 hours, respectively, due to low OH concentrations. As a result, the PAR1-3

480 calculated the similar IEPOX production rate (1.9 Tg yr⁻¹) from the ISOPOOH + OH reaction compared to the full chemistry (1.8 Tg yr⁻¹) for the southeastern US, but the disagreement was larger for the Amazon (4.8 Tg yr⁻¹ in the PAR1-3 vs 3.9 Tg yr⁻¹) in the full chemistry). We anticipate that the discrepancy in source regions will be reduced in the future version of GEOS-Chem, because GEOS-Chem with the most up to date isoprene mechanism predicts higher OH concentrations (up to 250% increase) in Amazon,

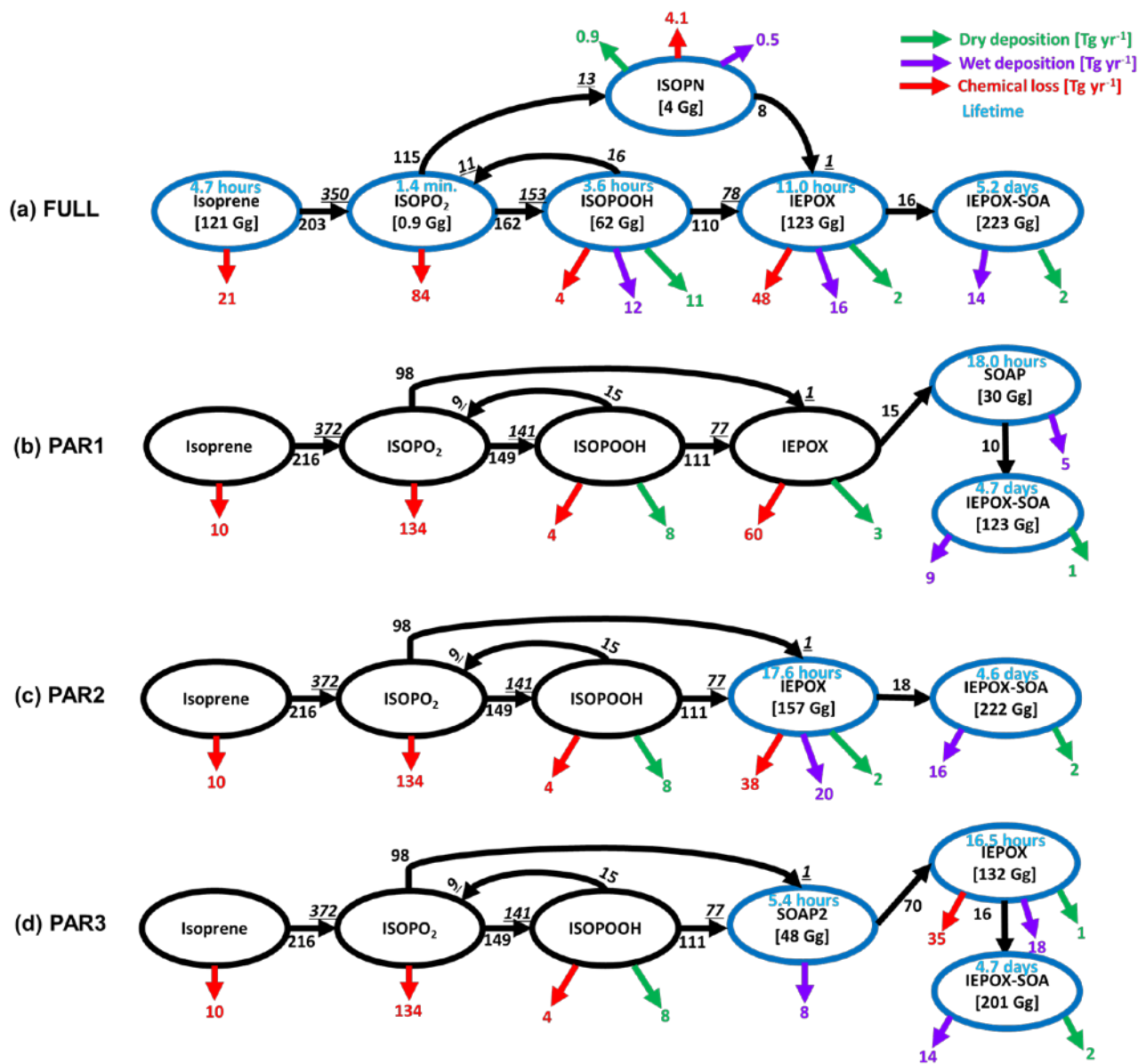
485 central Africa, and Borneo regions compared to the isoprene mechanism used in this study (Fig. S17 in Bates and Jacob, 2019).





490 Figure 4. (a) Scatterplots of parameterized (y-axis) versus full chemistry IEPOX-SOA (x-axis) concentrations within the troposphere for July 2013 – June 2014. Each point represents monthly averaged
 495 model grid value of IEPOX-SOA concentration. Colors represent the density of points, where densities were calculated by dividing x and y axis ranges into 100 by 100 grid cells. (b) Vertical profiles of global annual mean average IEPOX-SOA concentrations. The vertical locations of the markers indicate the mid levels of the vertical grid boxes in GEOS-Chem. (c) Timeseries of global tropospheric burdens of IEPOX-SOA [Gg]. (d) Timeseries of IEPOX-SOA concentrations simulated by the box model. The VBS was not

500 *calculated with the box model, as it requires additional partitioning calculation with pre-existing aerosols, which are calculated online in GEOS-Chem. Input chemical/meteorological fields were averaged from GEOS-Chem results for four major isoprene source regions [the Southeastern United States: 30°N – 40°N, 100°W – 80°W, Amazon: 10°S – 0°S, 70°W – 60°W, Central Africa: 5°N – 15°N, 10°E – 30°E, Borneo: 5°S – 5°N, 105°E – 120°E]. Input values represent annual mean values, which were calculated by using the first two days of each month model outputs at 30 minutes interval averaged within the PBL.*



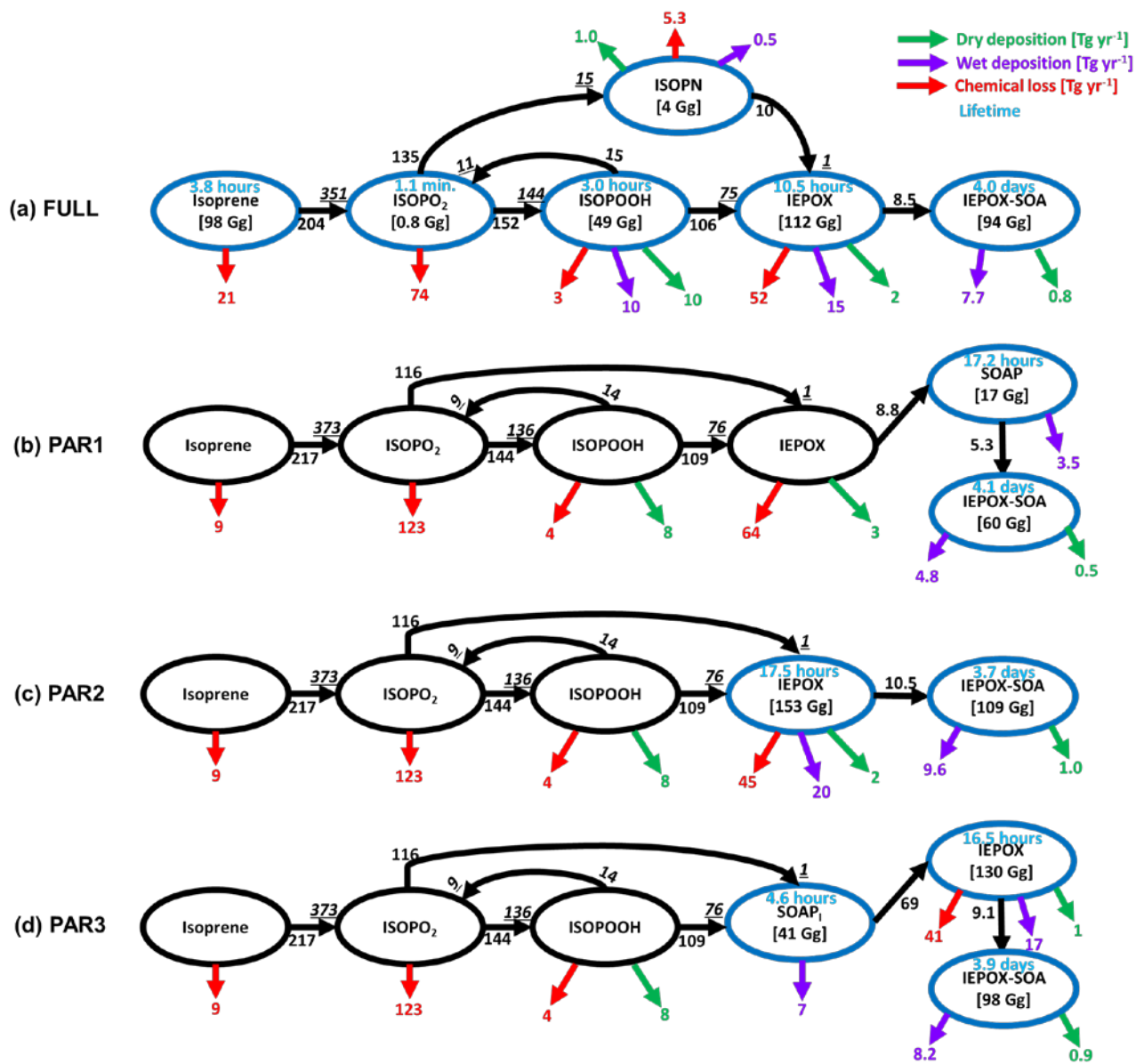
505

510

Parameterizations using chemical fields (PAR1–3) captured the variability of IEPOX-SOA well with R^2 values of 0.89–0.94. PAR3 always showed the best R^2 and slopes in terms of not only annual mean (Fig. 4a) but also monthly mean evaluation (Fig. S11), due to the fact that the structure of PAR3 was closer to that of full chemistry compared to other parameterizations. PAR3 requires three tracers and has a slightly higher computational cost than PAR1 and PAR2 that need two tracers to simulate IEPOX-SOA (Table 1).

In terms of vertical profiles (Fig. 4b), PAR2 and PAR3 again showed the best results, although these parameterizations slightly overestimated surface concentrations. On the other hand, PAR1, the VBS, and the 3% yield substantially underestimated concentrations below 4 km.

515 The annual mean global tropospheric burden of IEPOX-SOA by full chemistry was 94 Gg, vs. 60, 108, 98, 48, and 82 Gg for PAR1, PAR2, PAR3, the VBS, and the 3%, respectively. Global IEPOX-SOA burden of PAR3 was within ~5% of IEPOX-SOA burden simulated by full chemistry. Furthermore, we found that PAR2 and PAR3 showed similar monthly variations to the full chemistry (Fig. 4c). It also applied to the seasonal patterns of the hemispheric burden when we separated them for the northern and
520 southern hemispheres as shown in Fig. S12. We also found that the fixed 3% yield generally well reproduced the global burden amount of IEPOX-SOA, which gave some confidence in using the 3% yield derived from the Southeastern US summer conditions in terms of reproducing the global burden of IEPOX-SOA.



525

530

Figure 5. Global budget analysis of IEPOX-SOA formation from isoprene on a total annual mean basis (July 2013 – June 2014). Black arrows with numbers show the IEPOX-SOA formation pathways. Two numbers are shown if the loss amount of reactant differs from the production amount of product (underline italic), which are caused by the different molecular weights and product yields. *Isoprene nitrate (ISOPN) production pathway from isoprene + NO₃ reaction is not shown.* Chemical losses that are not leading to IEPOX-SOA formation are shown in red arrows. Dry and wet deposition amounts are presented in green and purple arrows, respectively. Tropospheric burdens are given in brackets if species

is explicitly simulated in the model. Blue circles are used for species that are explicitly simulated in each case.

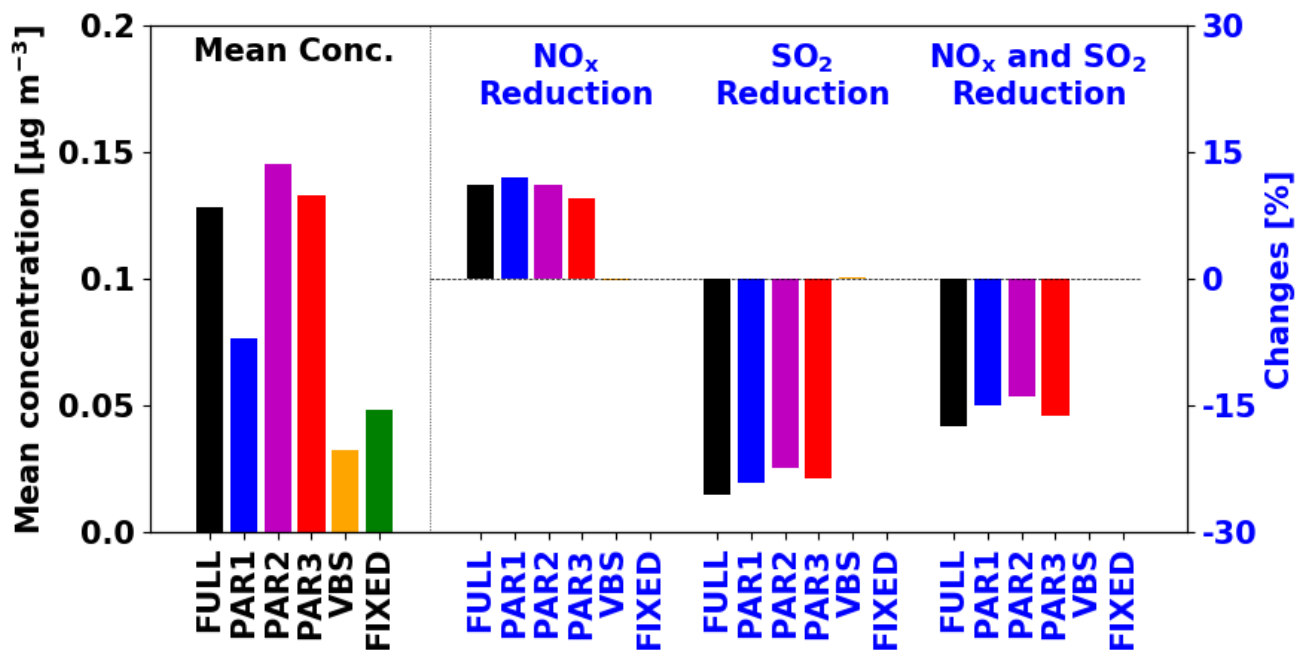
535 ~~Parameterizations using chemical fields (PAR1, PAR2, and PAR3) captured the variability of IEPOX-SOA well with R² values of 0.88–0.93. PAR3 always showed the best R² and slopes in terms of not only annual mean (Fig. 4a) but also monthly mean evaluation (Fig. S7), due to the fact that the structure of PAR3 was closer to that of full chemistry compared to other parameterizations. PAR3 requires three tracers and has a slightly higher computational cost than PAR1 and PAR2 that need two tracers to simulate~~
540 ~~IEPOX-SOA (Table 1).~~

~~In terms of vertical profiles (Fig. 4b), PAR2 and PAR3 again showed the best results, although these parameterizations slightly overestimated surface concentrations and underestimated upper troposphere concentrations. The slightly shorter average lifetime of IEPOX-SOA by PAR2/PAR3 (4.6–4.7 days) vs. full chemistry (5.2 days) (Fig. 5) resulted in slightly reduced upward transport. On the other hand, PAR1, the VBS, and the 3% yield substantially underestimated both surface and free tropospheric concentrations.~~

545 ~~The annual mean global tropospheric burden of IEPOX-SOA by full chemistry was 223 Gg, vs. 123, 222, 201, 49, and 82 Gg for PAR1, PAR2, PAR3, the VBS, and the 3%, respectively. Global IEPOX-SOA burdens of PAR2 and PAR3 were within ~10% of IEPOX-SOA burden simulated by full chemistry. Furthermore, we found that PAR2 and PAR3 showed similar monthly variations for global burdens; as well as, absolute values compared to full chemistry (Fig. 4c).~~

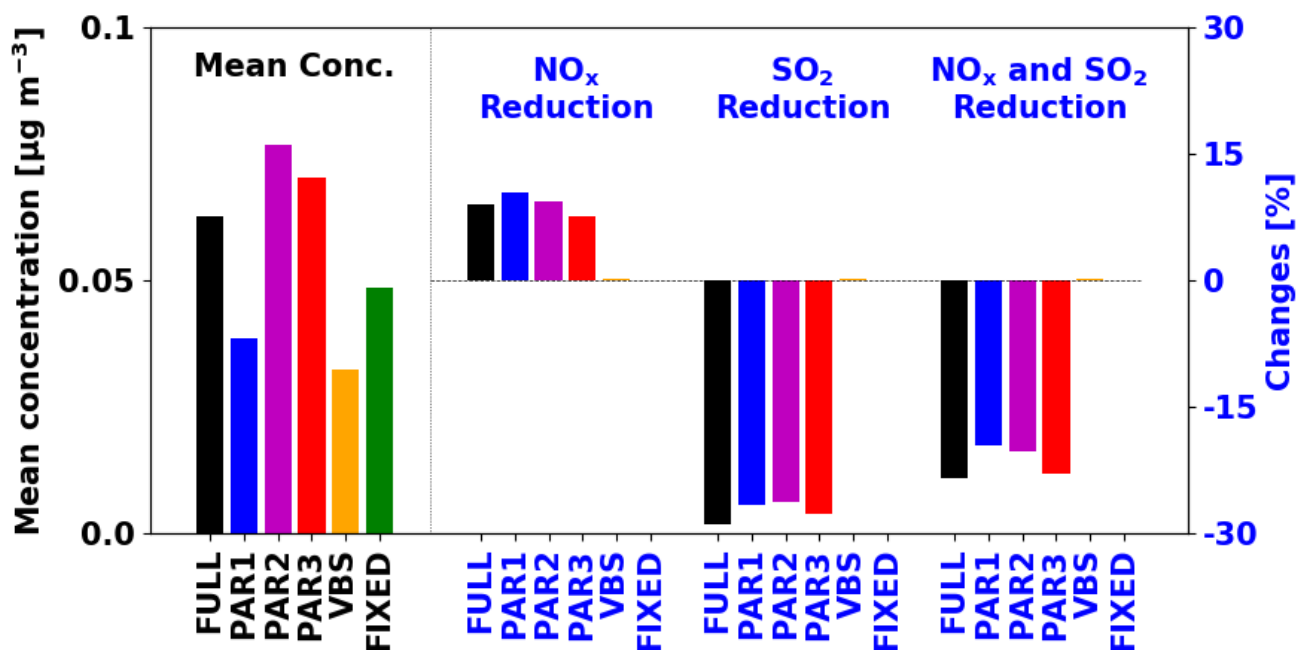
We calculated the annual mean global budgets of IEPOX-SOA simulated by the full chemistry and the parameterizations developed in this study (Fig. 5). Generally, each term is of the same order, with some differences in some cases, which are mainly due to the diurnal variation of the chemical fields. For example, the isoprene loss by O₃ and NO₃ was 21 Tg yr⁻¹ for the full chemistry, but this loss was reduced
555 to ~~109~~ 123 Tg yr⁻¹ in our parameterizations. Because NO₃ concentration was very low during the daytime when isoprene was emitted (Fig. S6S8), our parameterizations using the instantaneous yield applied to isoprene emission underestimated isoprene loss by NO₃. On the other hand, ISOPO₂ loss was higher in our parameterizations (~~134~~ 123 Tg yr⁻¹) than in the full chemistry (~~8474~~ Tg yr⁻¹) because chemical species affecting ISOPO₂ loss (~~CH₃O₂ and CH₃CO₃~~ in Fig. S6S8) had similar diurnal variation patterns compared
560 to the isoprene emission.

Although there were some differences between the results of the parameterizations and the full chemistry above, the parameterizations generally showed similar source and sink values compared to the full chemistry. The full chemistry showed annual production of ~~153~~144 Tg yr⁻¹ ISOPOOH, which was similar to the value estimated by the parameterizations (~~141~~136 Tg yr⁻¹). That was also the case for the annual production of IEPOX (~~78~~75 Tg yr⁻¹ vs. ~~70~~76 Tg yr⁻¹). Results in Fig. 5 imply that chemical reaction-based parameterizations can capture global budgets of IEPOX-SOA chemistry with reasonable accuracy without explicit calculation of all intermediates. Furthermore, we found that the flux from IEPOX (or SOAP) to IEPOX-SOA was important for IEPOX-SOA simulation capability. For example, the flux from IEPOX to IEPOX-SOA in PAR3 was ~~16~~9.1 Tg yr⁻¹, which was ~~same~~similar to the flux (~~16~~8.5 Tg yr⁻¹) in the full chemistry, and PAR3 showed the best results. On the other hand, the production of IEPOX-SOA was ~~10~~5.3 Tg yr⁻¹ in PAR1, which was the main reason for the IEPOX-SOA underestimation in that case.



575 When the explicit full chemistry changed, and the resulting IEPOX-SOA burden was increased by a factor of two, our parameterizations showed very similar statistical parameters and evaluation results compared to the full chemistry (See Figs. 3 and 4 in the discussion paper and response to reviewers for more details). In other words, our parameterizations are robust to the changes of chemistry. This characteristic can be further confirmed by emission sensitivity tests as discussed below.

580



585 *Figure 6. Global PBL averaged IEPOX-SOA concentrations (left, black) and the concentration changes with anthropogenic emission reductions (right, blue) for July – August 2013. The anthropogenic emissions were decreased by 50% for each sensitivity case.*

Finally, we investigated the effects of anthropogenic emission reductions on the simulated IEPOX-SOA concentrations. We conducted additional sensitivity tests for two months by reducing NO_x and SO₂ emissions by 50%. New parameterizations (PAR1–3) showed similar sensitivities to the full chemistry case, but the VBS and fixed 3% parameterizations did not reproduce changes relative to emission reductions (Fig. 6). Isoprene SOA concentrations by the fixed 3% parameterizations remain the same because they are using the constant yield.

The VBS showed negligible sensitivities (less than 0.3%). For the VBS, ~~changes~~the change in the rate of oxidation of isoprene is the most important factor that can affect ~~the~~isoprene SOA ~~changes~~change. We found that OH concentrations were decreased in the NO_x reduction case (Fig. S8aS13a). However, isoprene concentrations were increased (Fig. S8bS13b) due to the reduced oxidant fields affecting isoprene loss (OH, O₃, and NO₃), because the chemical loss is the only pathway for isoprene loss (i.e. no

isoprene is lost by dry and wet deposition) and isoprene emissions are unaffected. As a result, the initial rate oxidation of isoprene (rate constant \times [isoprene] \times [OH]) did not show the significant changes (Fig. S8dS13d), as is also observed for isoprene SOA (Fig. S8fS13f).

However, in the explicit full chemistry, for the sensitivity case of NO_x emission reduction, the contribution of HO₂ pathway was increased compared to the NO pathway, making more IEPOX and IEPOX-SOA. The reduced sulfate aerosol caused by the SO₂ emission reduction increases aerosol pH and decreases available aerosol surface area, which eventually decreases IEPOX reactive uptake. New parameterizations successfully captured these tendencies, indicating that they will be much more accurate compared to the current parameterizations in simulating the response of isoprene SOA to different scenarios, such as the response to future climates or anthropogenic emission reduction scenarios.

Table 1. Computational time estimation for the simulation of IEPOX-SOA using the full chemistry and parameterization cases in the box model and GEOS-Chem. The box model results are mean values of 1,000 simulations based on 5-days integration time. The VBS was not simulated in the box model, because the VBS requires the partitioning calculation with pre-existing aerosol concentrations, which are not available in the box model, and are calculated online in GEOS-Chem. For GEOS-Chem, values were based on 7-days simulation using 32 cores on NCAR Cheyenne machine. The Gprof performance analysis tool was used to calculate how much time was spent in subroutines with Intel Fortran Compiler 17.0.1 with '-p' option. Values were estimated by multiplying the total time spent in each process by the contribution of related reactions/species for each case, except for time estimates for chemistry of parameterizations¹). For example, transport time in full chemistry was calculated by multiplying 2978 s (total transport time in Table S4) by 10 (Total number of the full chemistry species) / 173 (Total number of advected species).

	Box model [s]	GEOS-Chem [s]				
	Chemistry	Chemistry	Transport	Dry deposition	Wet deposition	Total

FULL	1.5285	559	172	30	380	1141
VBS	-	7	120	20	253	400
PAR1	0.0028 ¹⁾	47	34	7	84	172
PAR2	0.0023 ¹⁾	13	34	7	84	138
PAR3	0.0028 ¹⁾	48	52	7	127	234
FIX FIXED	0.0012 ¹⁾	1	34	3	42	80

4.2. Computational time estimation

We estimated computational time related ~~with~~to IEPOX-SOA simulation for the full chemistry and the
630 different parameterizations. The box model was used for estimating the time needed for chemistry calculation using chemical reactions and dry depositions in Table S1. All the parameterizations showed much faster integration time compared to the full chemistry.

For estimation within GEOS-Chem, we used the Gprof function profiling program and categorized the results according to four major processes (chemistry, transport, dry deposition, and wet deposition), as
635 shown in Table 1. One of ~~the~~ main ~~advantage~~~~advantages~~ of using a function profiling program is that all of ~~the~~ timings are estimated at once without ~~the~~ need for multiple simulations. Because model computational time varies between individual executions even for the same machine and code (Philip et al., 2016), and because we examined a minority (IEPOX-SOA chemistry) of total GEOS-Chem model reactions, computational time estimation using multiple runs can lead to significant errors.

640 Our parameterizations (PAR1–3) reduced the computational time by factors ~5 and ~2 compared to the full chemistry and the VBS, respectively. There was a factor of two difference among parameterizations due to two main reasons. First, the difference between PAR1 and PAR2 arose from the additional calculation of formation timescale in PAR1 (Eq. 12). Second, the number of species was a key factor making ~~the~~ difference between PAR1 (2 species) and PAR3 (3 species). The 3% showed the best
645 efficiency—the cost of the 3% case was ~2–3 times less than those of the PAR1–3, given its simplest structure.

When using GEOS-Chem, the full chemistry can still be chosen if the computational cost is not important or the detailed gas-phase chemical reactions are needed. Our developed parameterizations (PAR1–3) can be useful for researchers who are not interested in the details of isoprene SOA, but who
650 still want to have realistic aerosol concentrations in their simulations. PAR3 adds significant accuracy compared to the 3% yield GEOS-Chem default for limited additional cost. The ~~VBS~~default VBS in
GEOS-Chem v11-02-rc requires more computational cost than all of the parameterizations while being less accurate, and we recommend against its use in future simulations. Although we have used GEOS-Chem as a convenient development platform, the parameterizations may be especially useful for climate
655 models for long-term simulations using other codes.

5 Conclusions

IEPOX-SOA is thought to dominate the contribution of isoprene to SOA, but it is formed by complex multiphase chemistry which cannot be accurately simulated by the commonly used lumped volatility-basis-set or fixed yield SOA schemes. A detailed isoprene chemistry mechanism has been recently
660 developed and implemented in some models, and recent studies have found good agreement between observed and simulated IEPOX-SOA concentrations. However, the detailed chemistry requires higher computational cost than the lumped SOA schemes, which may not be applicable for long-term multi-scenario simulations in climate and similar models. The likely addition of other explicit SOA mechanisms
665 as knowledge improves in the future would exacerbate this problem.

Here we developed parameterization methods to enable accurate yet fast IEPOX-SOA formation for climate model applications that mostly require having the correct SOA mass, spatio-temporal distribution, and response to changes in important precursors, for accurate calculations of the aerosol radiative effects. First, we developed a method to calculate the yield of IEPOX-SOA from isoprene emissions based on an
670 approximate analytical solution of the full mechanism. Numerical fitting to box model results was introduced when the reaction could not be directly implemented for yield calculation. Formation timescales of key products were also used to more accurately represent the characteristic time of formation

of IEPOX-SOA. Therefore, our parameterizations used two (PAR1 and PAR2) or three tracers (PAR3) to simulate IEPOX-SOA without the full chemical mechanism.

675 The parameterizations (especially ~~PAR2 and~~ PAR3) generally captured the spatial and temporal variations of IEPOX-SOA including sources, sinks, burdens, surface concentrations, and vertical profiles. Furthermore, the parameterizations showed better performance and lower computational cost compared to the current fixed yield or VBS schemes in GEOS-Chem. Therefore, these parameterizations can be used for more accurate predictions of surface concentrations; as well as, climate effects such as direct
680 radiative forcing calculation.

The parameterizations can be easily updated if new values of key parameters are adopted by the community (e.g. ~~the~~ Henry's law constant of IEPOX). The differences between the parameterizations and the full chemistry were mostly explained by non-linear effects due to the diurnal variation of chemical/meteorological fields, which cannot be captured without additional complexity. One caveat is
685 that some climate models use monthly mean fields of VOCs and oxidants. Because the diurnal variation was found to be important for accurate predictions of IEPOX-SOA, this may reduce the accuracy of the results for such models. We recommend that climate models account for diurnal variations for each chemical field in order to obtain more accurate IEPOX-SOA concentrations.

Detailed mechanistic studies in the laboratory, often aided by new mass spectrometry instrumentation
690 with higher molecular detail, are leading to the development of many detailed SOA mechanisms, which will challenge global and especially climate models with their increased computational cost. The method developed in this study can be used to simplify other SOA mechanisms, allowing more accurate SOA simulations while limiting computational cost.

695 *Code and Data Availability.* The KinSim box model ~~will be publicly available on the web (can be~~
downloaded from [http://eires1.colorado.edu/jimenez-](http://eires1.colorado.edu/jimenez-group/wiki/index.php/Analysis_Software#tinyurl.com/kinsim-release)
[group/wiki/index.php/Analysis_Software#tinyurl.com/kinsim-release](http://eires1.colorado.edu/jimenez-group/wiki/index.php/Analysis_Software#tinyurl.com/kinsim-release) (preferred, due to updates) or from
the supporting information
700 (https://pubs.acs.org/doi/suppl/10.1021/acs.jchemed.9b00033/suppl_file/ed9b00033_si_001.zip) of Peng

705 and Jimenez (2019). The different KinSim_Software) but it is currently available upon request (jose.jimenez@colorado.edu). chemical mechanisms used for the box model are available in the supplement of this paper, and also at <https://tinyurl.com/kinsim-cases>. They can be directly loaded into KinSim to reproduce the calculations in this work. GEOS-Chem v11-02-rc and meteorological data can be downloaded from GEOS-Chem [website/wiki](http://wiki.seas.harvard.edu/geos-chem/index.php/Downloading_GEOS-Chem_source_code_and_data) (http://wiki.seas.harvard.edu/geos-chem/index.php/Downloading_GEOS-Chem_source_code_and_data). GEOS-Chem code modifications for new parameterizations and global model data are available upon email request ~~submitted to the corresponding author~~ (jose.jimenez@duseong.jo@colorado.edu).

710 *Author contributions.* JLJ, AH, LKE, and ~~LKE~~DSJ designed the research. ZP developed the KinSim box model and supported the implementation of the full IEPOX-SOA chemistry in it. WH conducted the IEPOX reactive uptake calculation within Igor Pro. DSJ and EAM conducted global model simulations. BAN ~~conceived~~contributed to the ~~ideas of~~ aerosol pH calculation. PCJ analyzed the IEPOX-SOA data. DSJ, JLJ, and AH developed the parameterizations. DSJ and JLJ wrote the original paper, and all authors
715 contributed to the review and editing of the paper.

Competing interests. The authors declare that they have no conflict of interest.

720 *Acknowledgements.* This publication was supported by US EPA STAR 83587701-0, NOAA NA18OAR4310113, DOE (BER/ASR) DE-SC0016559, NSF AGS-1822664, and the European Research Council (grant No. 819169). It has not been formally reviewed by EPA. The views expressed in this document are solely those of the authors and do not necessarily reflect those of the Agency. EPA does not endorse any products or commercial services mentioned in this publication. We thank Prasad Kasibhatla for useful discussions.

725

730

735

740

745 **References**

Allen, H. M., Draper, D. C., Ayres, B. R., Ault, A., Bondy, A., Takahama, S., Modini, R. L., Baumann, K., Edgerton, E., Knote, C., Laskin, A., Wang, B. and Fry, J. L.: Influence of crustal dust and sea spray supermicron particle concentrations and acidity on inorganic NO_3^- aerosol during the 2013 Southern Oxidant and Aerosol Study, *Atmos. Chem. Phys.*, 15, 10669–10685, doi:10.5194/acp-15-10669-2015, 750 2015.

~~Anttila, T., Kiendler-Scharr, A., Tillmann, R. and Mentel, T. F.: On the Reactive Uptake of Gaseous Compounds by Organic Coated Aqueous Aerosols: Theoretical Analysis and Application to the Heterogeneous Hydrolysis of N_2O_5 , *J. Phys. Chem. A*, 110, 10435–10443, doi:10.1021/jp062403e, 2006.~~

- 755 [Bates, K. H. and Jacob, D. J.: A new model mechanism for atmospheric oxidation of isoprene: global effects on oxidants, nitrogen oxides, organic products, and secondary organic aerosol, Atmos. Chem. Phys. Discuss., 2019, 1–46, doi:10.5194/acp-2019-328, 2019.](#)
- Bates, K. H., Crounse, J. D., St. Clair, J. M., Bennett, N. B., Nguyen, T. B., Seinfeld, J. H., Stoltz, B. M. and Wennberg, P. O.: Gas phase production and loss of isoprene epoxydiols, *J. Phys. Chem. A*, 118, 760 1237–1246, doi:10.1021/jp4107958, 2014.
- Bey, I., Jacob, D. J., Yantosca, R. M., Logan, J. A., Field, B. D., Fiore, A. M., Li, Q.-B., Liu, H.-Y., Mickley, L. J. and Schultz, M. G.: Global Modeling of Tropospheric Chemistry with Assimilated Meteorology: Model Description and Evaluation, *J. Geophys. Res.*, 106, 73–95, doi:10.1029/2001JD000807, 2001.
- 765 Bondy, A. L., Bonanno, D., Moffet, R. C., Wang, B., Laskin, A. and Ault, A. P.: The diverse chemical mixing state of aerosol particles in the southeastern United States, *Atmos. Chem. Phys.*, 18, 12595–12612, doi:10.5194/acp-18-12595-2018, 2018.
- Budisulistiorini, S. H., Nenes, A., Carlton, A. G., Surratt, J. D., McNeill, V. F. and Pye, H. O. T.: Simulating Aqueous-Phase Isoprene-Epoxydiol (IEPOX) Secondary Organic Aerosol Production during 770 the 2013 Southern Oxidant and Aerosol Study (SOAS), *Environ. Sci. Technol.*, 51, 5026–5034, doi:10.1021/acs.est.6b05750, 2017.
- Carlton, A. G., Wiedinmyer, C. and Kroll, J. H.: A review of Secondary Organic Aerosol (SOA) formation from isoprene, *Atmos. Chem. Phys.*, 9, 4987–5005, doi:10.5194/acp-9-4987-2009, 2009.
- Carlton, A. G., de Gouw, J., Jimenez, J. L., Ambrose, J. L., Attwood, A. R., Brown, S., Baker, K. R., 775 Brock, C., Cohen, R. C., Edgerton, S., Farkas, C. M., Farmer, D., Goldstein, A. H., Gratz, L., Guenther, A., Hunt, S., Jaeglé, L., Jaffe, D. A., Mak, J., McClure, C., Nenes, A., Nguyen, T. K., Pierce, J. R., de Sa, S., Selin, N. E., Shah, V., Shaw, S., Shepson, P. B., Song, S., Stutz, J., Surratt, J. D., Turpin, B. J., Warneke, C., Washenfelder, R. A., Wennberg, P. O. and Zhou, X.: Synthesis of the Southeast Atmosphere Studies: Investigating Fundamental Atmospheric Chemistry Questions, *Bull. Am. Meteorol. Soc.*, 99, 780 547–567, doi:10.1175/BAMS-D-16-0048.1, 2018.

- St. Clair, J. M., Rivera-Rios, J. C., Crouse, J. D., Knap, H. C., Bates, K. H., Teng, A. P., Jorgensen, S., Kjaergaard, H. G., Keutsch, F. N. and Wennberg, P. O.: Kinetics and Products of the Reaction of the First-Generation Isoprene Hydroxy Hydroperoxide (ISOPOOH) with OH, *J. Phys. Chem. A*, 120, 1441–1451, doi:10.1021/acs.jpca.5b06532, 2016.
- 785 Fairlie, T. D., Jacob, D. J. and Park, R. J.: The impact of transpacific transport of mineral dust in the United States, *Atmos. Environ.*, 41, 1251–1266, 2007.
- Fountoukis, C. and Nenes, A.: ISORROPIA II : a computationally efficient thermodynamic equilibrium model for K^+ - Ca^{2+} - Mg^{2+} - Na^+ - SO_4^{2-} - NO_3^- - Cl^- - H_2O aerosols, *Atmos. Chem. Phys.*, 7, 4639–4659, 2007.
- 790 Fu, T., Jacob, D. J., Wittrock, F., Burrows, J. P., Vrekoussis, M. and Henze, D. K.: Global budgets of atmospheric glyoxal and methylglyoxal, and implications for formation of secondary organic aerosols, *J. Geophys. Res.*, 113, 2008.
- Gaston, C. J., Riedel, T. P., Zhang, Z., Gold, A., Surratt, J. D. and Thornton, J. A.: Reactive uptake of an isoprene-derived epoxydiol to submicron aerosol particles, *Environ. Sci. Technol.*, 48, 11178–11186, 795 2014a.
- Gaston, C. J., Thornton, J. A. and Ng, N. L.: Reactive uptake of N_2O_5 to internally mixed inorganic and organic particles: the role of organic carbon oxidation state and inferred organic phase separations, *Atmos. Chem. Phys.*, 14, 5693–5707, 2014b.
- Guo, H., Sullivan, A. P., Campuzano-Jost, P., Schroder, J. C., Lopez-Hilfiker, F. D., Dibb, J. E., Jimenez, 800 J. L., Thornton, J. A., Brown, S. S., Nenes, A. and Weber, R. J.: Fine particle pH and the partitioning of nitric acid during winter in the northeastern United States, *J. Geophys. Res.*, 121, 10355–10376, doi:10.1002/2016JD025311, 2016.
- Hatch, L. E., Creamean, J. M., Ault, A. P., Surratt, J. D., Chan, M. N., Seinfeld, J. H., Edgerton, E. S., Su, Y. and Prather, K. A.: Measurements of Isoprene-Derived Organosulfates in Ambient Aerosols by 805 Aerosol Time-of-Flight Mass Spectrometry - Part 1: Single Particle Atmospheric Observations in Atlanta, *Environ. Sci. Technol.*, 45, 5105–5111, doi:10.1021/es103944a, 2011.

- Hodzic, A. and Jimenez, J. L.: Modeling anthropogenically controlled secondary organic aerosols in a megacity: A simplified framework for global and climate models, *Geosci. Model Dev.*, 4, 901, 2011.
- Hu, W., Palm, B. B., Day, D. A., Campuzano-Jost, P., Krechmer, J. E., Peng, Z., De Sa Suzane, S., Martin, S. T., Alexander, M. L., Baumann, K., Hacker, L., Kiendler-Scharr, A., Koss, A. R., De Gouw, J. A., Goldstein, A. H., Seco, R., Sjostedt, S. J., Park, J. H., Guenther, A. B., Kim, S., Canonaco, F., Prévôt, A. S. H., Brune, W. H. and Jimenez, J. L.: Volatility and lifetime against OH heterogeneous reaction of ambient isoprene-epoxydiols-derived secondary organic aerosol (IEPOX-SOA), *Atmos. Chem. Phys.*, 16, 11563–11580, doi:10.5194/acp-16-11563-2016, 2016.
- 815 Hu, W. W., Campuzano-Jost, P., Palm, B. B., Day, D. A., Ortega, A. M., Hayes, P. L., Krechmer, J. E., Chen, Q., Kuwata, M., Liu, Y. J., De Sá, S. S., McKinney, K., Martin, S. T., Hu, M., Budisulistiorini, S. H., Riva, M., Surratt, J. D., St. Clair, J. M., Isaacman-Van Wertz, G., Yee, L. D., Goldstein, A. H., Carbone, S., Brito, J., Artaxo, P., De Gouw, J. A., Koss, A., Wisthaler, A., Mikoviny, T., Karl, T., Kaser, L., Jud, W., Hansel, A., Docherty, K. S., Alexander, M. L., Robinson, N. H., Coe, H., Allan, J. D.,
- 820 Canagaratna, M. R., Paulot, F. and Jimenez, J. L.: Characterization of a real-time tracer for isoprene epoxydiols-derived secondary organic aerosol (IEPOX-SOA) from aerosol mass spectrometer measurements, *Atmos. Chem. Phys.*, 15, 11807–11833, doi:10.5194/acp-15-11807-2015, 2015.
- Jaeglé, L., Quinn, P. K., Bates, T. S., Alexander, B. and Lin, J.-T.: Global distribution of sea salt aerosols: new constraints from in situ and remote sensing observations, *Atmos. Chem. Phys.*, 11, 3137–3157, 2011.
- 825 Jimenez, J. L., Canagaratna, M. R., Donahue, N. M., Prevot, A. S. H., Zhang, Q., Kroll, J. H., DeCarlo, P. F., Allan, J. D., Coe, H., Ng, N. L., Aiken, A. C., Docherty, K. S., Ulbrich, I. M., Grieshop, A. P., Robinson, A. L., Duplissy, J., Smith, J. D., Wilson, K. R., Lanz, V. A., Hueglin, C., Sun, Y. L., Tian, J., Laaksonen, A., Raatikainen, T., Rautiainen, J., Vaattovaara, P., Ehn, M., Kulmala, M., Tomlinson, J. M., Collins, D. R., Cubison, M. J., Dunlea, E. J., Huffman, J. A., Onasch, T. B., Alfarra, M. R., Williams, P.
- 830 I., Bower, K., Kondo, Y., Schneider, J., Drewnick, F., Borrmann, S., Weimer, S., Demerjian, K., Salcedo, D., Cottrell, L., Griffin, R., Takami, A., Miyoshi, T., Hatakeyama, S., Shimono, A., Sun, J. Y., Zhang, Y. M., Dzepina, K., Kimmel, J. R., Sueper, D., Jayne, J. T., Herndon, S. C., Trimborn, A. M., Williams, L. R., Wood, E. C., Middlebrook, A. M., Kolb, C. E., Baltensperger, U. and Worsnop, D. R.: Evolution of

- organic aerosols in the atmosphere, *Science* (80-.), 326, 1525–1529, doi:10.1126/science.1180353, 835 2009.
- Kim, P. S., Jacob, D. J., Fisher, J. A., Travis, K., Yu, K., Zhu, L., Yantosca, R. M., Sulprizio, M. P., Jimenez, J. L., Campuzano-Jost, P., Froyd, K. D., Liao, J., Hair, J. W., Fenn, M. A., Butler, C. F., Wagner, N. L., Gordon, T. D., Welti, A., Wennberg, P. O., Crouse, J. D., St. Clair, J. M., Teng, A. P., Millet, D. B., Schwarz, J. P., Markovic, M. Z. and Perring, A. E.: Sources, seasonality, and trends of southeast US 840 aerosol: an integrated analysis of surface, aircraft, and satellite observations with the GEOS-Chem chemical transport model, *Atmos. Chem. Phys.*, 15, 10411–10433, doi:10.5194/acp-15-10411-2015, 2015.
- Knote, C., Hodzic, A., Jimenez, J. L., Volkamer, R., Orlando, J. J., Baidar, S., Brioude, J., Fast, J., Gentner, D. R., Goldstein, A. H., Hayes, P. L., Knighton, W. B., Oetjen, H., Setyan, A., Stark, H., 845 Thalman, R., Tyndall, G., Washenfelder, R., Waxman, E. and Zhang, Q.: Simulation of semi-explicit mechanisms of SOA formation from glyoxal in aerosol in a 3-D model, *Atmos. Chem. Phys.*, 14, 6213–6239, doi:10.5194/acp-14-6213-2014, 2014.
- Koo, B., Knipping, E. and Yarwood, G.: 1.5-Dimensional volatility basis set approach for modeling organic aerosol in CAMx and CMAQ, *Atmos. Environ.*, 95, 158–164, 2014.
- 850 Krechmer, J. E., Coggon, M. M., Massoli, P., Nguyen, T. B., Crouse, J. D., Hu, W., Day, D. A., Tyndall, G. S., Henze, D. K., Rivera-Rios, J. C., Nowak, J. B., Kimmel, J. R., Mauldin, R. L., Stark, H., Jayne, J. T., Sipilä, M., Junninen, H., St. Clair, J. M., Zhang, X., Feiner, P. A., Zhang, L., Miller, D. O., Brune, W. H., Keutsch, F. N., Wennberg, P. O., Seinfeld, J. H., Worsnop, D. R., Jimenez, J. L. and Canagaratna, M. R.: Formation of Low Volatility Organic Compounds and Secondary Organic Aerosol from Isoprene 855 Hydroxyhydroperoxide Low-NO Oxidation, *Environ. Sci. Technol.*, 49, 10330–10339, doi:10.1021/acs.est.5b02031, 2015.
- Lamarque, J. F., Bond, T. C., Eyring, V., Granier, C., Heil, A., Klimont, Z., Lee, D., Mieville, A. and Owen, B.: Historical(1850-2000) gridded anthropogenic and biomass burning emissions of reactive gases and aerosols: methodology and application, *Atmos. Chem. Phys.*, 10, 7017–7039, 2010.

- 860 Liu, J., D'Ambro, E. L., Lee, B. H., Lopez-Hilfiker, F. D., Zaveri, R. A., Rivera-Rios, J. C., Keutsch, F. N., Iyer, S., Kurten, T., Zhang, Z., Gold, A., Surratt, J. D., Shilling, J. E. and Thornton, J. A.: Efficient Isoprene Secondary Organic Aerosol Formation from a Non-IEPOX Pathway, *Environ. Sci. Technol.*, 50, 9872–9880, doi:10.1021/acs.est.6b01872, 2016.
- Mao, J., Carlton, A., Cohen, R. C., Brune, W. H., Brown, S. S., Wolfe, G. M., Jimenez, J. L., Pye, H. O. T., Lee Ng, N., Xu, L., McNeill, V. F., Tsigaridis, K., McDonald, B. C., Warneke, C., Guenther, A., Alvarado, M. J., de Gouw, J., Mickley, L. J., Leibensperger, E. M., Mathur, R., Nolte, C. G., Portmann, R. W., Unger, N., Tosca, M. and Horowitz, L. W.: Southeast Atmosphere Studies: learning from model-observation syntheses, *Atmos. Chem. Phys.*, 18, 2615–2651, doi:10.5194/acp-18-2615-2018, 2018.
- 870 Marais, E. A.: ~~Fixes for isoprene SOA for consistency with Marais et al. (2016), [online] Available from: http://wiki.seas.harvard.edu/geos-chem/index.php/Secondary_organic_aerosols#Fixes_for_isoprene_SOA_for_consistency_with_Marais_et_al._.282016.29 (Accessed 7 January 2019), 2018.~~
- ~~Marais, E. A.,~~ Jacob, D. J., Jimenez, J. L., Campuzano-Jost, P., Day, D. A., Hu, W., Krechmer, J., Zhu, L., Kim, P. S., Miller, C. C., Fisher, J. A., Travis, K., Yu, K., Hanisco, T. F., Wolfe, G. M., Arkinson, H. L., Pye, H. O. T., Froyd, K. D., Liao, J. and McNeill, V. F.: Aqueous-phase mechanism for secondary organic aerosol formation from isoprene: Application to the southeast United States and co-benefit of SO₂ emission controls, *Atmos. Chem. Phys.*, 16, 1603–1618, doi:10.5194/acp-16-1603-2016, 2016.
- 875 Marais, E. A., Jacob, D. J., Turner, J. R. and Mickley, L. J.: Evidence of 1991–2013 decrease of biogenic secondary organic aerosol in response to SO₂ emission controls, *Environ. Res. Lett.*, 12, 54018, 2017.
- 880 Middlebrook, A. M., Murphy, D. M., Lee, S. H., Thomson, D. S., Prather, K. A., Wenzel, R. J., Liu, D. Y., Phares, D. J., Rhoads, K. P., Wexler, A. S., Johnston, M. V, Jimenez, J. L., Jayne, J. T., Worsnop, D. R., Yourshaw, I., Seinfeld, J. H. and Flagan, R. C.: A comparison of particle mass spectrometers during the 1999 Atlanta Supersite Project, *J. Geophys. Res.*, 108, 2003.
- Murphy, D. M., Froyd, K. D., Bian, H., Brock, C. A., Dibb, J. E., DiGangi, J. P., Diskin, G., Dollner, M., Kupc, A., Scheuer, E. M., Schill, G. P., Weinzierl, B., Williamson, C. J. and Yu, P.: The distribution of sea-salt aerosol in the global troposphere, *Atmos. Chem. Phys. Discuss.*, 2018, 1–27, doi:10.5194/acp-

2018-1013, 2018.

890 Nault, B. A., Campuzano-Jost, P., Douglas Day, Hu, W., Palm, B., Schroder, J. C., Bahreini, R., Bian, H., Chin, M., Clegg, S. L., Colarco, P. R., Crouse, J. D., Dibb, J. E., Kim, M. J., Kodros, J., Lopez-Hilfiker, F., Marais, E. A., Middlebrook, A. M., Neuman, J. A., Nowak, J. B., Pierce, J. R., Scheuer, E. M., Thornton, J. A., Veres, P. R., Wennberg, P. O. and Jimenez, J. L.: Global Survey of Submicron Aerosol Acidity (pH), Abstract A53A-06 presented at American Geophysical Union Fall Meeting 2018, 10-14, December, Washington, D.C., 2018.

Nguyen, T. B., Crouse, J. D., Teng, A. P., Clair, J. M. S., Paulot, F., Wolfe, G. M. and Wennberg, P. O.:
895 Rapid deposition of oxidized biogenic compounds to a temperate forest, Proc. Natl. Acad. Sci., 112, E392–E401, 2015.

Noble, C. A. and Prather, K. A.: Real-time measurement of correlated size and composition profiles of individual atmospheric aerosol particles, Environ. Sci. Technol., 30, 2667–2680, 1996.

Pankow, J. F.: An absorption model of the gas/aerosol partitioning involved in the formation of secondary
900 organic aerosol, Atmos. Environ., 28, 189–193, 1994.

Park, R. J., Jacob, D. J., Chin, M. and Martin, R. V: Sources of carbonaceous aerosols over the United States and implications for natural visibility, J. Geophys. Res. Atmos., 108, doi:10.1029/2002JD003190, 2003.

Park, R. J., Jacob, D. J., Kumar, N. and Yantosca, R. M.: Regional visibility statistics in the United States:
905 Natural and transboundary pollution influences, and implications for the Regional Haze Rule, Atmos. Environ., 40, 5405–5423, doi:10.1016/j.atmosenv.2006.04.059, 2006.

Paulot, F., Crouse, J. D., Kjaergaard, H. G., Kürten, A., St. Clair, J. M., Seinfeld, J. H. and Wennberg, P. O.: Unexpected Epoxide Formation in the Gas-Phase Photooxidation of Isoprene, Science (80-.), 325, 730–733, doi:10.1126/science.1172910, 2009.

910 Peng, Z., Day, D. A. A., Stark, H., Li, R., Lee-Taylor, J., Palm, B. B. B., Brune, W. H. H. and Jimenez, J. L. L.: HO_x radical chemistry in oxidation flow reactors with low-pressure mercury lamps systematically examined by modeling, Atmos. Meas. Tech., 8, 4863–4890, doi:10.5194/amt-8-4863-2015, 2015. and

915 [Jimenez, J. L.: KinSim: A Research-Grade, User-Friendly, Visual Kinetics Simulator for Chemical-Kinetics and Environmental-Chemistry Teaching, J. Chem. Educ., 96, 806–811, doi:10.1021/acs.jchemed.9b00033, 2019.](#)

Philip, S., Martin, R. V and Keller, C. A.: Sensitivity of chemistry-transport model simulations to the duration of chemical and transport operators: a case study with GEOS-Chem~v10-01, *Geosci. Model Dev.*, 9, 1683–1695, doi:10.5194/gmd-9-1683-2016, 2016.

920 Pye, H. O. T., Liao, H., Wu, S., Mickley, L. J., Jacob, D. J., Henze, D. J. and Seinfeld, J. H.: Effect of changes in climate and emissions on future sulfate-nitrate-ammonium aerosol levels in the United States, *J. Geophys. Res.*, 114 [online] Available from: <http://www.scopus.com/inward/record.url?eid=2-s2.0-62149132476&partnerID=40&md5=e43a4dcf73bdf0fcf1fb016bbd1eb87d>, 2009.

925 Pye, H. O. T., Chan, A. W. H., Barkley, M. P. and Seinfeld, J. H.: Global modeling of organic aerosol: The importance of reactive nitrogen (NO_x and NO₃), *Atmos. Chem. Phys.*, 10, 11261–11276, doi:10.5194/acp-10-11261-2010, 2010.

930 Shrivastava, M., Fast, J., Easter, R., Gustafson, W. I., Zaveri, R. A., Jimenez, J. L., Saide, P., Hodzic, A., Gustafson Jr, W. I., Zaveri, R. A., Jimenez, J. L., Saide, P., Hodzic, A., Gustafson, W. I., Zaveri, R. A., Jimenez, J. L., Saide, P. and Hodzic, A.: Modeling organic aerosols in a megacity: comparison of simple and complex representations of the volatility basis set approach, *Atmos. Chem. Phys.*, 11, 6639–6662, doi:doi:10.5194/acp-11-6639-2011, 2011.

Sindelarova, K., Granier, C., Bouarar, I., Guenther, A., Tilmes, S., Stavrou, T., Müller, J. F., Kuhn, U., Stefani, P. and Knorr, W.: Global data set of biogenic VOC emissions calculated by the MEGAN model over the last 30 years, *Atmos. Chem. Phys.*, 14, 9317–9341, doi:10.5194/acp-14-9317-2014, 2014.

935 Stadtler, S., Kühn, T., Schröder, S., Taraborrelli, D., Schultz, M. G. and Kokkola, H.: Isoprene derived secondary organic aerosol in a global aerosol chemistry climate model, *Geosci. Model Dev. Discuss.*, 2017, 1–35, doi:10.5194/gmd-2017-244, 2017.

Stocker, T. F., Qin, D., Plattner, G. K., Tignor, M. M. B., Allen, S. K., Boschung, J., Nauels, A., Xia, Y., Bex, V. and Midgley, P. M.: Climate change 2013: the physical science basis: Working Group I

contribution to the fifth assessment report of the intergovernmental panel on climate change, Cambridge
940 Univ. Press. Cambridge, United Kingdom New York, NY, USA, 1535 pp,
doi:10.1017/CBO9781107415324, 2013.

Surratt, J. D., Chan, A. W. H., Eddingsaas, N. C., Chan, M., Loza, C. L., Kwan, A. J., Hersey, S. P.,
Flagan, R. C., Wennberg, P. O. and Seinfeld, J. H.: Reactive intermediates revealed in secondary organic
aerosol formation from isoprene, *Proc. Natl. Acad. Sci.*, 107, 6640–6645, 2010.

945 Taylor, K. E., Stouffer, R. J. and Meehl, G. A.: An Overview of CMIP5 and the Experiment Design, *Bull.*
Am. Meteorol. Soc., 93, 485–498, doi:10.1175/BAMS-D-11-00094.1, 2011.

Tsigaridis, K. and Kanakidou, M.: The Present and Future of Secondary Organic Aerosol Direct Forcing
on Climate, *Curr. Clim. Chang. Reports*, 4, 84–98, doi:10.1007/s40641-018-0092-3, 2018.

Tsigaridis, K., Daskalakis, N., Kanakidou, M., Adams, P. J., Artaxo, P., Bahadur, R., Balkanski, Y.,
950 Bauer, S. E., Bellouin, N. ~~and Benedetti, A.: The AeroCom evaluation and intercomparison of organic
aerosol in global models, *Atmos. Chem. Phys.*, 14, 10845–10895.~~ Benedetti, A., Bergman, T., Berntsen,
T. K., Beukes, J. P., Bian, H., Carslaw, K. S., Chin, M., Curci, G., Diehl, T., Easter, R. C., Ghan, S. J.,
Gong, S. L., Hodzic, A., Hoyle, C. R., Iversen, T., Jathar, S., Jimenez, J. L., Kaiser, J. W., Kirkevåg, A.,
Koch, D., Kokkola, H., H Lee, Y., Lin, G., Liu, X., Luo, G., Ma, X., Mann, G. W., Mihalopoulos, N.,
955 Morcrette, J. J., Müller, J. F., Myhre, G., Myriokefalitakis, S., Ng, N. L., O'donnell, D., Penner, J. E.,
Pozzoli, L., Pringle, K. J., Russell, L. M., Schulz, M., Sciare, J., Seland, Shindell, D. T., Sillman, S.,
Skeie, R. B., Spracklen, D., Stavrou, T., Steenrod, S. D., Takemura, T., Tiitta, P., Tilmes, S., Tost, H.,
Van Noije, T., Van Zyl, P. G., Von Salzen, K., Yu, F., Wang, Z., Wang, Z., Zaveri, R. A., Zhang, H.,
Zhang, K., Zhang, Q. and Zhang, X.: The AeroCom evaluation and intercomparison of organic aerosol in
960 global models, *Atmos. Chem. Phys.*, 14, 10845–10895, doi:10.5194/acp-14-10845-2014, 2014.

Yantosca, B.: Species in GEOS-Chem (Full-chemistry), [online] Available from:
http://wiki.seas.harvard.edu/geos-chem/index.php/Species_in_GEOS-Chem#Full-chemistry (Accessed 7
January 2019), 2016.

Yantosca, B.: GEOS-Chem v11-02 release candidate, [online] Available from:

965 http://wiki.seas.harvard.edu/geos-chem/index.php/GEOS-Chem_v11-02#GEOS-Chem_v11-02_release_candidate (Accessed 7 January 2019), 2018.

Zhang, Q., Jimenez, J. L., Canagaratna, M. R., Allan, J. D., Coe, H., Ulbrich, I., Alfarra, M. R., Takami, A., Middlebrook, A. M. and Sun, Y. L.: Ubiquity and dominance of oxygenated species in organic aerosols in anthropogenically-influenced Northern Hemisphere midlatitudes, *Geophys. Res. Lett.*, 34, 970 L13801, 2007.

Zhang, Y., Chen, Y., Lambe, A. T., Olson, N. E., Lei, Z., Craig, R. L., Zhang, Z., Gold, A., Onasch, T. B., Jayne, J. T., Worsnop, D. R., Gaston, C. J., Thornton, J. A., Vizueté, W., Ault, A. P. and Surratt, J. D.: Effect of the Aerosol-Phase State on Secondary Organic Aerosol Formation from the Reactive Uptake of Isoprene-Derived Epoxydiols (IEPOX), *Environ. Sci. Technol. Lett.*, acs.estlett.8b00044, 975 doi:10.1021/acs.estlett.8b00044, 2018.

Supporting Information:

A simplified parameterization of isoprene-epoxydiol-derived secondary organic aerosol (IEPOX-SOA) for global chemistry and climate models

5 Duseong S. Jo^{1,2}, Alma Hodzic^{3,4}, Louisa K. Emmons³, Eloise A. Marais⁵, Zhe Peng^{1,2}, Benjamin A. Nault^{1,2}, Weiwei Hu^{1,2}, Pedro Campuzano-Jost^{1,2}, and Jose L. Jimenez^{1,2}

¹Cooperative Institute for Research in Environmental Sciences (CIRES), University of Colorado, Boulder, CO, USA

10 ²Department of Chemistry, University of Colorado, Boulder, CO, USA

³Atmospheric Chemistry Observations and Modeling Lab., National Center for Atmospheric Research, Boulder, CO, USA

⁴Laboratoire d'Aérodologie, Université de Toulouse, CNRS, UPS, Toulouse, France

⁵Department of Physics and Astronomy, University of Leicester, Leicester, UK

15

Correspondence to: Jose L. Jimenez (jose.jimenez@colorado.edu)

20

25

1 IEPOX reactive uptake coefficient calculation

30 We use the resistor model equation by Gaston et al. (2014b) to calculate the reactive uptake coefficient of IEPOX (γ). The equation is as follows:

$$\frac{1}{\gamma} = \frac{\omega R_p}{4D_{gas}} + \frac{1}{\alpha} + \frac{\omega R_p}{4RT H_{org} D_{org} (q_{org} F - 1)} \quad (S1a)$$

$$F = \frac{\coth(q_{org}) + h(q_{aq}, q_{org}^*)}{1 + \coth(q_{org}) h(q_{aq}, q_{org}^*)} \quad (S1b)$$

$$h(q_{aq}, q_{org}^*) = -\tanh(q_{org}^*) \frac{\frac{H_{aq} D_{aq}}{H_{org} D_{org}} (q_{aq} \coth(q_{aq}) - 1) - (q_{org}^* \coth(q_{org}^*) - 1)}{\frac{H_{aq} D_{aq}}{H_{org} D_{org}} (q_{aq} \coth(q_{aq}) - 1) - (q_{org}^* \tanh(q_{org}^*) - 1)} \quad (S1c)$$

$$35 \quad q_{org} = R_p \sqrt{\frac{k_{org}}{D_{org}}}, \quad q_{aq} = R_c \sqrt{\frac{k_{aq}}{D_{aq}}}, \quad q_{org}^* = \frac{R_c}{R_p} q_{org} \quad (S1d)$$

where ω is the mean molecular speed of IEPOX (m s^{-1}), R_p is the particle radius (m), D_{gas} is the gas-phase diffusion coefficient of IEPOX ($10^{-5} \text{ m}^2 \text{ s}^{-1}$), α is the mass accommodation coefficient (0.1), R is the universal gas constant ($8.2057 \times 10^{-2} \text{ L atm mol}^{-1} \text{ K}^{-1}$), T is temperature (K), H_{aq} and H_{org} are Henry's law coefficients in the aqueous core ($1.7 \times 10^7 \text{ M atm}^{-1}$) and in the organic layer ($2 \times 10^6 \text{ M atm}^{-1}$), D_{aq} and D_{org} are diffusion coefficients of IEPOX in the aqueous core ($10^{-9} \text{ m}^2 \text{ s}^{-1}$) and in the organic layer (discussed below), and R_c is the inorganic aqueous core radius (m). k_{aq} is the first-order reaction rate constant in the aqueous phase (s^{-1}), calculated as follows:

$$k_{aq} = (k_{H^+}[H^+]) + (k_{nuc}[nuc]a_{H^+}) + k_{ga}[ga] \quad (S2)$$

where k_{H^+} is the reaction rate constant due to acid-catalyzed ring-opening ($0.036 \text{ M}^{-1} \text{ s}^{-1}$), $[H^+]$ is the proton concentration (M), a_{H^+} is the proton activity, k_{nuc} is the reaction rate constant due to the presence of specific nucleophiles (sulfate and nitrate) ($2 \times 10^{-4} \text{ M}^{-1} \text{ s}^{-1}$), $[nuc]$ is the concentration of nucleophiles (M), k_{ga} is the reaction rate constant due to the presence of general acids (bisulfate) ($7.3 \times 10^{-4} \text{ M}^{-1} \text{ s}^{-1}$), and $[ga]$ is the concentration of general acids (M). We assumed the reaction rate coefficient of IEPOX in the organic layer (k_{org}) is the same as k_{aq} . We note that the equation above is different from the IEPOX reactive uptake equation used by Zhang et al. (2018), which is based on Gaston et al. (2014a). The

equation from Gaston et al. (2014a) can be derived from the Taylor series approximation by assuming thin coatings (Anttila et al., 2006). Therefore, we used the equation S1 to avoid some possible errors from the cases that second or higher order Taylor terms become important.

55 The diffusion coefficient of IEPOX in the organic layer (D_{org}) substantially changes by several orders of magnitude over a range of relative humidity (RH) in the atmosphere. Based on Table S3 of Zhang et al. (2018), we considered the RH dependence for D_{org} values. Table S1 show D_{org} values we used for GEOS-Chem calculation.

60

65

70

Table S1. Chemical reactions and dry deposition processes used in this study. The GEOS-Chem default chemistry mechanism is shown in the left column, and the corresponding lumped reactions used as the starting point of this work are shown in the right column.

#	Reactions (GEOS-Chem v11-02-rc)	Reaction rate	Reactions (Lumped)	Reaction rate
1	ISOP + OH → 1.0 ISOPO ₂	3.1E-11*exp(360/T)	ISOP + OH → 1.0 ISOPO ₂	3.1E-11*exp(360/T)
2	ISOP + O ₃ → other products	1.00E-14*exp(-1970/T)	ISOP + O ₃ → other products	1.00E-14*exp(-1970/T)
3	ISOP + NO ₃ → other products	3.5E-12*exp(-450/T)	ISOP + NO ₃ → other products	3.5E-12*exp(-450/T)
4	ISOP + Cl → 1.0 ISOPO ₂	7.60E-11*exp(500/T)	ISOP + Cl → 1.0 ISOPO ₂	7.60E-11*exp(500/T)
5	ISOPO ₂ + HO ₂ → 0.628 ISOPOOH_A + 0.272 ISOPOOH_B + 0.037 ISOPOOH_D	2.06E-13*exp(1300/T)	ISOPO ₂ + HO ₂ → 0.937 ISOPOOH	2.06E-13*exp(1300/T)
6	ISOPO ₂ + NO → 0.009 ISOPND + 0.081 ISOPNB	2.7E-12*exp(350/T)	ISOPO ₂ + NO → 0.009 ISOPND + 0.081 ISOPNB	2.7E-12*exp(350/T)
7	ISOPO ₂ + CH ₃ O ₂ → other products	8.37E-14	ISOPO ₂ + CH ₃ O ₂ → other products	8.37E-14
8	ISOPO ₂ + ISOPO ₂ → other products	2.30E-12	ISOPO ₂ + ISOPO ₂ → other products	2.30E-12
9	ISOPO ₂ + CH ₃ CO ₃ → other products	1.68E-12	ISOPO ₂ + CH ₃ CO ₃ → other products	1.87E-12
	ISOPO ₂ + CH ₃ CO ₃ → other products	1.87E-13		
10	ISOPO ₂ → other products	4.07E+08*exp(-7694/T)	ISOPO ₂ → other products	4.07E+08*exp(-7694/T)
11	ISOPOOH_A + OH → 0.750 ISOPO ₂	6.13E-12*exp(200/T)	ISOPOOH + OH → 0.652 ISOPO ₂	5.69E-12*exp(200/T)
	ISOPOOH_B + OH → 0.480 ISOPO ₂	4.14E-12*exp(200/T)		
	ISOPOOH_D + OH → 0.250 ISOPO ₂	5.11E-12*exp(200/T)		
12	ISOPOOH_A + OH → 0.578 IEPOX_A	1.70E-11*exp(390/T)	ISOPOOH + OH → 0.697 IEPOX	2.26E-11*exp(390/T)
	ISOPOOH_B + OH → 0.680 IEPOX_A + 0.320 IEPOX_B	2.97E-11*exp(390/T)		
	ISOPOOH_D + OH → 0.500 IEPOX_D	2.92E-11*exp(390/T)		
13	ISOPND + OH → 0.1 IEPOX_D	1.20E-11*exp(652/T)	ISOPND + OH → 0.1 IEPOX	1.20E-11*exp(652/T)
14	ISOPNB + OH → 0.067 IEPOX_A + 0.033 IEPOX_B	2.40E-12*exp(745/T)	ISOPNB + OH → 0.1 IEPOX	2.40E-12*exp(745/T)
15	ISOPND + O ₃ → other products	2.90E-17	ISOPND + O ₃ → other products	2.90E-17
16	ISOPNB + O ₃ → other products	3.70E-19	ISOPNB + O ₃ → other products	3.70E-19
17	IEPOX_A + OH → other products	3.73E-11*exp(-400/T)	IEPOX + OH → other products	4.07E-11*exp(-400/T)
	IEPOX_B + OH → other products	5.79E-11*exp(-400/T)		

	IEPOX_D + OH → other products	3.20E-11*exp(-400/T)	
	IEPOX_A → IEPOX-SOA		
18	IEPOX_B → IEPOX-SOA		IEPOX → IEPOX-SOA
	IEPOX_D → IEPOX-SOA		
19	ISOPND + hv → other products		ISOPND + hv → other products
20	ISOPNB + hv → other products		ISOPNB + hv → other products
	ISOPOOH_A + hv → other products		
21	ISOPOOH_B + hv → other products		ISOPOOH + hv → other products
	ISOPOOH_D + hv → other products		
22	ISOPOOH(A,B,D) dry deposition		ISOPOOH dry deposition
23	IEPOX(A,B,D) dry deposition		IEPOX dry deposition

Table S2. Input parameter sets considered in this study for the evaluation of parameterizations using the box model.

#	Species	Values
1	NO [ppt]	1, 5, 10, 50, 100, 500, 1000, 5000, 10^4 , 5×10^4 , 10^5 , 5×10^5 , 10^6
2	OH [molecules cm^{-3}]	10^4 , 5×10^4 , 10^5 , 5×10^5 , 10^6 , 2×10^6 , 3×10^6 , 4×10^6 , 5×10^6
3	HO ₂ [ppt]	1, 2, 5, 10, 20, 50, 100
4	Aerosol pH [unitless]	-1,0,1,2,3,4
5	Aerosol surface area [$\mu\text{m}^2 \text{cm}^{-3}$]	10, 50, 100, 500, 1000, 5000, 10^4
6	O ₃ [ppb]	10, 20, 30, 40, 50, 60, 70, 80, 90, 100
7	NO ₃ [ppt]	1, 2, 5, 10, 20, 30
8	Cl [molecules cm^{-3}]	10, 100, 500, 1000, 5000
9	CH ₃ O ₂ [ppt]	5, 10, 20, 30, 40, 50, 60, 70, 80, 90, 100
10	CH ₃ CO ₃ [ppt]	0.5, 1, 2, 3, 4, 5, 6, 7, 8, 9, 10
11	Aerosol radius [nm]	50, 100, 150, 200, 250, 300, 500, 1000
12	Organic coating fraction [unitless]	0.0, 0.1, 0.2, 0.3, 0.4, 0.5, 0.6, 0.7, 0.8, 0.9
13	Temperature [K]	288, 293, 298, 303, 308, 313, 318
14	Planetary boundary layer height [m]	100, 200, 500, 1000, 1500, 2000, 2500, 3000, 3500, 4000
15	Photolysis rate of ISOPOOH [s^{-1}]	10^{-7} , 5×10^{-7} , 10^{-6} , 5×10^{-6} , 10^{-5} , 2×10^{-5}

5

10

15

Table S3. Fitting constants for Eq. (12).

Constant [Unit]	Value (PAR1)	Value (PAR3)
C ₀ [s]	1.2766x10 ⁶	8.6804x10 ⁵
C ₁ [s]	-2.5853x10 ⁵	-6.8531x10 ⁵
C ₂	0.7812	0.8651
C ₃ [s ⁻¹]	1.1910x10 ⁻⁶	7.6927x10 ⁻⁷
C ₄ [s]	-2.2937x10 ⁵	-1.8233x10 ⁵
C ₅	1.1969	0.91796
C ₆ [s ⁻¹]	3.2483x10 ⁻⁶	1.4389x10 ⁻⁶
C ₇ [s]	-7.8766x10 ⁵	-1.8034x10 ⁵
C ₈	1.0760	1.3762
C ₉ [s ⁻¹]	1.5886x10 ⁻⁶	3.2078x10 ⁻⁶
C ₁₀ [s]	-2.2735x10 ⁵	
C ₁₁	1.3584	
C ₁₂ [s ⁻¹]	3.3567x10 ⁻⁶	
C ₁₃	-17.9610	-9.084
C ₁₄	1.4992	-2.004
C ₁₅	2.6901x10 ¹	2.8313x10 ¹
C ₁₆	1.8906x10 ¹	9.9961
C ₁₇	4.5583x10 ⁻²	1.0903x10 ⁻¹

Table S4. Computational time estimation using the Gprof performance analysis tool. Intel Fortran compiler 17.0.1 with ‘-p’ option was used for the compilation process for function profiling. Values were based on 7-days simulation using 32 cores (2.3-GHz Intel Xeon E5-2697V4 processors) on the NCAR Cheyenne supercomputer. More than 1,000 subroutines in GEOS-Chem were analyzed with the Gprof but we classified subroutines to 12 categories by keywords. For example, if ‘gckpp’ was included in Fortran filename or subroutine name, it was considered as chemistry calculation process.

Process	Estimated time [s]	Keywords for classification
Chemistry	10728	gckpp, flexchem, state_chm
Photolysis and non-tropospheric chemistry	630	strat_chem, fast_j
Emission	1214	hco
Transport	2978	transport, convection, tpcore
Dry deposition	410	drydep, mixing
Wet deposition	4808	wetscav
Unit conversion	2146	unitconv
VBS	23	soa, chem_nvoc, zeroin
PAR1	47	par1 ¹⁾
PAR2	13	par2 ¹⁾
PAR3	48	par3 ¹⁾
3%	1	pari1 ¹⁾
Others	2732	All others

1) Not included in the standard version of GEOS-Chem

10

15

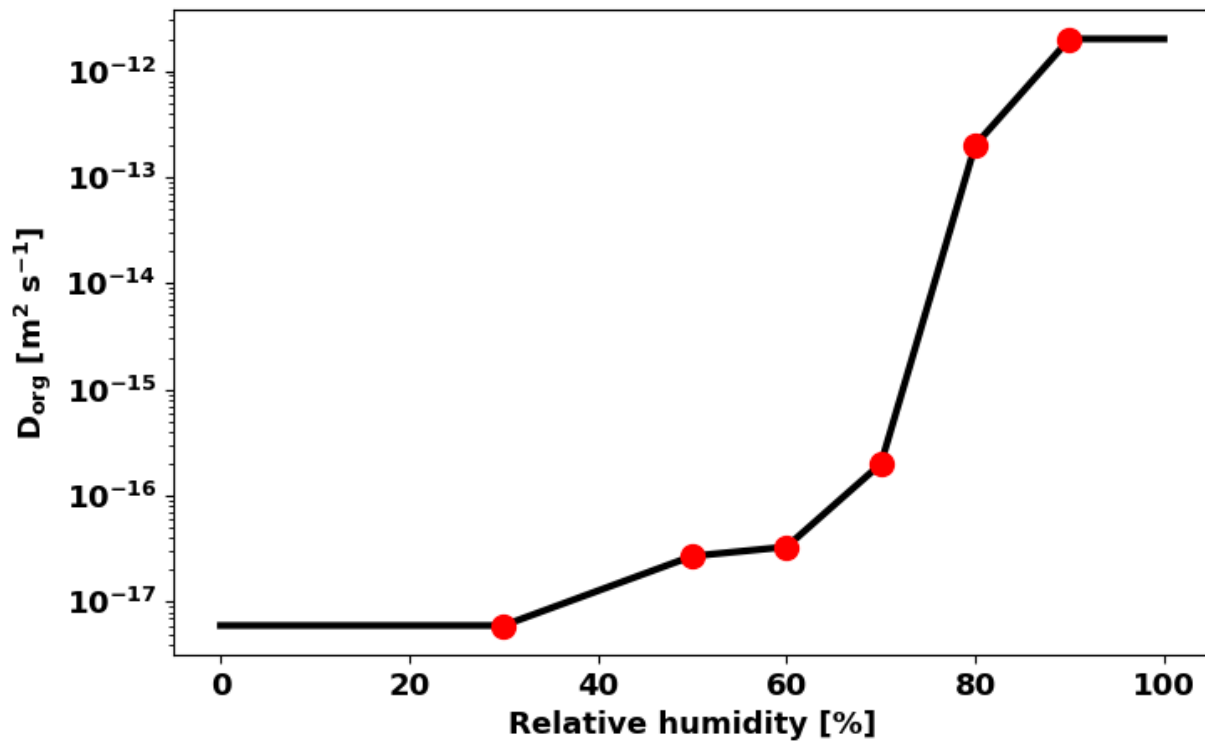
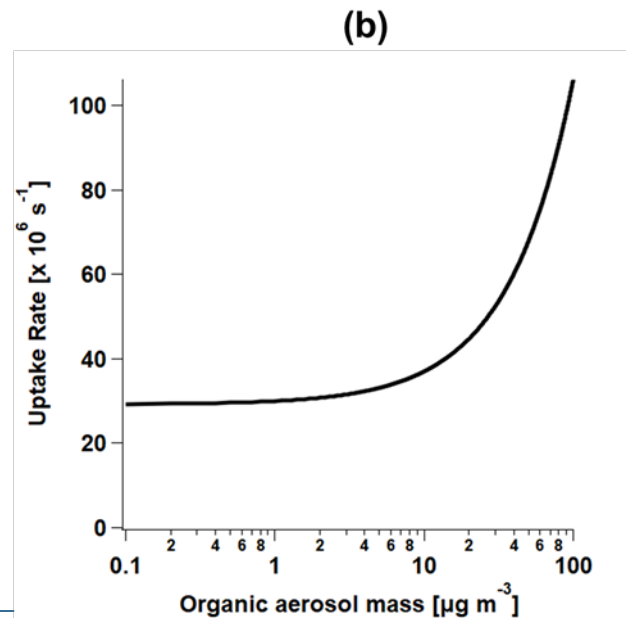
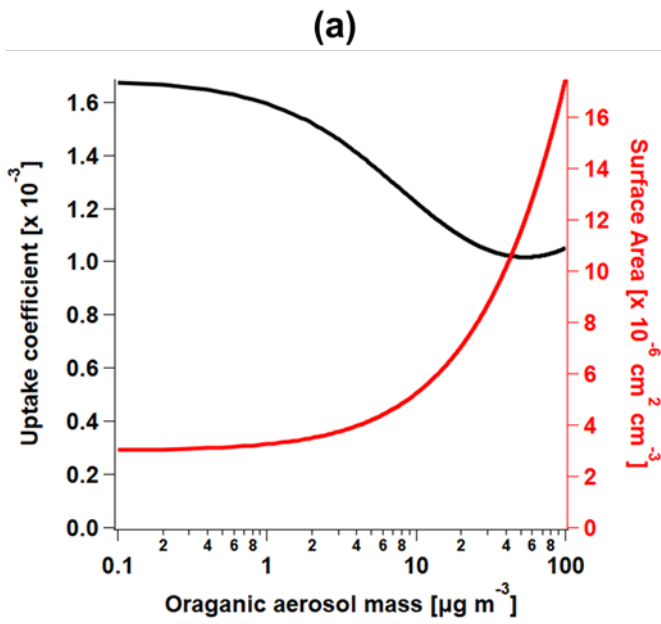


Figure S1. ~~(a)~~ The diffusion coefficient of IEPOX in the organic layer (D_{org}) as a function of RH. Red points indicate values calculated by Zhang et al. (2018). Values in between red points are log-linearly interpolated, and values below 30% RH or above 90% are set to be the constant values.

5

10

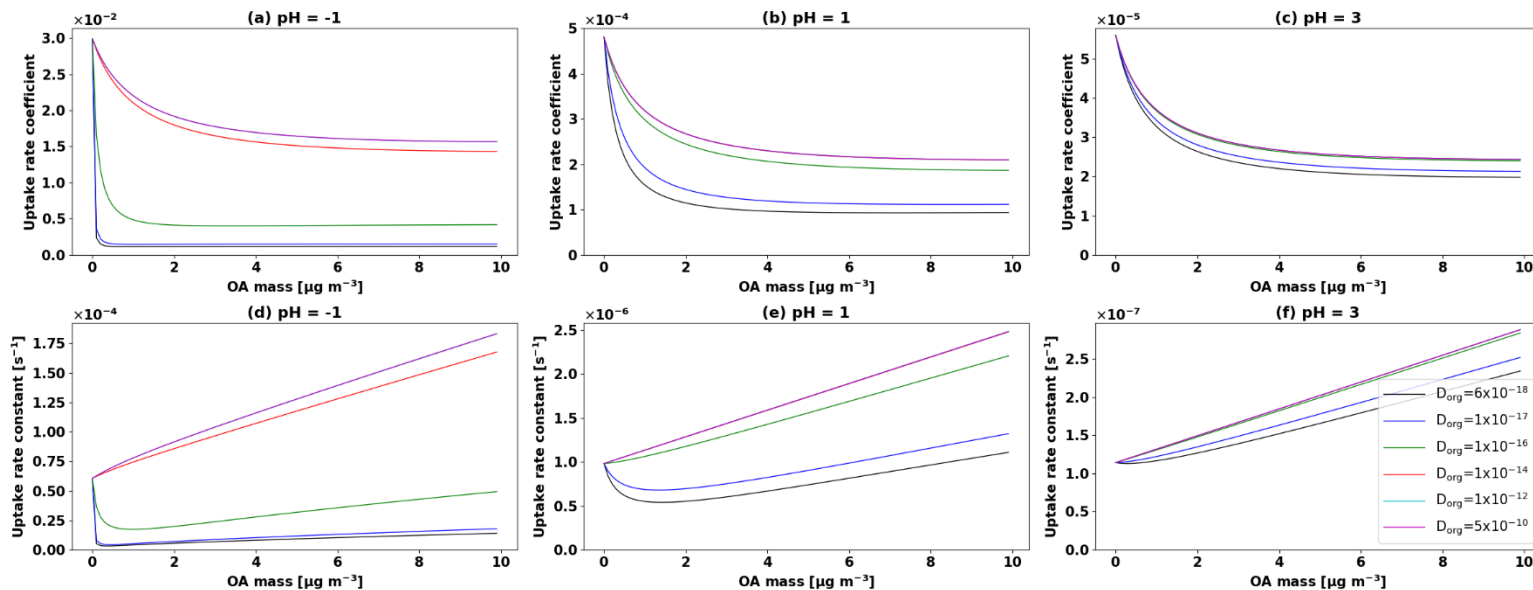
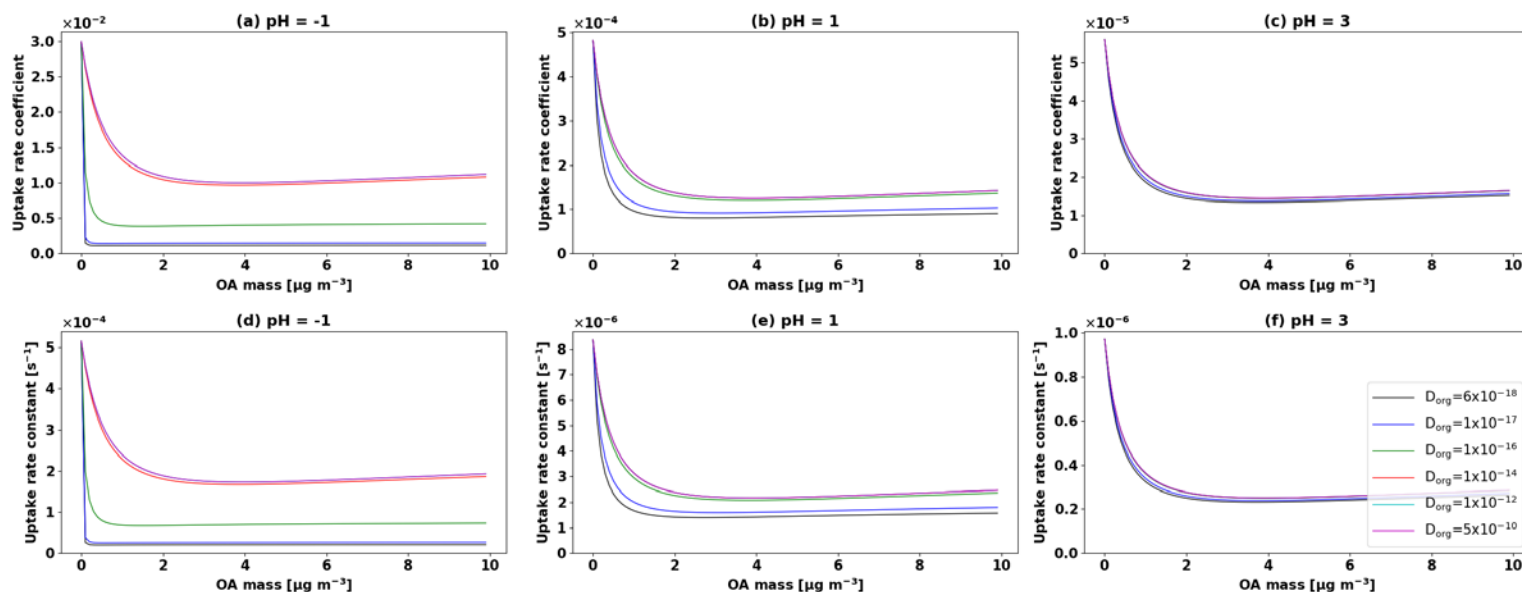


Figure S2. IEPOX reactive uptake coefficient (a,b,c) and surface area (S_a) uptake rate constant (d,e,f) as a function of OA mass concentration. (b) IEPOX condensation rate (k_{18}) as a function of OA mass concentrations. Different colors indicate D_{org} values ranging from 6×10^{-18} to $1 \times 10^{-12} \text{ m}^2 \text{ s}^{-1}$. Aerosol pH values were set to be -1 (a,d), 1 (b,e), and 3 (c,f), respectively. Sulfate aerosol mass concentration was assumed as $10 \mu\text{g m}^{-3}$. Initial surface area of $3 \times 10^{-6} \text{ cm}^2 \text{ cm}^{-3}$ was assumed for organic aerosol mass = $0 \mu\text{g m}^{-3}$. Densities of sulfate and organic aerosols were set to be 1.7 and 1.3 g cm^{-3} , respectively, based on densities used by GEOS-Chem v11-02-rc. Initial aerosol radius of 50 nm and aerosol surface area of $3 \times 10^{-6} \text{ cm}^2 \text{ cm}^{-3}$ were assumed for organic aerosol mass = $0 \mu\text{g m}^{-3}$. The changes of aerosol radius and aerosol surface area were calculated as OA mass increases, and aerosol inorganic core radius was fixed as 50 nm.



10 **Figure S3.** IEPOX reactive uptake coefficient (a,b,c) and uptake rate constant (d,e,f) as a function of OA mass concentrations. Different colors indicate D_{org} values ranging from 6×10^{-18} to $1 \times 10^{-12} \text{ m}^{-2} \text{ s}^{-1}$. Aerosol pH values were set to be -1 (a,d), 1 (b,e), and 3 (c,f), respectively. Sulfate aerosol mass concentration was assumed as $1 \mu\text{g m}^{-3}$. Densities of sulfate and organic aerosols were set to be 1.7 and 1.3 g cm^{-3} , respectively, based on densities used by GEOS-Chem v11-02-rc. Initial aerosol radius of 50 nm and aerosol surface area of $3 \times 10^{-6} \text{ cm}^2 \text{ cm}^{-3}$ were assumed for organic aerosol mass

= 0 $\mu\text{g m}^{-3}$. The changes of aerosol radius and aerosol surface area were fixed regardless of OA mass increase. Aerosol core radius was reduced in proportion to the OA mass increase (i.e. coating thickness increase).

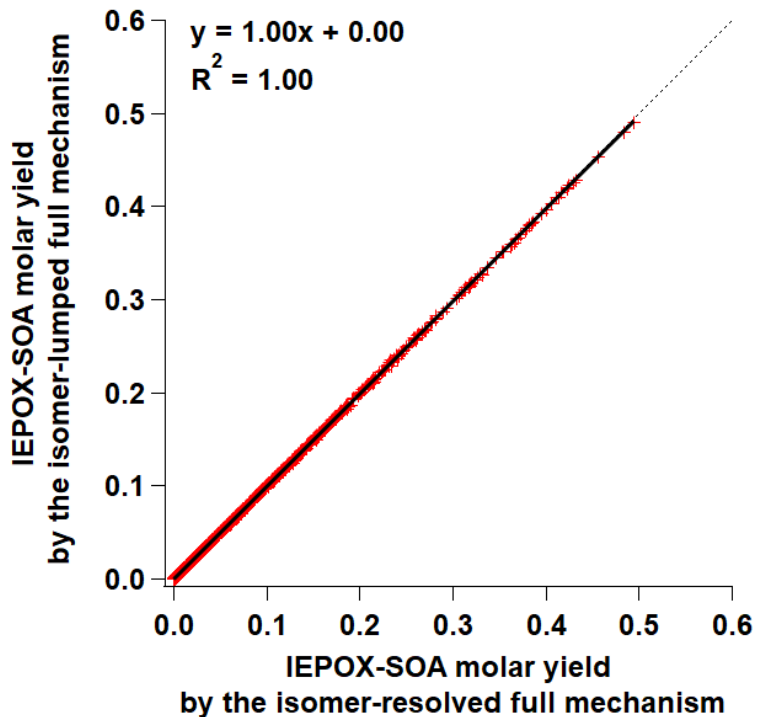


Figure S2S4. Point to point comparison of IEPOX-SOA molar yields for the isomer-lumped (y-axis) versus isomer-resolved full GEOS-Chem (x-axis) mechanisms. Yields were calculated by the box model using 14,000 simulations by systematically varying the input parameters in Table S2.

5

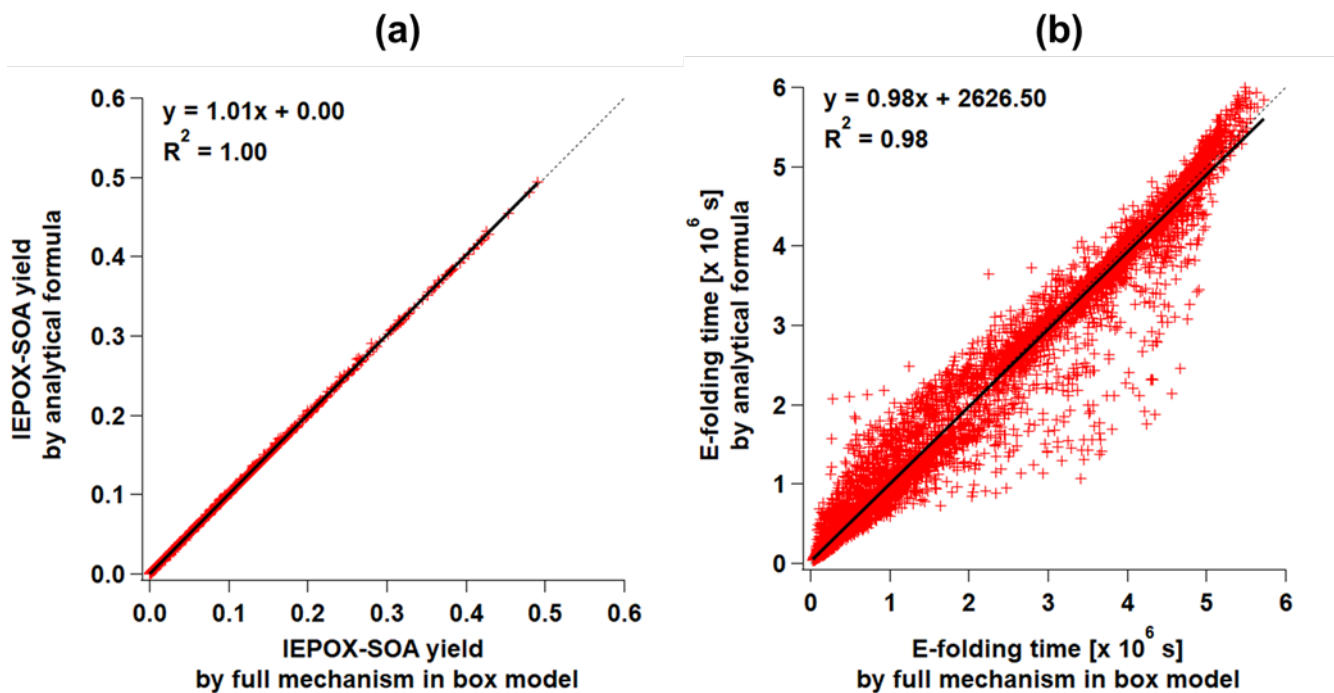
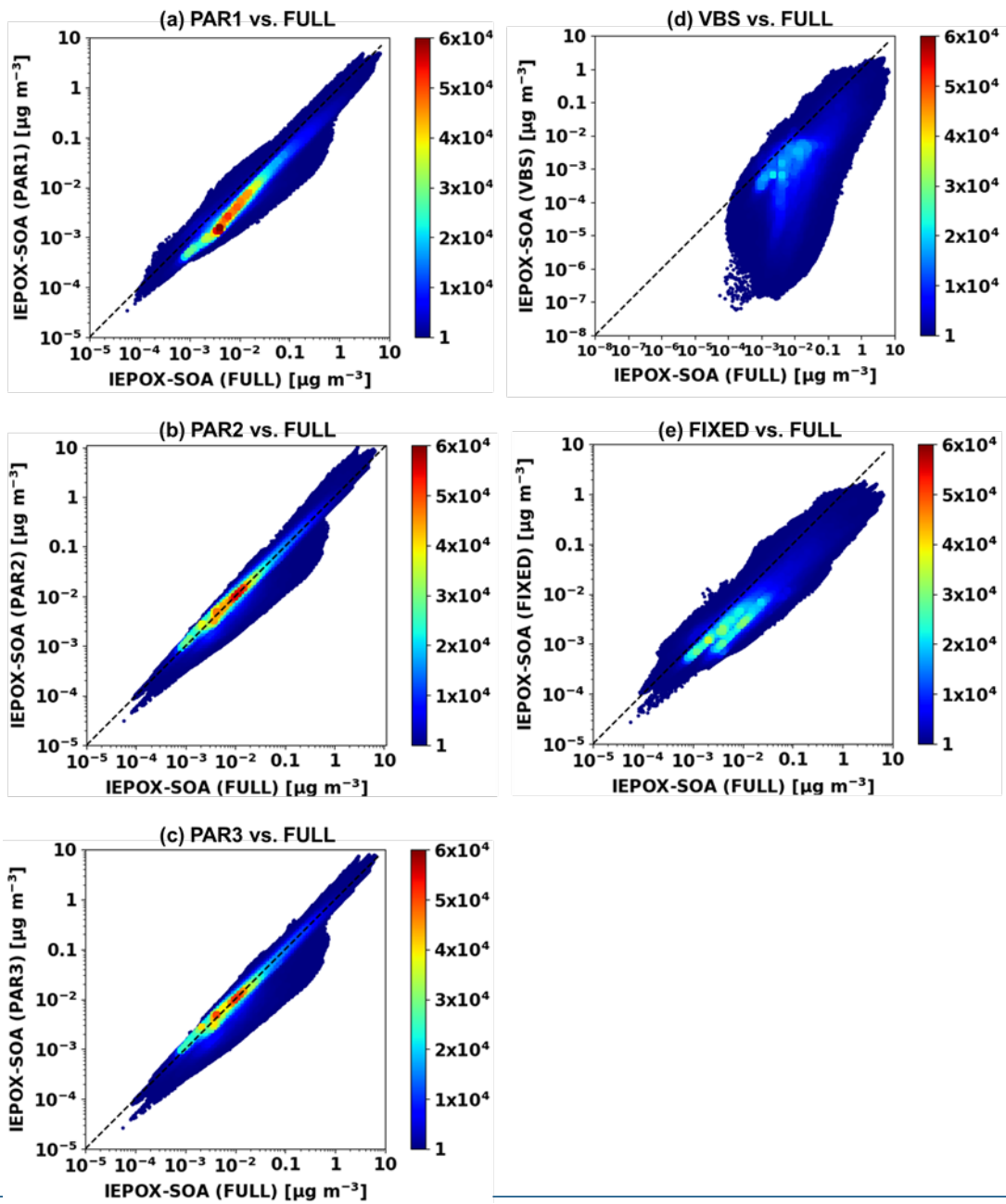


Figure S3S5. Scatterplots of parameterized (PAR1 case) (y-axis) versus simulated (x-axis) results by the box model for (a) IEPOX-SOA molar yield and (b) formation timescale with randomly selected parameters in Table S1 of 14,000 simulations.

5

10



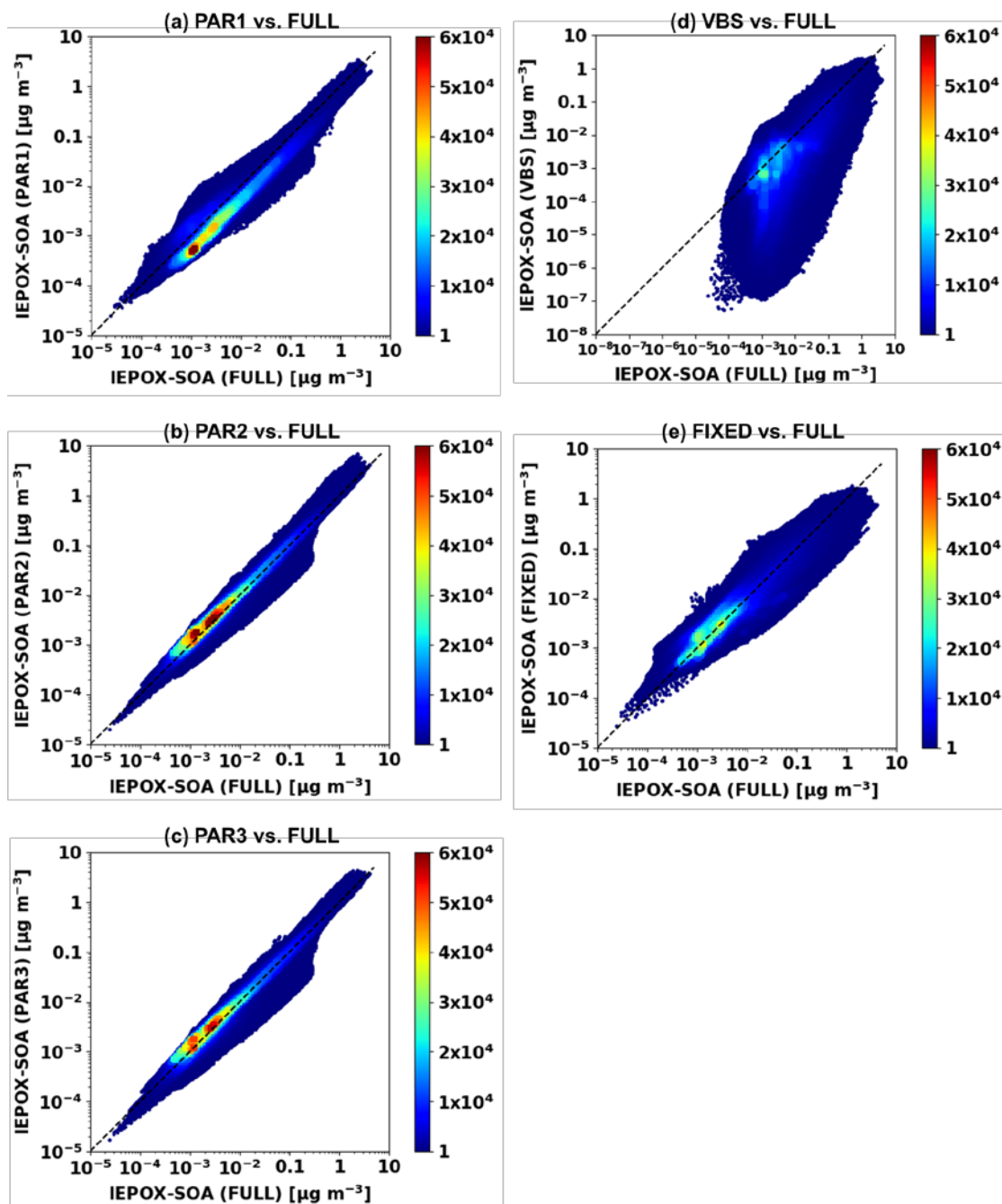
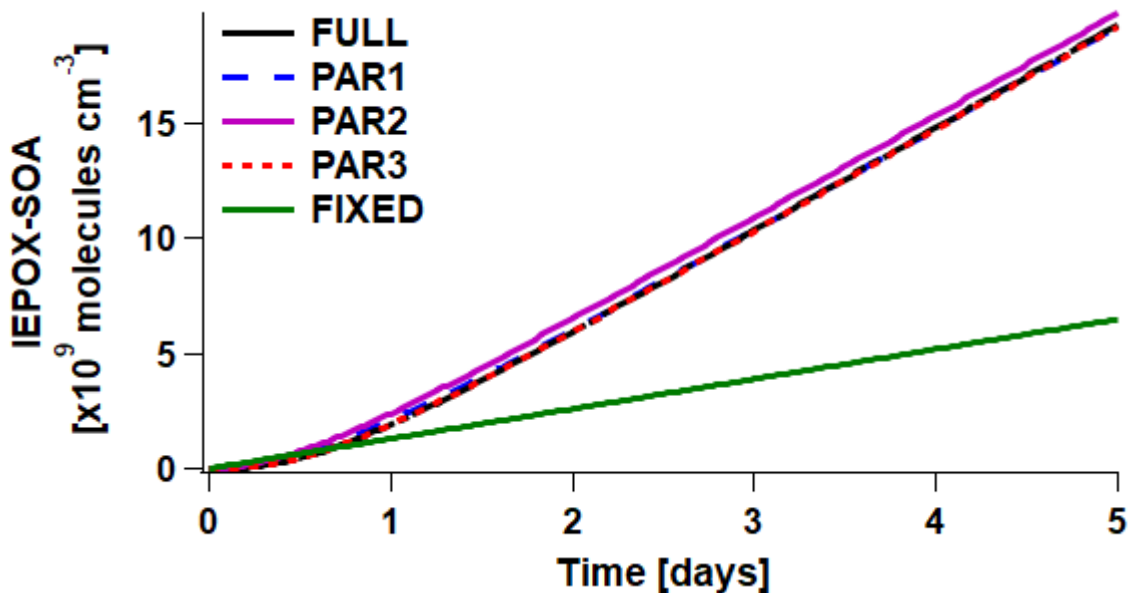


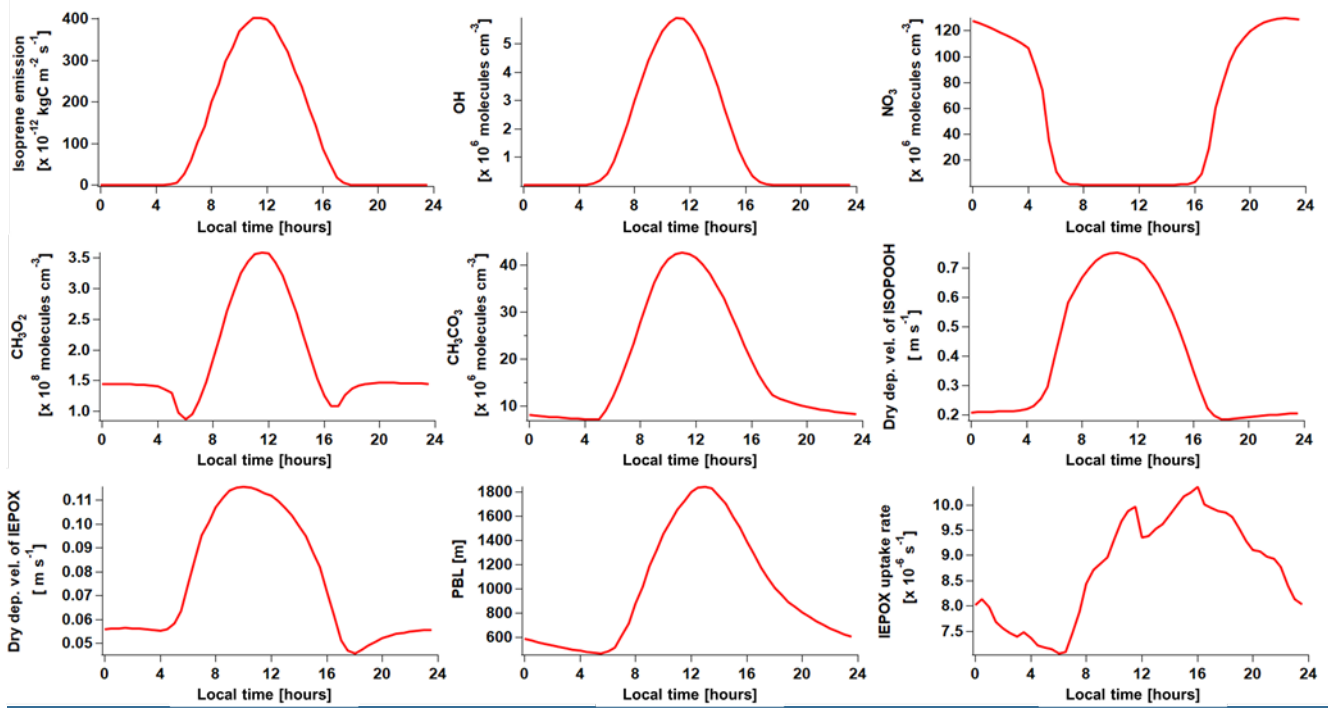
Figure S4S6. Scatterplots of parameterized (y-axis) versus full chemistry IEPOX-SOA (x-axis) concentrations within the troposphere for July 2013 – June 2014 shown on a log scale with base of 10. Each point represents monthly averaged model grid value of IEPOX-SOA concentration. Colors represent the density of points, where densities were calculated by dividing x and y axis ranges into 100 by 100 grid cells.



5 **Figure S5S7.** Same as Fig. 4d but IEPOX-SOA concentrations were simulated without diurnal variation of chemical/meteorological fields. Fixed values used for this calculation are: $\text{OH} = 10^6$ molecules cm^{-3} , $\text{HO}_2 = 100$ ppt, $\text{O}_3 = 50$ ppb, $\text{NO}_3 = 10$ ppt, $\text{Cl} = 10^3$ molecules cm^{-3} , $\text{NO} = 100$ ppt, $\text{CH}_3\text{O}_2 = 10$ ppt, $\text{CH}_3\text{CO}_3 = 10$ ppt, IEPOX uptake rate = 10^{-5} s^{-1} , Dry deposition rate of ISOPOOH and IEPOX = 10^{-6} s^{-1} , ISOPOOH photolysis rate = 10^{-5} s^{-1} , temperature = 298.15 K.

10

15



5

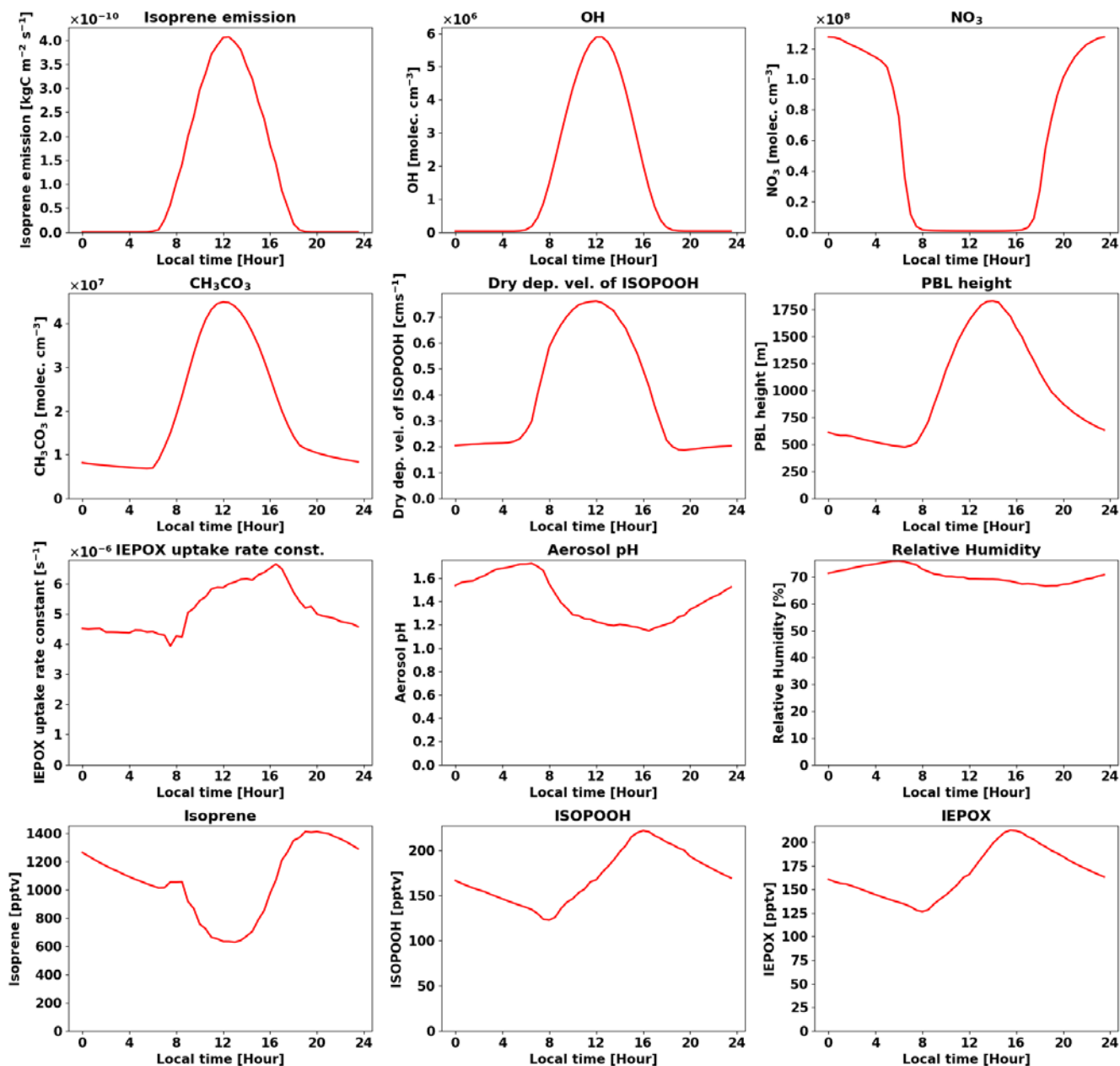
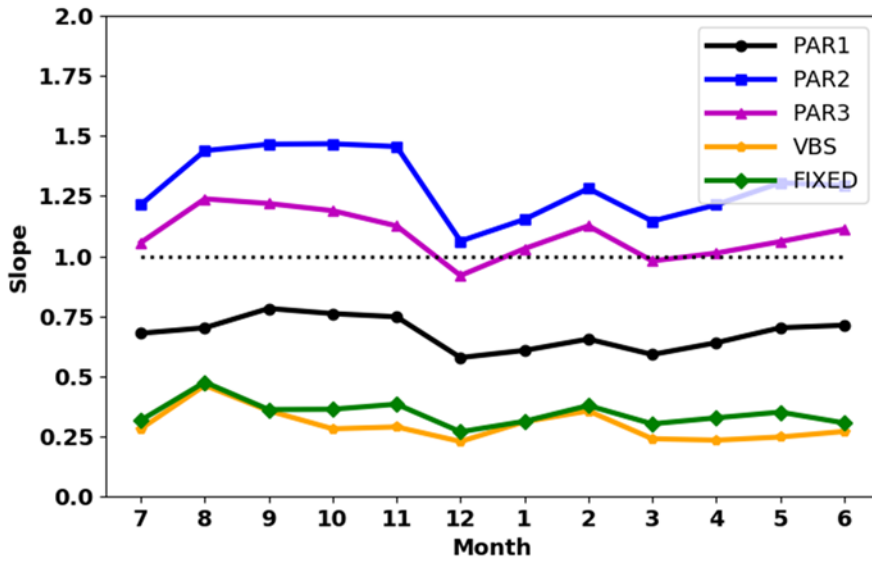
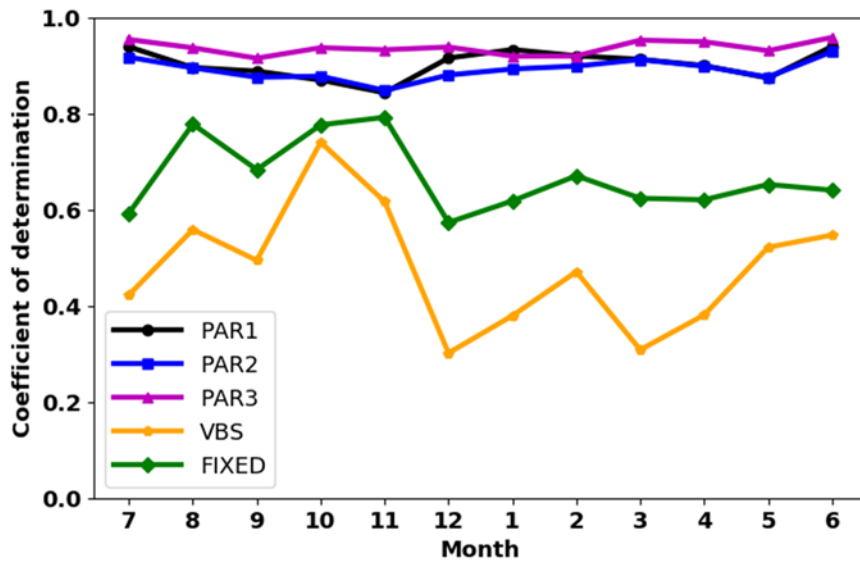


Figure S6S8. Diurnal variations of chemical/meteorological fields used in box model calculation (Fig. 5d). Values were extracted from GEOS-Chem global mean results for four major isoprene source regions [the Southeastern United States: 30°N – 40°N, 100°W – 80°W, Amazon: 10°S – 0°S, 70°W – 60°W, Central Africa: 5°N – 15°N, 10°E – 30°E, Borneo: 5°S – 5°N, 105°E – 120°E]. Figures represent approximate annual mean diurnal variation profiles, which were calculated by using the first two days of each month model outputs at 30 minutes interval averaged within the PBL, averaging points of the same local time.

(a)



(b)



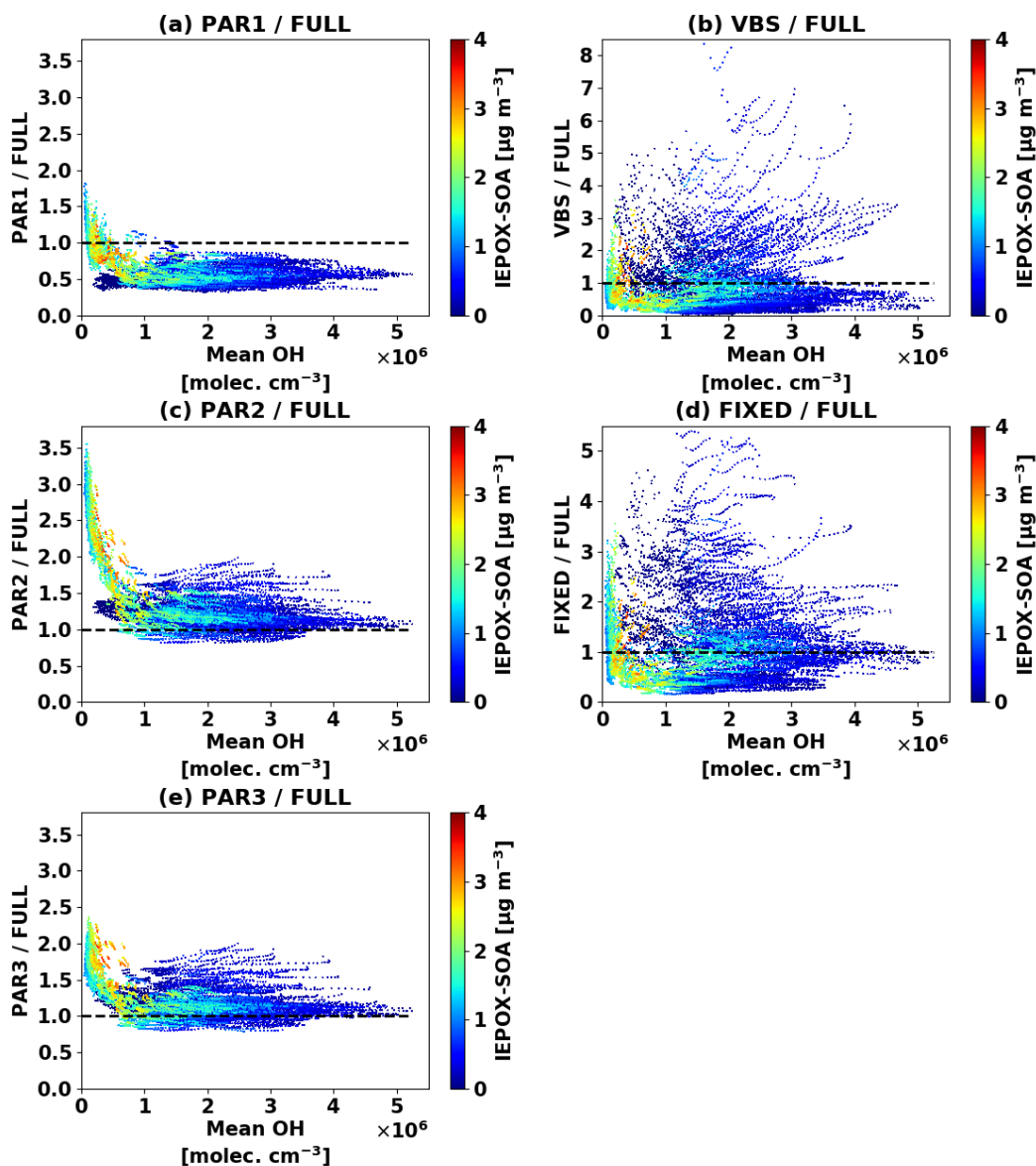


Figure S7.

Figure S9. Scatterplots of the IEPOX-SOA concentration ratio (five parameterizations against the explicit full chemistry) vs. OH concentration within the PBL. Each point represents the monthly averaged model grid value for four major isoprene source regions [the Southeastern United States: 30°N – 40°N, 100°W – 80°W, Amazon: 10°S – 0°S, 70°W – 60°W, Central Africa: 5°N – 15°N, 10°E – 30°E, Borneo: 5°S – 5°N, 105°E – 120°E]. Colors indicate the IEPOX-SOA concentration simulated by the full chemistry.

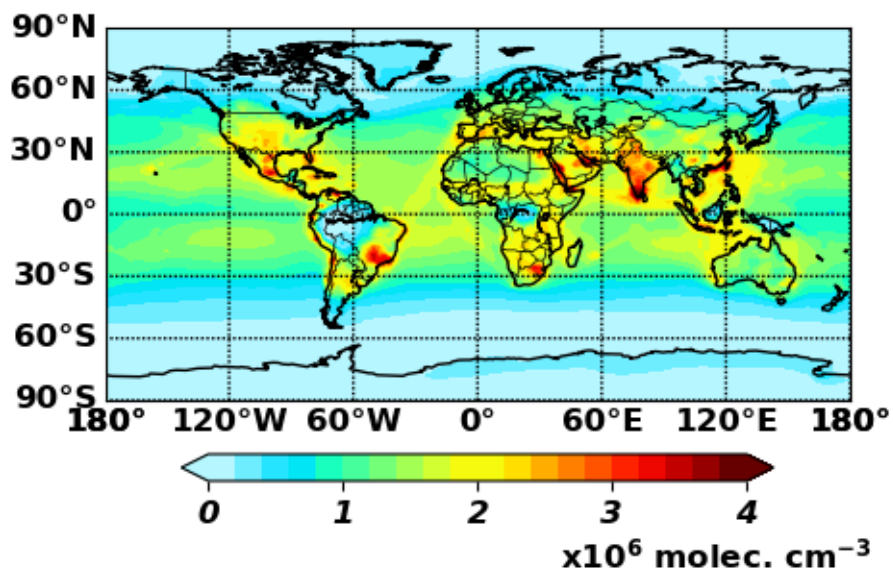


Figure S10. Global annual mean OH concentrations for July 2013 – June 2014 as predicted by the GEOS-Chem v11-02-rc used in this study.

5

10

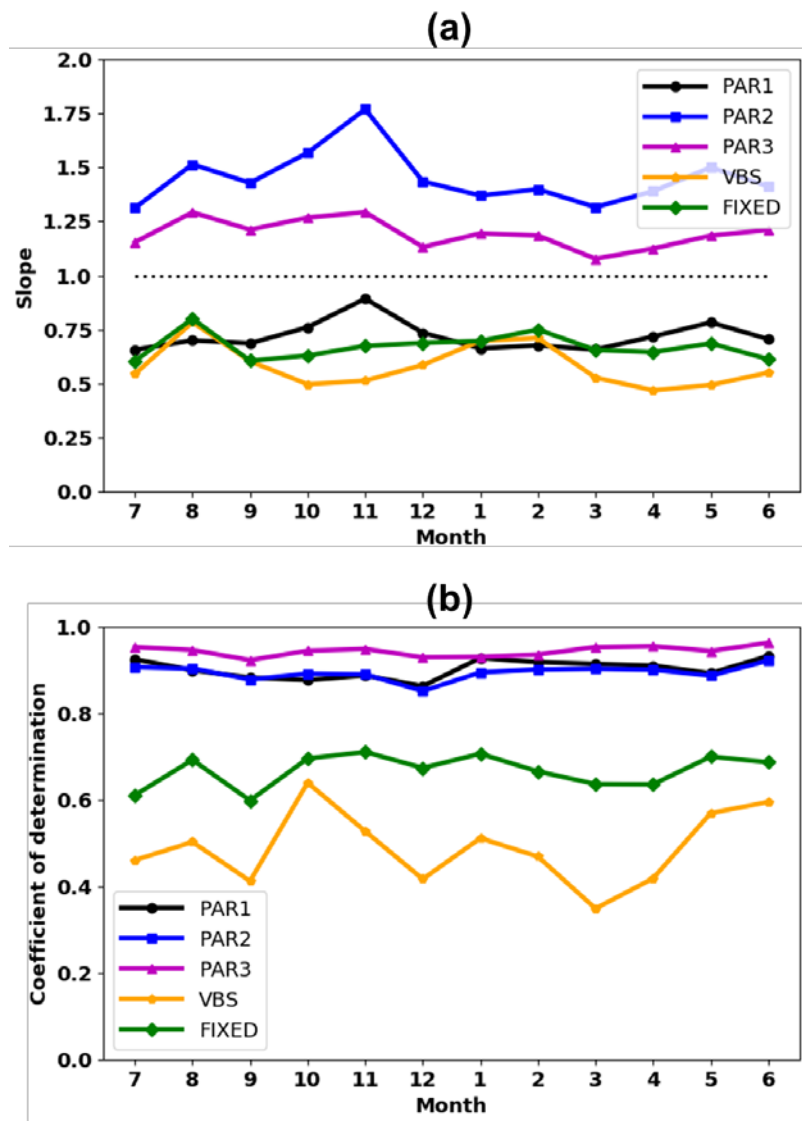


Figure S11. Timeseries of (a) regression slope and (b) R^2 for the full chemistry vs. parameterizations. Regression slope and R^2 are calculated for each month for concentrations within the troposphere.

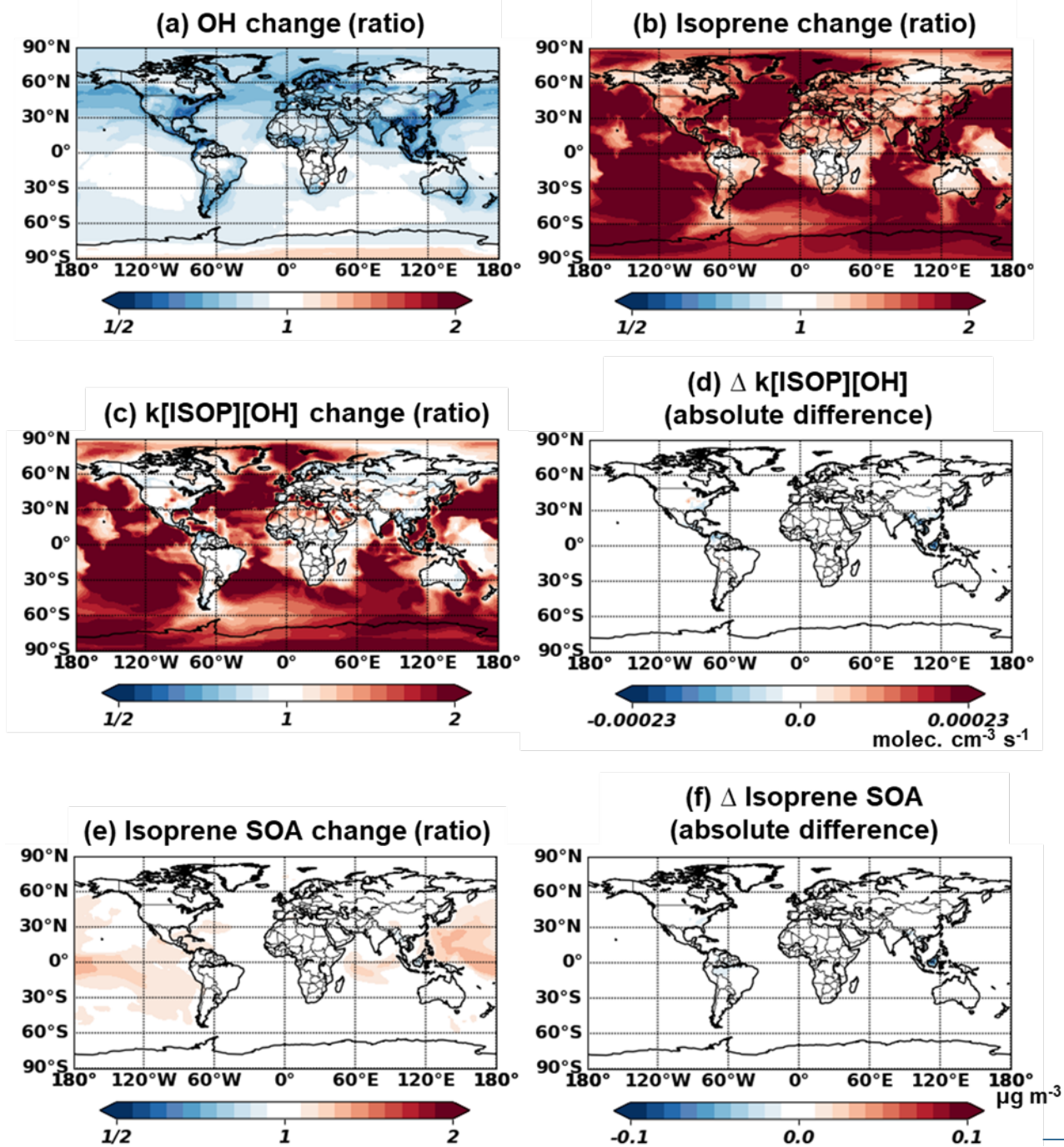


Figure S8.

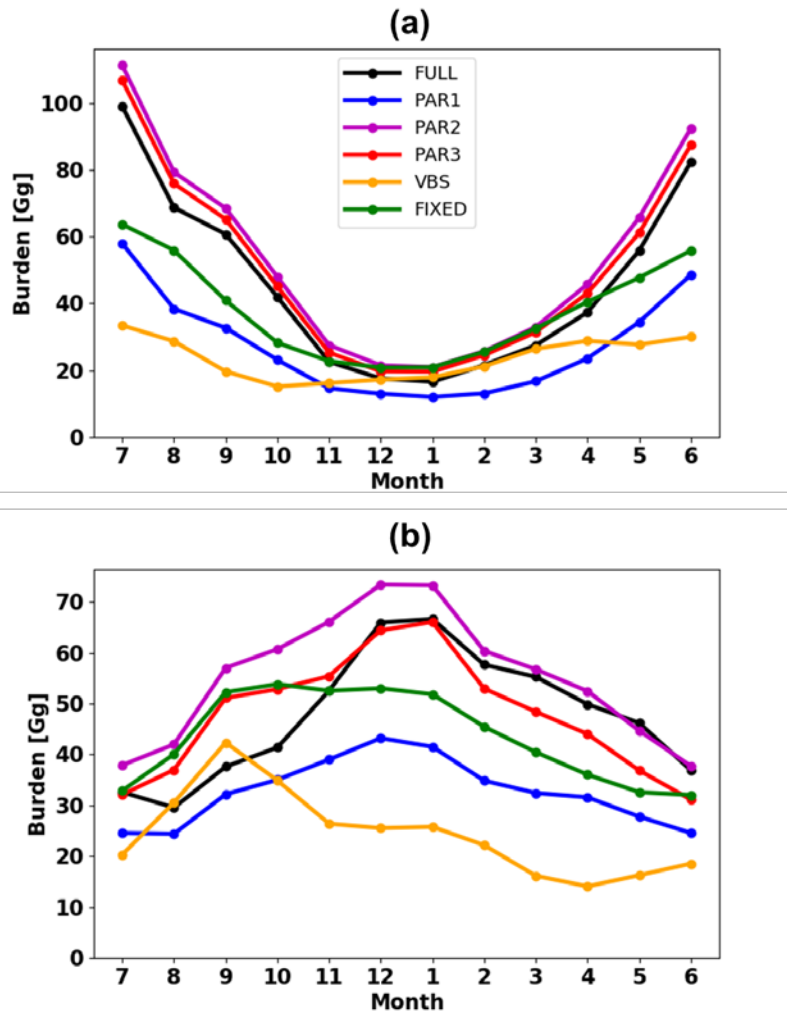
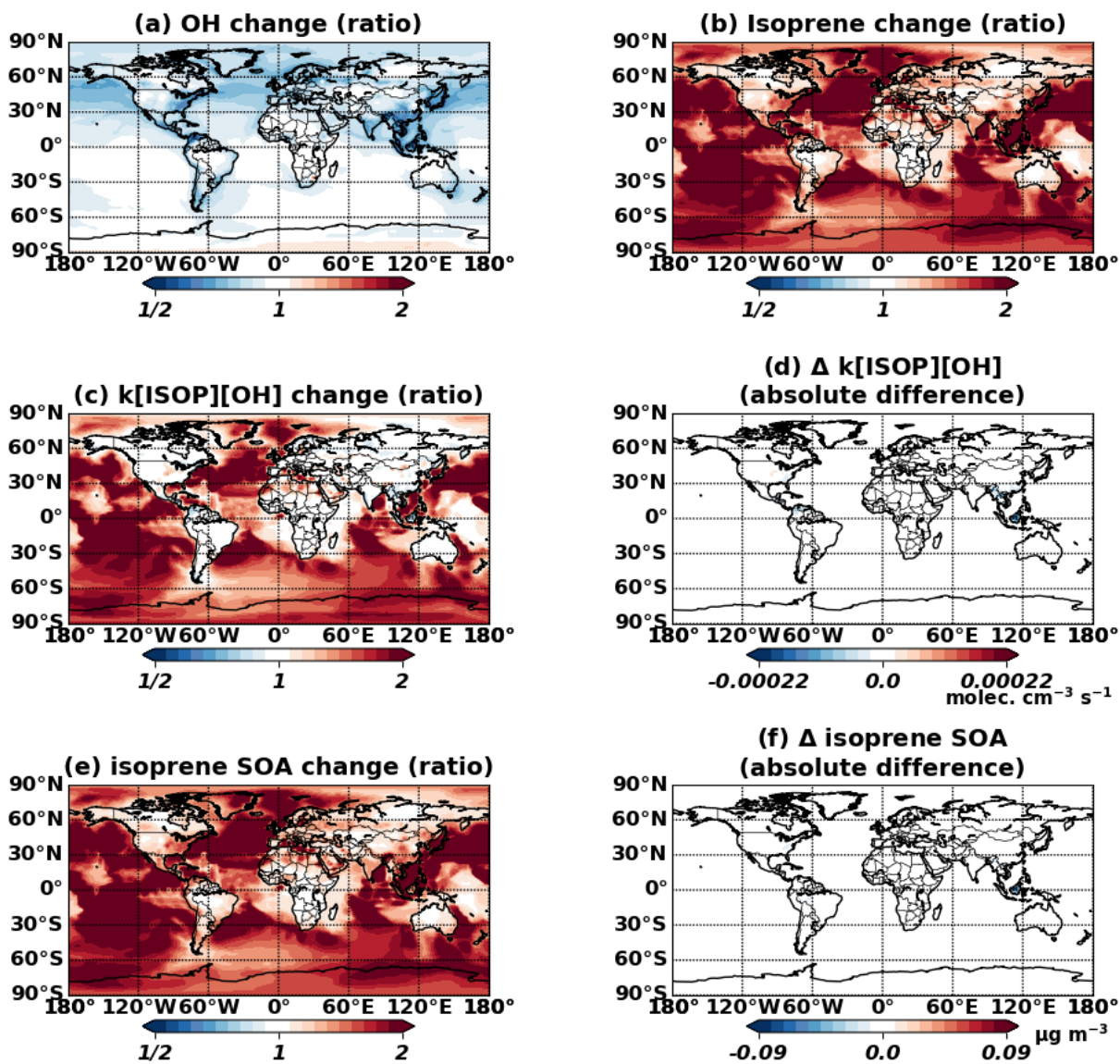


Figure S12. Same as Fig. 4c but for (a) Northern and (b) Southern Hemisphere.

5

10



5 **Figure S13.** Changes of chemical fields affecting the initial oxidation of isoprene and isoprene SOA concentrations simulated by the VBS. Ratios were computed as the 50% NO_x emission reduction case divided by the base case. All figures represent surface values for July – August 2013.